The interaction of UVA radiation with cultured human skin cells

Zhang, Jin

Award date:
2014

Awarding institution:
University of Bath

The interaction of UVA radiation with cultured human skin cells

Jin Zhang

A thesis submitted for the degree of Doctor of Philosophy

University of Bath

Department of Pharmacy and Pharmacology

July 2014

TO MY FAMILY

Table of Contents

ACKNOWLEDGEMENTS 6

ABSTRACT 8

ABBREVIATIONS 9

CHAPTER 1 INTRODUCTION 13

1.1 Human skin **13**

1.1.1 Human skin structure 13

1.1.2 Epidermal layer 13

1.1.3 Dermis layer 14

1.1.4 Hypodermal layer 14

1.2 UVA **15**

1.2.1 History of ultraviolet radiation 15

1.2.2 Main types of UV radiation 16

1.2.3 Harmful effects of UVR 17

1.3 Reactive oxygen species (ROS) **18**

1.3.1 Cytotoxicity of ROS 19

1.3.2 Consequences of oxidative stress 21

1.3.3 Origin of ROS in cells 23

1.3.4 UVA induced ROS in skin 24

1.4 NADPH oxidase (NOX) **27**

1.4.1 NADPH oxidase family 27

1.4.2 The NOX family in physiological and pathological process 29

1.4.3 Regulator proteins of NOX 33

1.4.4 NADPH oxidase and ROS 35

1.4.5 NADPH oxidase in skin 36

1.4.6 NADPH oxidase and HO-1 36

1.5 Cellular antioxidant defence **37**

1.5.1 Heme oxygenase (HO) 38

1.5.2 Bach family 44

1.5.3 Glutathione 46

1.6 RNA interference **49**

1.7 Aims and objectives **51**

CHAPTER 2 MATERIALS AND METHODS 53

2.1 Chemicals **53**

2.2 Cell culture **53**

2.3 Cell maintenance **54**

2.4 UVA irradiation **54**

2.5 Chemical treatment **55**

2.5.1 DPI treatment 55

2.5.2 Plumbagin treatment 55

2.5.3 Hemin treatment 55

2.6 siRNA transfection **56**

2.7 Cytotoxicity assay **58**

2.7.1 MTS assay 58

2.7.2 LDH assay 58

2.8 ROS generation assay **60**

2.8.1 Principle 60

2.8.2 Procedure 60

2.9 Flow cytometry (dual stain assay) apoptosis and necrosis assay **61**

2.9.1 Principle 61

2.9.2 Procedure 63

2.10 Trypan blue assay **63**

2.11 Total protein extraction **63**

2.12 Quantification of protein concentration **64**

2.13 Sodium dodecyl sulphate polyacrylamide gel electrophoresis (SDS-PAGE) **64**

2.14 Western blot analysis **66**

2.15 Confocal microscope cell imaging **67**

2.16 NADPH Oxidase activity assay **68**

2.16.1 Principle 68

2.16.2 Procedure 68

2.17 Statistical analysis **69**

CHAPTER 3. RESULTS 70

Part I: Potential protection of human skin cells against cell damage/inactivation via UVA-induced HO-1 ..... **70**

3.1 Silencing of Bach1 leads to no strong effect on cytotoxicity following UVA irradiation. **71**

3.2 Glutathione depletion of FEK4 cells by treatment with BSO results in a higher cytotoxicity following UVA irradiation. **74**

3.3 Silencing of Bach1 does not result in lower membrane damage in FEK4 cells **77**

3.4 Effect of siBach1/siHO-1 on ROS generation after UVA irradiation **80**

Part II: The Role of NADPH oxidase (NOX) in the response of human skin cells to UVA irradiation –ROS generation **85**

3.5 Comparisons of ROS generation in skin cells after UVA irradiation **85**

3.6 A comparison of UVA activated NOX activity in cultured skin cells following UVA irradiation **90**

3.7 A comparison of UVA activation of NOX proteins (NOX1 and NOX4) in cultured skin cells following UVA irradiation **95**

3.8 Effects of NOX inhibitors on UVA-mediated ROS generation. **99**

3.9 Effect of NOX1/NOX4 gene knockdown on ROS generation after UVA irradiation of skin cells. **117**

3.10 The effect of HO-1 knocking-down on NOX activity in cultured human skin keratinocytes after UVA irradiation. **128**

CHAPTER 4 DISCUSSIONS AND CONCLUSIONS 131

4.1 Role of Bach1 in protecting against UVA-induced skin cell damage.....132

4.2 Bach1/HO-1 involvement in UVA-induced ROS generation.....133

4.3 NOX involvement in UVA induced ROS generation 133

4.4 The contribution of NOX1/NOX4 subunits 134

4.5 The relationship between HO-1 and NOX.....136

4.6 Conclusions.....138

CHAPTER 5 REFERENCES.....140

APPENDIX 165

Acknowledgements

I am extremely grateful to my supervisor, Professor Rex Tyrrell for his excellent and constant supervision, guidance, and all the kindest understanding, and encouraging me to continually carry out the laboratory experimental work whenever I felt frustrated or depressed. All this helped brighten me up when I was lost in research. I'm deeply impressed with his brilliant research knowledge and keenness for science.

I wish to extend my thanks and appreciation to Dr Charareh Pourzand for helping me so much with practical suggestions and the kindness to give me the permission to access her laboratory. I am deeply thankful to Dr Olivier Reefs for his kind help and valuable advice and devoting himself to help me in certain experiments. I also thank Dr Asma Aroun for giving me training for the cell culture experiments. I would like to thank all the laboratory mates in 2.14 and 2.20, both past and current, especially Tina Ridka, for all the kindly support and friendly conversations; I also give my sincere thanks and appreciation to Dr Adrian Rogers for helping me with flow cytometry analysis. I would like to thank Dr Julia Zhong for her kindly support and training.

I give my appreciation to Mr Stephen Phillips and Mr Rod Murray for their kind technical support and friendly chat. I am also very appreciative to Mr Kevin Smith and Mrs Jo Carter for their practical help.

I would also like to thank Professor Randy Mrsny for his valuable suggestions on the siRNA work; Edward Carter for help with the practical experiment and James Heward for the gene work.

I also thank all to my dearest colleagues in the office 3.22, both past and present, for their friendly support and conversations. I would like to thank to Dr Rory Arrowsmith for support during my PhD as well as the proofreading of my thesis. I also would like to thank Nour Alhusein and Dr Supattra Rungsimakan for their friendly support that they gave me.

I am extremely thankful to the University of Bath for giving me the studentship and the Chinese government for the further sponsorship.

Last but not least, my greatest thanks for my family for all their unconditional love, support and encouragement.

Abstract

Heme oxygenase-1 (HO-1) is well known for being involved in antioxidant defence. BTB and CNC homology1 protein (Bach1) is involved in the transcriptional regulation of the HO-1 gene as a negative regulator. In human skin cells, HO-1 induction protects against UVA-induced cellular damage. Previous studies from this laboratory have found that during this process, suppressing the Bach1 level regulates HO-1 expression level. However little is known about whether repression of Bach1 would enhance HO-1 protection against UVA damage. In this study, we silenced Bach1 by specific siBach1 RNA and showed that Bach1 repression does not protect against UVA induced damage in cultured human skin fibroblasts. However, silencing of Bach1 in skin fibroblasts was shown to be involved in the process of UVA-induced ROS generation. We observed that UVA-induced ROS generation is independent of HO-1 induction. This led us to investigate further the mechanism by which UVA-induces ROS in cultured human skin cells; we targeted NADPH oxidase (NOX) as the major source of UVA-induced ROS generation in human skin cells, and showed that following UVA irradiation, NOX is activated to different extents in two cultured human skin cell lines (i.e. FEK4 cells and HaCaT cells). The possible involvement of different NOX proteins was then studied and the results showed that NOX1 and NOX4 both contribute to the NOX activation process but to different extents. NOX1 and NOX4 protein expression levels were also induced to different extents following UVA irradiation of FEK4 cells and HaCaT cells. The NOX general inhibitor, diphenylene iodonium (DPI), was used in this study to repress NOX, and we showed that this general inhibitor of the enzyme reduced ROS generation following UVA irradiation in human fibroblasts. This data is consistent with a previous study showing DPI inhibition of UVA-induced ROS generation in keratinocytes. However, using specific siRNA knock-down reagents, NOX1 and NOX4 were found to have only a limited contribution to the UVA-induced ROS generation process in human skin fibroblasts, a result consistent with the involvement of additional NOX proteins in this pathway.

Abbreviations

ATP	**Adenosine triphosphate**
APS	**Ammonium persulphate**
BSO	**Buthionine-S,R-sulphoximine**
bZip	**bZip basic leucine zipper**
BTB	**Broad complex, tramtrack, bric-a- brac**
Bach1/2	**BTB and CNC homology-1/2**
BSA	**Bovine serum albumin**
CNC	**Cap'n'collar**
CO	**Carbon monoxide**
CM-H_2DCFDA	**5-(and-6)-Chloromethyl-2',7'-dichlorodihydrofluorescein diacetate, acetyl ester**
dsRNA	**Double strand RNA**
DAPI	**4,6-Diamidino-2-phenylindole**
DMSO	**Dimethyl sulphoxide**
DPI	**Diphenylene iodonium**
DMEM	**Dulbecco's Modified Eagle's Medium**
DNA	**Deoxyribonucleic acid**
EMEM	**Earle's modified minimal essential medium**
EDTA	**Ethylenediaminetetracetic acid**
ES	**Endoplasmic reticulum**
FBS	**Foetal bovine serum**
FITC	**Fluorescein isothiocyanate**
FAD	**Flavin adenine dinucleotide**
FACS	**Fluorescence-activated cell sorting**
Fe	**Iron**
Fe^{2+}	**Ferrous iron**

Fe^{3+}	Ferric iron
GSH	Glutathione
GSSG	Glutathione disulphide (oxidised glutathione)
h	Hour/hours
s	Second/Seconds
HOCl	Hypochlorous acid
H_2O_2	Hydrogen peroxide
H_2O	Water
HO-1	Heme oxygenase 1
HO-2	Heme oxygenase 2
HO-3	Heme oxygenase 3
IL-1	Interleukin-1
Il-6	Interleukin-1
kJ/m^2	Kilo Joule per metre squared
Keap1	Kelch-like ECH-associated protein 1
LCR	Locus control regions
LPS	Lipopolysaccharide
mRNA	Messenger RNA
min	Minute
MTS	3-(4,5-dimethylthiazol-2-yl)-5-(3-carboxymethoxyphenyl)-2-(4-sulphophenyl)-2H-tetrazolium
MW	Molecular weight
MARE	Maf associated recognition elements
MAPK	Mitogen-activated protein kinase
Nrf2	NF-E2-Related factor 2
NADPH	Nicotinamide adenine dinucleotide phosphate
NOX	NADPH oxidase

NaOH	**Sodium hydroxide**
NF-E2	**Nuclear factor, erythroid-derived 2**
Nt	**Nucleotides**
O_3	**Ozone**
$O_2^{\cdot -}$	**Superoxide anion**
$^1O_2$	**Singlet oxygen**
O_2^{2-}	**Peroxide anion**
POZ	**Poxvirus, zinc finger**
PVDF	**Polyvinylidene difuoride**
PARP	**Nuclear poly-ADP-ribose-polymerase**
PBS	**Phosphate buffer saline**
PI	**Propidium Iodide**
PS	**Phosphatidylserine**
PMSF	**Phenylemethylsulphonyl fluoride**
PAGE	**Polyacrylamide gel electrophoresis**
RNA	**Ribonucleic acid**
RNAi	**RNA interference**
ROS	**Reactive oxygen species**
RNS	**Reactive nitrogen species**
RT	**Room temperature**
RISC	**RNA induced silencing complex**
$RO^{2\cdot}$	**Peroxyl**
$RO_{\cdot}$	**Alkoxyl**
γ-GC	**Gamma-glutamylcysteine**
GS	**Glutathione synthase**
SFM	**Serum free medium**
StRE	**Stress response elements**
sb	**Scrambled**

siRNA	**Small interfering RNA**
TEMED	**N,N,N',N'-tetramethylethylenediamine**
TGF	**Transforming growth factor**
TNF-α	**Tumour necrosis factor-α**
UV	**Ultraviolet**
UVR	**Ultraviolet rays**
UVA/B/C	**Ultraviolet A/B/C**
V	**Volts**
w/o	**With or without**
W/V	**Weight over volume**

Chapter 1 Introduction

1.1 Human skin

1.1.1 Human skin structure

Skin is responsible for various functions in the human body, such as absorption, secretion, protection by virtue of the barrier and sensitivity of thermal balance. Human skin is the most widely distributed organ and occupies the largest area of any one component of the human body. Since it is the first line of defence against the external environments of the human body, skin plays a crucial role in defending against various external toxic chemicals or physical factors which can induce damage and also acts as an important internal barrier in preventing water loss and maintaining temperature. Unlike the smooth surface perceived at a distance from the surface of the skin, the skin tissue is covered by grooves. The skin includes three major layers: epidermal layer, dermal layer, and subcutaneous tissue (Celleno and Tamburi, 2009).

1.1.2 Epidermal layer

The epidermal layer is the outer layer of the skin which separates the external environment from the skin. Its thickness varies from 0.5 mm of the thinnest area to 1.5 mm of the thickest area (Celleno et al., 2009). The epidermal layer is mainly keratinocyte cells which include: stratum basale, stratum granulosum and the outer layer, stratum corneum.

The function of keratinocytes is primarily to make the protein ‘keratin’; it is responsible for epidermal layer turnover since keratinocytes grow and die towards the external surface of the epidermal layer to keep the continual renewal of epidermis. Melanocytes are also an important component in the epidermal layer, in charge of producing melanin. Langerhans cells are situated just above the basal layer of the epidermis, and are involved in immune surveillance system (Celleno and Tamburi, 2009). Certain organs of the

human body contain Merkel cells such as finger tips and lips (Celleno and Tamburi, 2009).

Immediately under the epidermal layer is the basal membrane (epidermal-dermal junction) which makes up a complex structure to connect the epidermal crests and dermal papillae.

1.1.3 Dermis layer

Under the epidermal layer is the dermal layer of the skin. The dermal layer is much thicker than the epidermal layer (Evans et al., 2013). Dermal dendrocytes, mast cells and fibroblasts are the major cell types in dermal layer (Kanitakis, 2002). Fibroblasts synthesise fibres and they are the major cell type of the dermis, which includes two morphologically different sub layers known as the papillary and reticular dermis (Celleno et al., 2009). The reticular dermis contains collagen fibres and supports dermis structures to support the mechanical strength such as: collagen I and elastin (Evans et al., 2013). Furthermore, macrophages and lymphocytes are distributed all over the dermis.

1.1.4 Hypodermal layer

In the deepest layer of skin, is the hypodermal layer. The main cell type of this layer is the adipocyte. The hypodermal layer contains fat and is important in the storage of energy and the regulation of temperature (Kanitakis, 2002).

1.2 UVA

1.2.1 History of ultraviolet radiation

The word ultraviolet (UV), meaning "beyond violet", originated from the Latin word ultra, meaning beyond, and violet is the colour of the shortest wavelengths of visible light. The wavelengths of ultraviolet (UV) light are shorter than visible light but longer than X-rays. The discovery of solar UV radiation was a gradual process which spanned three centuries (Hockberger, 2002). Salsa made an observation in 1614 that sunlight turns silver nitrate crystals black. In 1801, Ritter noticed that the invisible rays beyond the violet end of the spectrum were more effective on dark silver chloride soaked paper, thus he named them “deoxidising rays”. The terms ultraviolet and infrared radiation were eventually used (Hockberger, 2002). After this, the term “chemical rays” was adopted and became popular throughout the 19th century. Many studies on chemical rays and their ability to stimulate chemical reactions were undertaken. In 1865, Maxwell proposed the theory that “the light and sound are part of larger spectrum of energy with wave-like properties” (Hockberger, 2002). Also, he named them “electromagnetic waves”. In the early 20th century, some new discoveries in photochemistry and photophysics helped the understanding of the theoretical behaviour of electromagnetic radiation.

In 1900, Planck proposed that electromagnetic radiation is comprised of packets of energy which were definite "quanta”, and then, Bohr discovered that electrons absorb light energy and also re-emit it at the wavelengths corresponding to the electron’s energy. Schrödinger suggested a theory of wave mechanics that treated electrons as waves rather than particles.

1.2.2 Main types of UV radiation

The electromagnetic spectrum of ultraviolet light can be subdivided in a number of ways. The draft ISO standard on determining solar irradiances (ISO-DIS-21348) describes the following ranges (Table 1):

Table 1 UV radiation types

Name	Abbreviation	Wavelength (nm)
Extreme	EUV	10-121
Vacuum	VUV	10-200
Far	FUV	122-200
Ultraviolet C	UVC	100-280
Middle	MUV	200-300
Ultraviolet B	UVB	280-315
Near	NUV	300-400
Ultraviolet A	UVA	315-400

Biologist use the term “UVC” to describe the ultraviolet radiation with wavelengths below 280 nm and this radiation is absorbed by the ozone layer. UVA (solar region between 315 and 400 nm) penetrates window glass and causes physiological effects on organisms. The UVB region of the solar spectrum is between that of UVC and UVA, and is believed to be the major region responsible for the deleterious effects of sunlight on living organisms. The ozone layer of the Earth blocks most solar UV radiation in the UVB and UVC region because they are strongly absorbed by the ozone layer and other molecules in the atmosphere. As a result, UVA contributes most of the ultraviolet radiation that reaches the surface of the earth.

1.2.3 Harmful effects of UVR

In humans, skin is the main organ exposed to UV radiation and long term exposure to solar UV radiation (UVR) may cause harmful effects on the human body. A report in 1928 by Findlay described that skin tumours developed in depilated albino mice exposed to UV rays for 8 months from a quartz Hg vapour lamp (Hockberger 2002). Tyrrell (1995) confirmed that UVA may cause more levels of cellular damage in human skin tissue than UVB radiation (Tyrrell, 1995). UVA penetrates deeply into human skin and, like UVB, it can cause sunburn. UVA generates highly reactive chemical intermediates such as hydroxyl and oxygen radicals, which in turn can cause damage indirectly.

1.3 Reactive oxygen species (ROS)

With two unpaired electrons the ground state of oxygen is the most stable. Oxygen can act as an oxidant, and singlet oxygen is a more reactive state that can be achieved by insertion of energy above the ground state of oxygen; singlet oxygen is a non-radical since it has both paired electrons (Fukuto et al., 2012). However, when a single electron is added to ground state oxygen, a superoxide radical ($O_2^{\cdot-}$) forms (Scheme 1). A peroxide anion (O_2^{2-}) forms when an additional electron is added to a superoxide radical; in the presence of two protons, hydrogen peroxide (H_2O_2) is then formed, when two electrons and two protons are added to hydrogen peroxide, the product is water (H_2O) (Fukuto et al., 2012; Miller et al., 1990).

$$O_2 \xrightarrow{1e^-} O_2^{\cdot-} \xrightarrow{1e^-} O_2^{2-} \xrightarrow{2H^+} H_2O_2 \xrightarrow{2e^-,\,2H^+} 2H_2O$$

Scheme 1. The major pathway of reactive oxygen species formation.

Reactive oxygen species (ROS) refer to a group of oxygen derived small molecules, which include radicals: peroxyl ($RO_2^{\cdot}$), alkoxyl ($RO^{\cdot}$); and also non-radicals that can be easily converted to radical molecules such as: hypochlorous acid (HOCl), ozone (O_3), singlet oxygen ($^1O_2$), and hydrogen peroxide (H_2O_2) (Guerin et al., 2001; Kodama, 1988).

Many findings revealed that ROS are involved in the host defence, and additional research on ROS indicated that they are widely involved in the regulation of many reversible physiological processes (Nose, 2000; Pourova et al., 2010). In normal aerobic systems, ROS are short-term and continuously generated small molecules. However, once excessive ROS have been generated, they interact with cellular lipids, membranes, proteins and nucleic acids to damage or alter the function of these molecules. Thus, ROS have been considered as a major source of damage in various biological organisms (Kohen, 1999). During these processes, $O_2^{\cdot-}$ reacts with a single proton to produce $HO_2^{\cdot}$, Which is more reactive than $O_2^{\cdot-}$. It can initiate lipid peroxidation,

with most of $O_2^{\cdot-}$ coming from the membrane bound system, thus either $O_2^{\cdot-}$ or $HO_2^{\cdot}$ could cause damage to cells since $O_2^{\cdot-}$ is highly reactive (Harman, 1956). $O_2^{\cdot-}$ can also reduce antioxidant enzyme activity, examples of which are catalase, ribonucleotide reductase and glutathione peroxidase (Harman, 1956). As a superoxide derived species, peroxynitrite is mostly produced by a fast reaction between $O_2^{\cdot-}$ and $NO^{\cdot}$.

1.3.1 Cytotoxicity of ROS

Excessive ROS can induce cytotoxicity including both apoptosis and necrosis (Matsuzawa and Ichijo, 2008). ROS are considered to be involved in programed cell death by activating a number of signalling pathways (Jacobson, 1996). For example, apoptosis signal-regulated kinase 1 (ASK1) can be activated in stress conditions by generating ROS (Tobiume et al., 2001). Studies have shown that ROS play an important role in the process of TNF-α induced cytotoxicity in murine fibrosarcoma cells (Goossens et al., 1995). In a neuron-degeneration system, Mitochondria–derived ROS can induce oxidative stress which then leads to the cytochrome C release, caspase3 activation and then finally results in apoptotic cell death (Honig and Rosenberg, 2000). Oxidative stress induced by high glucose leads to activation of various signal pathways that lead to apoptosis in vitro: P38, mitogen-activated protein kinase (MAPK) was activated in podocytes; Bax (Bcl-2 associated X) protein was increased in renal epithelial cells (Wagener et al., 2009).

1.3.2 Oxidative stress

As described above the term ‘oxidative/nitrosative stress’ refers to a serious imbalance of ROS/Reactive nitrogen species (RNS) production and antioxidants (Harman, 1956). ROS induced oxidative stress can provide various type of cellular and molecular damage (DNA modification, lipid peroxidation, protein damage and induction of inflammatory cytokines) which

are involved in human skin diseases including cancer (Briganti and Picardo, 2003). Oxidative stress may result from diminished antioxidant levels or increased production of ROS/RNS (Harman, 1956). Oxidative stress can be induced by both free radicals (superoxide anion radicals, nitric oxide radicals, hydroxyl radicals and trichloromethyl radicals) non-radical oxidants (hydrogen peroxide, peroxynitrite and disulphides) and non-radical thiol-reactive chemicals (Jones, 2008).

Although there was some debate about the term 'free radicals', the simple definition of free radicals refers to 'a species that has one or more unpaired electrons which are able to exist independently' (Halliwell and Gutteridge, 1999). The unpaired electron could become highly reactive. Radicals can form in several ways: either when a paired electron loses one electron or adding a single electron to a non-radical. Additionally, radicals form when homolytic or heterolyic fission occurs between covalent bonds (von Sonntag, 1987). Harman (1956) developed the first landmark theory claiming that free radicals contribute to the aging process.

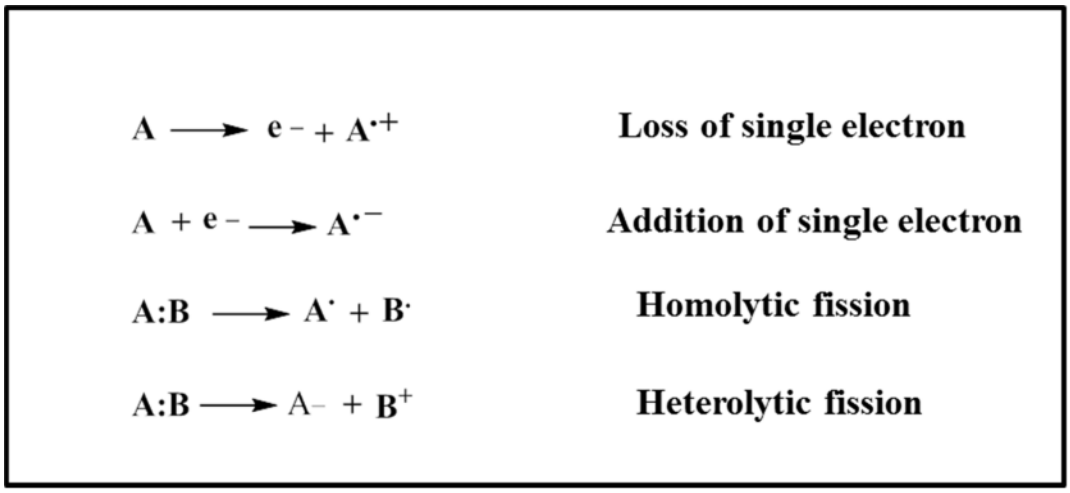

Figure 1 Several pathways of radical formation.

As free radicals are small and diffusible and have an unpaired electron, they have been considered as a major factor in damaging macromolecules. In biological systems, oxidative stress induced damage is more related to the free radical initiation procedure since free radical scavenging by antioxidant enzymes and chemicals (such as vitamins E&C) can completely prevent the free radical chain reaction when the antioxidant concentration is high enough (Jones, 2008).

1.3.2 Consequences of oxidative stress

In normal physiological environments, cells often incur a mild oxidative stress. To maintain the balance of oxidants and antioxidants, the mild oxidative stress can induce a cellular protective response such as control of gene expression to increase antioxidant defence (Godic et al., 2014). However, when the antioxidant cannot maintain the balance of the oxidants, cellular injury may occur.

Intracellular antioxidant enzymes are involved in prevention of oxidative stress and protect against ROS-induced potential cellular damage. These enzymes include glutathione peroxidase, catalase and superoxide dismutase. Glutathione peroxidase reduces hydrogen peroxide to water. Superoxide dismutase reduces super oxide anions to hydrogen peroxide. When the oxidant production is more than the antioxidants potential present, imbalance occurs. Oxidative stress is therefore also defined as excess levels of oxidants over antioxidants within a physiological system (Thannickal and Fanburg, 2000). The important consequence of oxidative stress is that the redox state changes to a more oxidising status for components of biological systems (membrane, nucleus and mitochondria) (Drummond et al., 2011).

Overall, oxidative stress can result in either adaptation or cellular damage. In cells, oxidative stress causes various types of damage to biomolecules

including lipids, proteins and DNA (Godic et al., 2014; Kehrer, 1993; Narendhirakannan and Hannah, 2013a). The sequence of injury differs depending on the type of oxidising agent. For example, double-stranded DNA breaks occur before detectable lipid peroxidation or protein damage in H_2O_2 damaged mammalian cells (Schraufstatter et al., 1986). Enzymes and receptors as well as transporter proteins are important targets in the early stages of oxidative stress damage to cells.

Since ROS are capable of modifying DNA chemically, they are therefore carcinogenic (Han and Chen, 2013). When exposed to molecular oxygen, especially in the presence of metal ions, a series of free radical oxidation chain reactions arises and will damage the cell membrane component of polyunsaturated fatty acids. This is also known as lipid peroxidation (Harman, 1956). Lipid peroxidation was originally defined as the oxidative deterioration of polyunsaturated lipids (composed of polyunsaturated fatty acids made up of two or more carbon-carbon double bonds) (Nowak, 2013). Lipid peroxidation begins with any species which can abstract a hydrogen atom from the methylene (CH_2) group. Hydroxyl radicals are able to attack lipids to directly initiate lipid peroxidation, $OH\cdot$ also interacts with surface proteins such as glycoproteins (Niki, 2009; Yin et al., 2011). When the lipid peroxidase is activated, carbon radicals form and then react with O_2 to initiate a chain reaction (Niki, 2014). It has been proven that proteins generate carbonyls and peroxides on the peptide backbone when under irradiation and that the selective amino acid side residue chains, amino acid peroxides became unstable as a result of heating or when transition metal ions are added (Denu and Tanner, 1998).

Oxidative stress may cause various cellular damage pathways for example, cell death, and ion status disruption as well as DNA damage. Severe oxidative stress in cells may cause suicide responses due to a failure of adenosine triphosphate (ATP) production as a result of depletion of cellular nicotinamide adenine dinucleotide/nicotinamide adenine dinucleotide phosphate

($NAD^+/NADP^+$) level by excessive poly (ADP-ribose) polymerase (PARP) activation (Schraufstatter et al., 1986). Necrosis and apoptosis also occur under severe oxidative stress. Necrotic cells can release iron and copper ions, superoxide releases iron from ferritin proteins; peroxide also releases iron by heme protein degradation; peroxynitrite can interact with iron-sulphur proteins and then release iron (Narendhirakannan and Hannah, 2013b; Tandara and Salamunic, 2012).

Oxidative stress can cause an increase in free intracellular Ca^{2+} levels and then activate certain signal transduction pathways (Booth et al., 2011). The consequence of this is membrane blebbing which arises from cytoskeleton disruption. Apart from deregulation of Ca^{2+} levels, oxidative stress also interferes with iron in cells (Aroun et al., 2012).

ROS lead to DNA damage by direct chemical attack and by indirect pathways, $OH\cdot$ interacts with DNA to generate various products through attacking sugars, purines and pyrimidines (Breen and Murphy, 1995).

1.3.3 Origin of ROS in cells

ROS are mainly generated by cellular metabolism pathways such as NADPH oxidase, xanthine oxidase and oxidative phosphorylation or external stimuli which includes UVA radiation (Brieger et al., 2012; Guerin et al., 2001).

There are two major types of intracellular sources of ROS by metabolism pathways: enzymatic and non-enzymatic sources. The smooth endoplasmic reticulum (ER) contains enzymes which catalyse harmful metabolic products from lipid or membrane soluble drugs. For example, cytochromes P-450 oxidises unsaturated fatty acid and reduces molecular oxygen to superoxide anion or hydrogen peroxide (Thannickal and Fanburg, 2000). Peroxisomes are considered to be a major source of total cellular hydrogen peroxide production

(Boveris et al., 1972). Intracellular soluble enzymes also generate ROS through the catalytic cycling procedure. These enzymes include: xanthine oxidase, aldehyde oxidase, flavoprotein dehydrogenase (McKelvey et al., 1988). Peroxidase, nitric oxide synthase and tryptophan dioxygenase can also generate superoxide radicals (Harman, 1956). During the respiration process, NADPH oxidase can produce ROS (Brieger et al., 2012). The non-enzymatic source include the single electron transfer from flavins or iron clusters (Turrens, 2003).

1.3.4 UVA induced ROS in skin

As an oxidative stress inducing agent, UVA radiation is a major factor in generating excessive ROS in human skin to cause an imbalance between antioxidants and oxidants. This will potentially lead to pathological results in the skin (Bickers and Athar, 2006).

As one of the most important organs in human body, the human skin serves as a biological barrier that protect against external insults. Skin is the most widely and frequently exposed organ to environmental agents such as physical and chemical pollutants and is therefore much easier to damage than other human body components. These agents include: oxygen, chemicals applied in daily life, UV light, bacteria and excretion of sweat (Gutteridge et al., 1985a; Narendhirakannan and Hannah, 2013a). Transition metal ions (such as iron and copper) in sweat are potentially involved in free radical reactions. The cytotoxic products of these reactions can also aid the growth of bacteria (Gutteridge et al., 1985b).

The major insult that skin normally faces is UV light. Despite the beneficial effect that UV light can have such as Vitamin D synthesis, hormone and mood regulation (Polefka et al., 2012), too much exposure to UVR causes either

acute or chronic; direct or indirect damage to skin cells (Matsumura and Ananthaswamy, 2004). For direct exposure, cellular molecules which absorb UV light may undergo structural modifications, with resultant functional damage including to the DNA. This can occur by disruption of DNA repair or replication or a gene mutation (p53) which may lead to cell cycle dys-function and apoptosis (Trouba et al., 2002). Indirect exposure happens when photosensitisers (porphyrins, flavins) in the skin absorb a photon from UV radiation and are excited to a higher energy state; the excited photosensitisers are then capable of undergoing electron transfer reactions to form reactive oxygen species. This leads to cellular oxidative stress and damage (Wondrak et al., 2006).

With reference to acute damage, exposure to UVR causes skin roughness, skin redness (Masaki, 2010) and oedema (Kevin J. Trouba). Since the skin is constantly exposed to the oxidative stress caused by UVR, oxidised skin lipids/membranes and protein could lead to various skin pathologies. UVA radiation can cause cellular DNA damage by indirect mechanisms which involves cellular chromophores which can act as endogenous photosensitisers (Kielbassa et al., 1997; Tyrrell, 1990). Various oxidative DNA modifications such as strand breaks, sites of base loss and DNA-protein cross links are also generated by UVA (Kielbassa et al., 1997).

In human skin, the chronic exposure of UV leads to photo ageing and carcinogenesis (Tyrrell and Reeve, 2006). Long-term exposure to sunlight is the main risk in development of human skin cancers including basal or squamous cell carcinomas and melanoma. UVA penetrates deeply into the dermis, and acts as an oxidising carcinogen in mice (Tyrrell and Reeve, 2006). These pathological events are both cumulative with UV dose and wavelength dependent. Work from this laboratory has shown that labile iron (Pourzand et al., 1999) and free heme (Kvam et al., 1999b) are released as a result of UVA irradiation of cells. UVA radiation can generate various active oxygen intermediates. It produces peroxides, hydroxyl radicals, superoxide anions

and singlet oxygen from cellular chromophores; the major biological effects of UVA radiation depend on oxygen and can be modified by antioxidants (Tyrrell and Reeve, 2006).

1.4 NADPH oxidase (NOX)

1.4.1 NADPH oxidase family

Nicotinamide adenine dinucleotide phosphate (NADPH) oxidase refers to a trans-membrane protein family which transfers electrons and was first discovered in phagocytes. A gene coding the subunit of phagocyte NADPH oxidase (NOX) was found in the 1980s; namely, $gp91^{phox}$, and is also known as NOX2. A wide range of NADPH oxidases were later found in other cell types such as fibroblasts, tumour cells and vascular smooth muscle cells (Griendling et al., 1994; Meier et al., 1991). Rossi and Zatti (1964) first proposed that NADPH oxidase was responsible for the respiratory burst. NADPH oxidase transfers electrons across biological membranes via flavin adenine dinucleotide (FAD) to oxygen (Figure 2). The two heme groups in NOX function as an electron donor to reduce oxygen to superoxide (Paletta-Silva et al., 2013).

The NADPH oxidase family includes seven isoforms: NOX1, NOX2, NOX3, NOX4, NOX5, Dual oxidase 1 (DUOX1) and DUOX2. Furthermore, six more subunits have been recognised, which include $p47^{phox}$ and NOXO1 as two organizer subunits; $p67^{phox}$ and NOXA1 as two activator subunits and DUOXA1 and DUOXA2 as DUOX-specific maturation factors (Bedard and Krause, 2007). NOX family activation requires several additional subunits and regulatory proteins: $p22^{phox}$; NOXO1 (organiser subunits), $p47^{phox}$; $p67^{phox}$ and NOXA1 (activator subunits); $p40^{phox}$; Rac GTPsae.

All of the NOX isoforms have the common structure of six trans-membrane domains (Figure 2). The central trans-membrane domains contain two histidine residues and the heme-binding region. Both a conserved FAD binding site and a NADPH binding site are located in the cytoplasmic COOH

terminus. It was proposed that NOX transfers electrons firstly from NADPH to FAD, then to heme and finally to oxygen (Bedard and Krause, 2007).

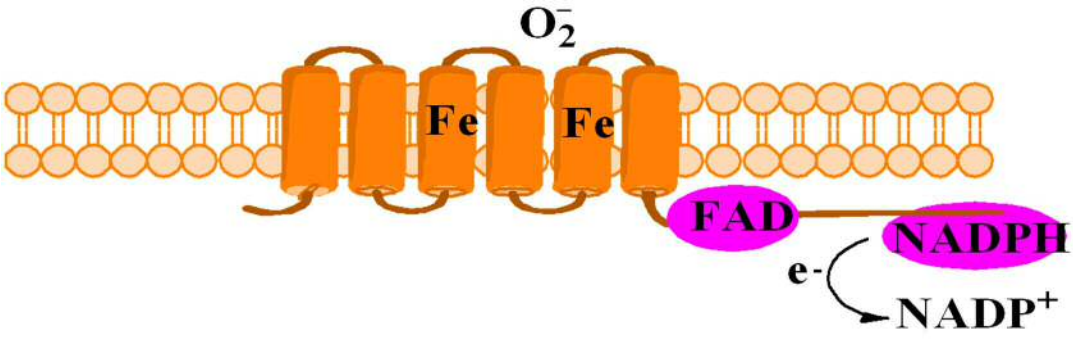

Figure 2 NADPH oxidase structure.

1.4.2 The NOX family in physiological and pathological process

The NOX family are believed to be essential in normal physiological process, such as, cell growth and apoptosis (Brown and Griendling, 2009). Different isoforms of the NOX family play different roles and dysfunction of the isoforms may induce various pathologies (Table 2).

NOX1

NOX1 was first purified from colon epithelial cells (Paletta-Silva et al., 2013). Later, NOX1 expression was found in various tissues and cell lines including retinal pericytes, prostate, endothelial cells and vascular smooth cells (Bánfi et al., 2000; Bedard and Krause, 2007; Suh et al., 1999). NOX1 performs varying physiological roles in different organs of the body including the cardiovascular system, the nervous system, the lung and the colon (Katsuyama et al., 2012). NOX1 derived ROS may plays an important role in the initiation of inflammatory bowel disease (Paletta-Silva et al., 2013). The overexpression of NOX1 in nude mouse generates ROS for tumorigenic and angiogenic functions indicating that dys-function of NOX1 in the colon may induce carcinogenesis (Rokutan et al., 2006; Suh et al., 1999).

NOX2

NOX2 was the first member of the NOX family to be identified in phagocytes, with a wider distribution found later in tissues such as colon, ovary, prostate, placenta and small intestine (Cheng et al., 2001). NOX2 is believed to be involved in the host defence system in microorganisms (Rada et al., 2008) and in hypertension (Paletta-Silva et al., 2013). Absence of NOX2 or its subunit causes chronic granulomatous disease (CGD) (Brown and Griendling, 2009).

NOX3

NOX3 was found to play a critical role in organ development (Paletta-Silva et al., 2013). NOX3 activation requires $p22^{phox}$ subunit, $p47^{phox}$ or NOXO1, $p67^{phox}$ or NOXA1 and Rac1 (Banfi et al., 2004a; Nakano et al., 2007; Ueyama et al., 2006). NOX3 is strongly expressed in the inner ear, skull bone and brain (Banfi et al., 2004a). Foetal spleen (Kikuchi et al., 2000) and kidney (Bedard and Krause, 2007) also express NOX3.

NOX4

High levels of NOX4 have been found in kidney (Geiszt et al., 2000) and the enzyme is also expressed in skin cells including fibroblasts (Dhaunsi et al., 2004), keratinocytes (Chamulitrat et al., 2004), and melanoma cells (Brar et al., 2002) as well as endothelial cells (Hu et al., 2005), osteoclasts (Yang et al., 2001), smooth muscle cells (Ellmark et al., 2005), hematopoietic stem cells (Piccoli et al., 2005) and neurons (Vallet et al., 2005). NOX4 activation does not require the cytosolic subunit for activity, but it does requires $p22^{phox}$ (Martyn et al., 2006). Some studies show that NOX4 might be constitutively activated, although this proposal is debated (Bedard and Krause, 2007). NOX4 is induced by various factors such as shear stress, hypoxia, ischemia and reticulum stress (Bedard and Krause, 2007).

NOX5

NOX5 was characterised by two groups in 2001 (Banfi et al., 2001; Cheng et al., 2001). NOX5 differs from other NOX isoforms by containing a Ca^{2+} binding site on the intracellular NH_2 terminal and also an EF-hand domain (Banfi et al., 2004b). Importantly, NOX5 doesn't need an activation subunit as it is a calcium related homologue (Geiszt et al., 2000; Katsuyama et al., 2012). NOX5 is not glycosylated and can only catalyse reactions with NADPH and not NADH. The activation of NOX5 does not require any organiser or regulatory subunits. Instead, NOX5 activation is regulated by the cytoplasmic Ca^{2+} concentration (Banfi et al., 2001; Banfi et al., 2004b).

DUOXs

The DUOXs (DUOX1 and DUOX2) were first found in the thyroid gland (Dupuy et al., 1999), and function as part of the Golgi apparatus processing procedure (Morand et al., 2004). DUOX enzymes also contain a membrane spanning region and a peroxidase-like domain (Katsuyama et al., 2012).

Although DUOX's function as a peroxidase has not yet been fully characterised, a recent study suggests the DUOXs primary product is superoxide (Ameziane-El-Hassani et al., 2005). DUOX1 can be induced by IL-13 and IL-4 while DUOX2 can be induced by interferon-Ɣ (Harper et al., 2005).

Table 2: Characteristics of NOX isoforms

NOX isoforms	Main Location	Other distribution	Related Dys-function
NOX1	Colon	Endothelium, uterus, prostate, osteoclasts, retina, placenta, smooth muscle.	Hypertension, inflammation, lung injury.
NOX2	Phagocytes	Lymphocytes, neurons, endothelium, smooth muscle, neurons,	Heart failure, cardiac hypertrophy, Alzheimer's disease, Parkinson's disease,
NOX3	Inner ear	Skull bone, brain	Loss of hearing. diabetes
NOX4	Kidney, Blood Vessels	Endothelium, smooth muscle, skin (fibroblasts, keratinocytes, melanoma cells), neurons.	Renal cancer,
NOX5	Testis, Lymph Node	Endothelium, smooth muscle, uterus, stomach	Prostate cancer
DUOX1	Thyroid	Testis, airway epithelia	Host defence
DUOX2	Thyroid	Airway epithelia, rectal glands,	Host defence, hypothyroidism

Modified from Bedard and Krause (2007)

1.4.3 Regulator proteins of NOX

a. p22^{phox}

The 22 kDa membrane protein, p22^{phox} is not glycosylated and it dimerises with NOX2 in a 1:1 ratio (Parkos et al., 1987). The structure contains two transmembrane domains with both the NH_2 terminus and the COOH terminus in the cytoplasm (Burritt et al., 1998). p22^{phox} was shown to translocate coupling of NOX1 (Laude et al., 2005), NOX2 (DeLeo et al., 2000), NOX3 (Kawahara et al., 2005) and NOX4 (Ambasta et al., 2004) for activation, thus the major function of p22^{phox} is to stabilise NOX proteins and organizer proteins.

b. Organiser subunits

NOXO1 and p47^{phox} (namely, NOXO2) both have phox domains through which they can cooperate with phospholipids. They also both have an SH-3 domain for interacting with p22^{phox} through the proline rich COOH terminus (Leto et al., 1994). These two organiser proteins are responsible for combining with the activator proteins to activate NOX1 or NOX2.

c. Activator subunits

NOXA1 and p67^{phox} (namely NOXA2) are both unglycosylated, cytoplasmic proteins containing a SH-3 domain on the COOH terminus which interact with the proline repeats on NOXO1 and NOXO2 and tetratricopeptide repeats at the NH_2 terminus that interact with Rac. The structure of NOXA1 differs from NOXA2 by lacking a central SH-3 domain and the PB1 domain. This means it cannot interact with p40^{phox}. NOXA1 can combine with NOX1, NOX2 and NOX3 via the activating domain (Takeya et al., 2003).

d. p40^{phox}

The p40^{phox} protein contains a SH-3 domain, a PX domain and a PB1 domain. It is only stable when bound to NOXO1, and is important in NOX2 regulation; however it is not necessary for NOX2 activity (Bedard and Krause, 2007).

e. Rac GTPase

There are three Rac GTPase homologous, Rac1, Rac2, and Rac3 domains. Rac GTPase engages in NOX2 regulation of phagocytes (Bedard and Krause, 2007). The Rac protein is also involved in NOX1 activation (Miyano et al., 2006), but it is still debated whether they are involved in NOX3 or NOX4 regulation.

In summary, the NOX proteins require various coupling subunits for activation (e.g. NOX1: Rac, p22^{phox}, NOXO1/p47^{phox} NOXA1/p67phox; NOX2: Rac, p22^{phox}, p40^{phox}, p47^{phox}, p67^{phox}; NOX3: Rac, p22^{phox,} NOXA1/p67^{phox}, NOXO1/p47^{phox}; NOX4: p22^{phox}; DUOX1: DUOXA1; DUOX2: DUOXA2).

1.4.4 NADPH oxidase and ROS

NOX has been considered a major source of ROS generation. NOX derived ROS include superoxide and hydrogen peroxide. NOX derived ROS can have a big impact on major cellular process as they can regulate signalling pathways. Neutrophil NOX generates a large amount of superoxide anion as part of the oxidative burst system. Physiological and pathophysiological functions that could be influenced by NOX derived ROS include host defence and inflammation, cell signalling, apoptosis, cell proliferation, oxygen sensing protein cross-linking, angiogenesis, ECM regulation and cytokine gene expression (Bedard and Krause, 2007).

There is evidence that NOX is a major source of oxidative stress in ischemic injury of the cardiovasculature (Kleikers et al., 2012). The first recognition of NOX2 as responsible for ROS generation was in phagocytes (Royer-Pokora et al., 1986; Teahan et al., 1987). Later on, the other NOX proteins were gradually found to be involved in ROS generating events.

In cells from patients with impaired ROS generation, it was found to be a result of NOX4 reduction (Park et al., 2005). Quantitative real-time PCR results in human dermal fibroblasts revealed that 3-deoxyglucosone (3-DG) collagen induced ROS generation is dependent on NOX4 overexpression and fibroblasts pre-treated with the NOX general inhibitor apocynin also had reduced ROS generation (Loughlin and Artlett, 2010). In hairless mouse skin, UVB induced NOX4 expression (Rahman et al., 2011). Silencing the NOX4 gene augments melanin formation and largely decreased the basal and alpha melanocyte stimulating hormone (α-MSH) induced ROS generation in B16 melanoma cells (Liu et al., 2012). In HaCaT cells, gene knock-down of either NOX1 or NOX4 decreased production of ROS during early stages of wound healing. This indicated that NOX1 and NOX4 are involved in the NOX derived ROS production in HaCaT cells (Nam et al., 2010). Conversely, in vascular cells, NOX4 is considered to have a protective role (Schroder et al., 2012).

Silencing of NOX4 in human dermal fibroblasts abolished dehydroascorbic acid (DHA)-induced ROS generation (Rossary et al., 2007).

1.4.5 NADPH oxidase in skin

It has been observed that in skin cells ROS generation can be induced by various agents including ultraviolet light (Beak et al., 2004) and phorbol esters (Steinbrenner et al., 2005). More interestingly, both were inhibited by NOX inhibitors and that may indicate that NOX is involved (Meier et al., 1991). In keratinocytes, ROS generation in response to UV light was inhibited by a NOX inhibitor, indicating that NOX may be involved in this event (Beak et al., 2004). Fibroblasts have also been shown to generate ROS via NOX by various factors for example: very-long-chain fatty acids, insulin, IL-1 and, platelet-derived factors (Bedard and Krause, 2007).

1.4.6 NADPH oxidase and HO-1

Given that NOX contains heme as a prosthetic group, it is reasonable to hypothesise that there may be some links/interactions between HO-1 and NOX. Both in vitro and in vivo, induction of HO-1 in macrophages both decreases NOX activity and superoxide anion release. It is proposed that breakdown of heme upon HO-1 induction may be the mechanism by which HO-1 influences NOX activity and could explain the protective role of HO-1 induction during oxidative stress (Taille et al., 2004). Similar results were found in apolipoprotein E–deficient mice (Datla et al., 2007), where HO-1 induction decreased NOX activity and superoxide generation. Bilirubin also decreased NOX generated superoxide induced by oxidative stress in human neutrophil-like HL-60 cells (Datla et al., 2007).

1.5 Cellular antioxidant defence

In response to excessive ROS conditions, our body engages antioxidant protection defense systems (Gomes et al., 2012). The antioxidant defense pathways are normally through scavenging the ROS and interaction with ROS products (Godic et al., 2014).

Antioxidants include two major categories, either non-inducible or inducible by oxidising agents (e.g. UVA).

The non-inducible antioxidants include enzymatic and non-enzymatic. Enzymatic antioxidants include catalase, glutathione peroxidase, superoxide dismutase and thioredoxin (Cheeseman and Slater, 1993; Holmgren, 1985). These antioxidant molecules have strong free radical scavenging properties; non-enzymatic antioxidants include vitamin E, vitamin C, glutathione, uric acid, and ubiquinol (Pandel et al., 2013; Poljsak et al., 2013).

Among these two major categories, the antioxidants also distinguish as endogenous and exogenous. Asorbic acid, vitamin E and coenzyme Q10, belong to exogenous antioxidants. Glutathione peroxidase, superoxide dismutase and catalase belong to endogenous antioxidants (Pandel et al., 2013).

1.5.1 Heme oxygenase (HO)

UVA radiation causes damage as a result of ROS, which are induced by oxygen-dependent photosensitisation reactions (Reeve and Tyrrell, 1999). UVA can also induce genes encoding antioxidant proteins (e.g. glutathione peroxidase, superoxide dismutase etc.) which protect against the presence of ROS (Reeve and Tyrrell, 1999). In 1989, Tyrrell (Tyrrell and Pidoux, 1989) reported that a major 32 kDa stress protein, identified as heme oxygenase, was induced by UVA radiation (HO; EC 1.14.99.3) (Tyrrell and Pidoux, 1989). UVA radiation of human skin fibroblasts can cause induction of heme oxygenase messenger RNA (mRNA) and protein (Keyse and Tyrrell, 1987; Keyse and Tyrrell, 1989). It can also release heme, from microsomal heme-containing proteins which correlates with UVA-mediated HO-1 activation (Kvam et al., 1999a).

1.5.1.1 Heme

The term heme refers to a group of an iron chelated in a porphyrin ring; the porphyrin ring is known as protoporphyrin IX. The chelated iron is involved in the oxidation state when heme compounds are biological catalysts (Maines and Kappas 1977). There are three major kinds of biological heme, heme A, heme B and heme C. Heme B is the most common type. Hemes are commonly recognised as components of hemeoproteins.

1.5.1.2 Hemeoproteins

A hemeprotein is a metalloprotein which contains a heme group, either covalently or non-covalently bound to the protein itself. Hemeoproteins have several biological functions including diatomic gas transport, biological catalysis as enzymes and electron transfer.

1.5.1.3 Heme oxygenase structure and function

Heme oxygenase (HO) is a protein with the function of degrading heme. All studies have shown that HO is a distinct enzyme which can degrade heme. HO starts to degrade heme by binding to heme at a 1:1 ratio. It then converts heme to biliverdin, in this process oxygen and NADPH are required (Figure 3) (Tenhunen et al., 1968; Tenhunen et al., 1969). HO consists mostly of a helix in the folding domain. The substrate of heme is connected by the proximal helices and distal helices as a sandwich (Unno et al., 2007).

When reducing agents are present, heme oxygenase degrades heme into biliverdin, iron and CO. Each of the products has different properties. Biliverdin is then reduced by its reductase to bilirubin in mammals. Although bilirubin is considered to be an antioxidant, excessive amounts are harmful. Iron can also trigger lipid peroxidation (Unno et al., 2007). CO can participate in various biological functions such as: regulation of neuroendocrine (Pozzoli et al., 1994) and vascular tone (Kaide et al., 2001) and hemeorrhagic shock (Pannen et al., 1998). Fe^{2+} is a crucial metal in the Haber-Weiss reaction (Figure 4).

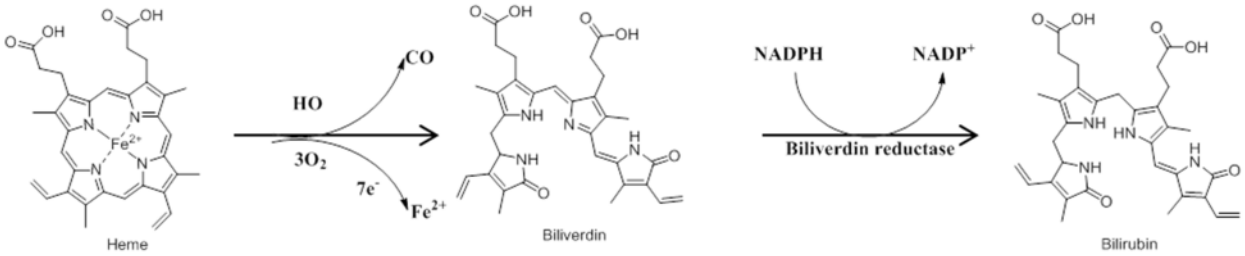

Figure 3 Mechanism of Heme oxygenase degrading heme (Modified from Unno et,al., 2007).

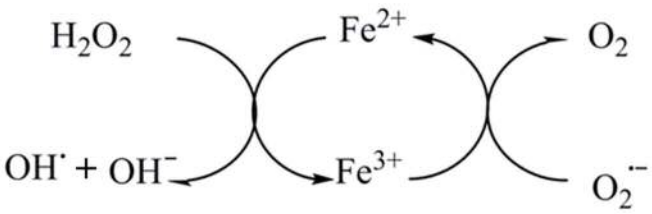

Figure 4 A diagram of the Haber-Weiss reaction.

1.5.1.4 Types of heme oxygenase and their functions

There are two major types of heme oxygenase (HO) known so far, which are HO-1, HO-2 (Maines et al., 1986; Trakshel et al., 1986). HO-1 and HO-2 were first identified in the microsomal fraction of rat liver (Maines et al., 1986). Among the two major types of heme oxygenase HO-1 and HO-2, HO-1 is inducible whereas HO-2 is not. HO-1 activity can be activated by environmental agents such as cadmium, hypoxia, UV light and heat shock (Khan and Quigley, 2011).

1.5.1.5 Mechanism of HO-1 protection

Oxidative stress can lead to cellular pro-oxidant protection (Applegate et al., 1991). Heme has been shown to be pro-inflammatory and produce ROS. Accumulation of free heme in cells can cause cell damage (Balla et al., 1991; Balla et al., 1993), so that removal of excess heme prevents potential cell damage. Since HO degrades free cellular heme to iron, CO and biliverdin, it serves a general function of maintaining cellular heme homeostasis. All the by-products of free heme degradation reaction may participate in cellular protection. Normally, CO is characterised as a poisonous gas, and it binds to hemeoglobin to deplete O_2. However, a crucial role of CO has been characterised in cellular protective process such as anti-inflammatory and anti-apoptotic responses (Brouard et al., 2000; Ryter et al., 2006). HO-1 has also been proposed to play an important role in several disease conditions which include: psoriasis, transplant rejection and alzheimer's disease (Raval., 2008).

UVA radiation strongly activates HO-1 in human skin fibroblasts (Keyse and Tyrrell, 1989). UVA therefore induces the heme-catabolising enzyme, heme oxygenase in mammalian skin. This enzyme is associated with a major anti-inflammatory response in several tissues and has been shown to protect against several disease states (Tyrrell and Reeve, 2006).

1.5.1.6 UVA-mediated HO-1 gene activation

It is important to understand the UVA-mediated regulation of HO-1 gene activation. Recent studies have shown that under normal physiological conditions, HO-1 expression is repressed by Bach1, and increased heme levels displace Bach1 from the promoter and allowing activators to bind to it (Sun et al., 2002).

The human HO-1 gene is located on chromosome 22q12; it has five exons and spans up to 14 kb (Hill-Kapturczak et al., 2003; Kutty et al., 1994). In 2003, Hill-Kapturczak demonstrated that the human HO-1 gene promoter has two upstream regions, one between -4.5 and -4.0, and another one between -9.1 and -4.5, which are required for activation of the HO-1 gene by heme (Hill-Kapturczak, Sikorski et al. 2003). Both these enhancer regions contain multiple stress responsive elements (StRE) and Maf recognition elements (MARE).

Under stress conditions, HO-1 is activated and, during this process, it has been shown that the NF-E2-related factor (Nrf2) along with the small musculoaponeurotic fibrosarcoma (Maf) protein form a heterodimer which can then bind to the MARE site of the HO-1 gene promoter (Sun et al., 2004). Nrf2 is stabilized in the cytoplasm by Keap1 protein under normal conditions, but is then released in response to the various stimuli. As a repressor protein, Bach1 competes with Nrf2 under normal conditions to form the heterodimer with Maf protein that binds to the MARE site on the HO-1 promoter (Figure 5A). Under stress condition (e.g. UVA irradiation), Bach1 binds to heme and is released from the MARE sites. This allows the activator protein (MafK/Nrf2) to bind to the same site for HO-1 gene activation (Sun et al., 2004) (Figure 5B).

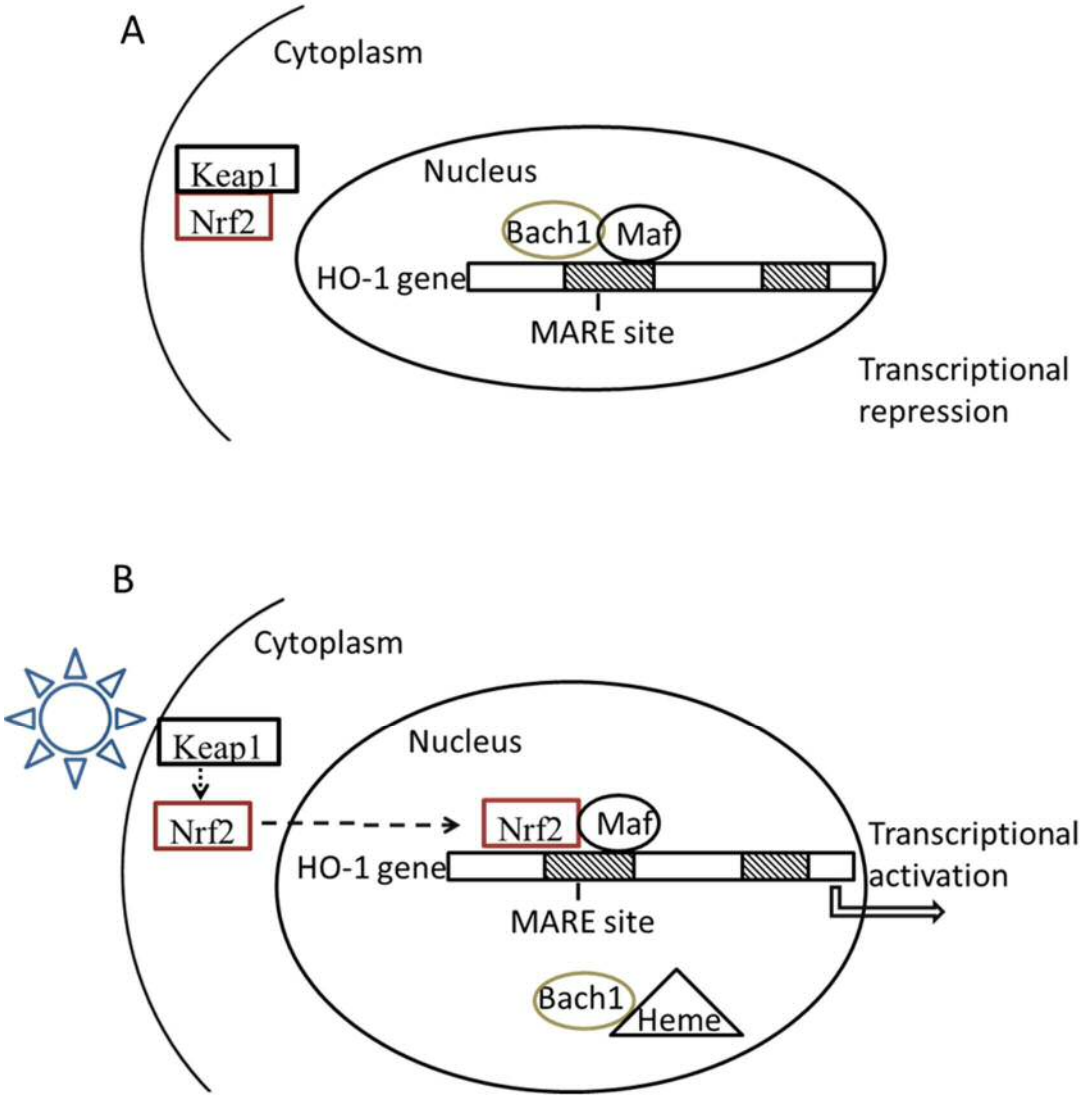

Figure 5 HO-1 gene regulations. A: Under normal conditions, Nrf2 is bound by Keap1 in the cytoplasm and Bach1 combines with Maf to occupy the MARE site of the HO-1 gene promoter and represses the transcription. B: Following UVA irradiation, free heme released by UVA binds to Bach1 and releases it's binding to the promoter. This allows Nrf2 to occupy the MARE site and activate HO-1 gene transcription.

1.5.2 Bach family

Basic leucine zipper proteins (bZip) are responsible for interactions with several different families of transcription factors through forming heterodimers. Such heterodimer formation controls gene regulation during the process of cellular organism development (Oyake et al., 1996b).

Transcriptional factor NF-E2 is one of the proteins containing the bZip subunit thereby providing it with DNA binding activity (Oyake et al., 1996b). NF-E2 consists of a large and a small bZip subunit (Andrews, Erdjument-Bromage et al. 1993). The large subunit belongs to the Cap'n'collar (CNC)-type bZip protein family, which is also named p45. The CNC family includes p45, NF-E2, Nrf1/LCRF1/TCF11 and Nrf2 (Caterina et al., 1994; Chan et al., 1993; Luna et al., 1994; Moi et al., 1994).

It has been proven that Bach protein belongs to the BTB (Broad complex–Tramtrack–Bric-abrac-Basic Leucine Zipper) transcription factors which can regulate certain genes and interact with small Maf family protein such as MafK, Maf F and Maf G, which are also bZip proteins (Oyake et al., 1996a) These complex heterodimers can therefore activate or repress gene transcription. The Bach family also contains a BTB domain (Oyake et al., 1996a; Zollman et al., 1994). Bach 1 and Bach2 were first identified as novel parts of the bZip family by Oyake and Itoh in 1996 (Oyake et al., 1996a).

1.5.2.1 Bach1

A study in Bach1 deficient mice showed high expression of HO-1 (Ochiai et al., 2008). Warnatz and Schmidt (Warnatz et al., 2011) recently reported that Bach1 interacts with genes involved in the process of oxidative stress as well as the cell cycle. Bach1 has also been shown to be engaged in apoptotic pathways and transport processes. The observation report about Bach1

binding to hyaluronan-mediated motility receptor, suggest that Bach1 is involved in cellular transport processes (Warnatz et al., 2011).

The Bach1 gene plays a crucial role in induction of HO-1 expression by UVA radiation (Raval., 2008). Tyrrell and Keyse (1989) have shown that in human skin fibroblasts, UVA irradiation strongly induced HO-1 transcription and activation. UVA radiation induction of Bach1 protein accumulation in human skin fibroblasts has also been reported (Raval et al., 2012). Bach1 deficient mice showed depression of oxidative stress induced pancreatic β-cell injury, and were susceptible to alloxan induced HO-1 induction (Kondo et al., 2013). Thus, it is reasonable to assume that a protective role of Bach1 may arise through HO-1 up-regulation. Zhong (2010) showed that Bach1 deficiency increased both basal and UVA-induced HO-1 expression in human HaCaT cells indicating that Bach1 is involved in UVA mediated HO-1 induction. In addition, silencing Bach1 reduced UVA-induced membrane damage in HaCaT cells (Zhong et al., 2010).

1.5.2.2 Bach2

Unlike Bach1, Bach2 is mainly distributed in neuronal cells and in B cells during differentiation (Rosbrook et al., 2012).

1.5.3 Glutathione

Glutathione (GSH) is distributed in most organisms and is essential for maintaining cellular protein thiol status. As a tripeptide structure, GSH is synthesized from the amino acids L-glutamate, L-cysteine and L-glycine (Glu-Cys-Gly) (Ehrlich et al., 2007). The function of glutathione is crucial to maintaining the cellular antioxidant/oxidant homeostasis as well as viability of cells (Fitzpatrick et al., 2012). GSH is one of the major cytosolic non-enzymatic antioxidants and scavenges free radicals (Ehrlich et al., 2007; Galano and Alvarez-Idaboy, 2011); including peroxynitrite and hydroxyl. It can also convert H_2O_2 to water. During this process, a GSH radical is formed, that would immediately be neutralized by binding to another GSH radical to form GSSG (Massaad and Klann, 2011). GSH reductase can covert GSSG back to the oxidized form GSH in the presence of NADPH (Fitzpatrick et al., 2012) (Figure 6). The disruption of intracellular glutathione levels will cause dys-regulation of the GSH/GSSG ratio, which in turn leads to a disrupted cellular ROS homeostasis (Johnson et al., 2012). The decreased GSH level was observed in various pathologies such as: acute lung disease, Parkinson's disease (Ehrlich et al., 2007), this reduction was believed to cause impaired ROS generation which consequently leads to related pathologies due to lack of the protection role of GSH against the impaired ROS generation.

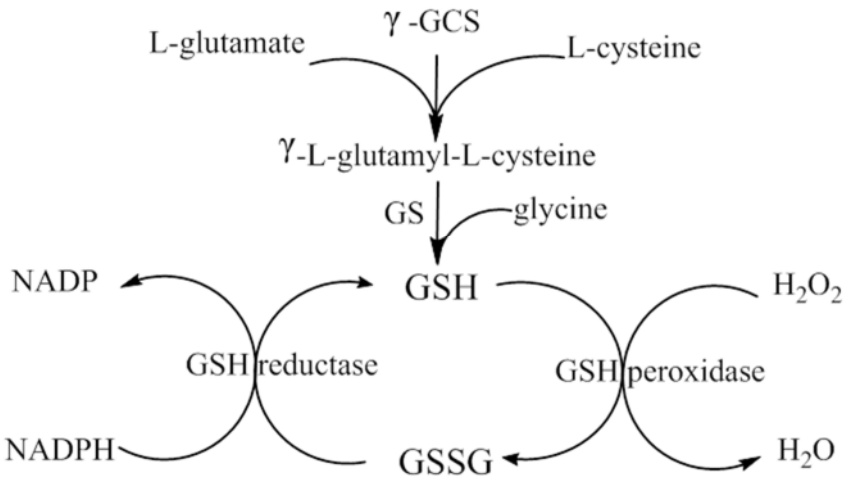

Figure 6 A diagram of the Glutathione (GSH) redox pathway. GSSG: reduced form of GSH, γ-GCS: gamma-glutamylcysteine synthase, GS: glutathione synthase.

The role of glutathione in UVA induced human skin damage has been examined in this laboratory, Tyrrell and Pidoux (1988) reported that glutathione depletion by D,L-buthionine-S,R-sulphoximine (BSO) in both skin fibroblasts and keratinocytes led to enhanced sensitivity to UVA irradiation. This suggests that glutathione functions as an antioxidant involved in protecting against UVA-induced human skin damage. In agreement with this, depletion of glutathione has been shown to increase the UVA-induced ROS level in HaCaT cells (Tobi et al., 2000). In contrast, if cellular glutathione levels are raised using NAC, ROS levels are little changed by UVA treatment (Tobi et al., 2000). These studies demonstrated the antioxidant role of glutathione. Depletion of cellular glutathione has been found to enhance the ROS level in UVA-irradiated cells (Tobi et al., 2000). Cellular glutathione depletion results in sensitization to lethal damage induced by UVA irradiation in both skin fibroblasts and keratinocytes (e.g. colony forming viability) (Tyrrell and Pidoux, 1988). Another study from this laboratory has shown that the UVA induction of HO-1 strongly correlates with the intracellular glutathione level (Lautier et al., 1992). There is also evidence that glutathione depletion in human keratinocytes (HaCaT cells) increased UVA–induced ROS generation (Tobi et al., 2000).

1.6 RNA interference

RNA interference (RNAi) refers to the phenomenon of exogenous short RNAs hybridizing to endogenous messenger RNA and interfering with translation (Montgomery et al., 1998). This process has been used to silence specific genes in vivo and in vitro. Reduction of specific gene activity using double strand RNA was first found in caenorhabditis elegans, and later was also found in plants as well as mammalian cells (Montgomery et al., 1998).

Fire and Mello first established that delivery of small double stranded RNA could result in more specific interference efficiency (Fire et al., 1998). Later, Hamilton and Baulcombe confirmed the mechanism of RNAi in mammalian cells (Elbashir et al., 2001). The enzyme Dicer degrades long double-stranded RNA (dsRNA) into small interfering RNAs (siRNA), 9~22 nucleotides (nt) in length (Tang, 2005), which can then be integrated into the RNA induced silencing complex (RISC). RISC contains a splicing protein which can cleave the targeted mRNA (Figure 7).

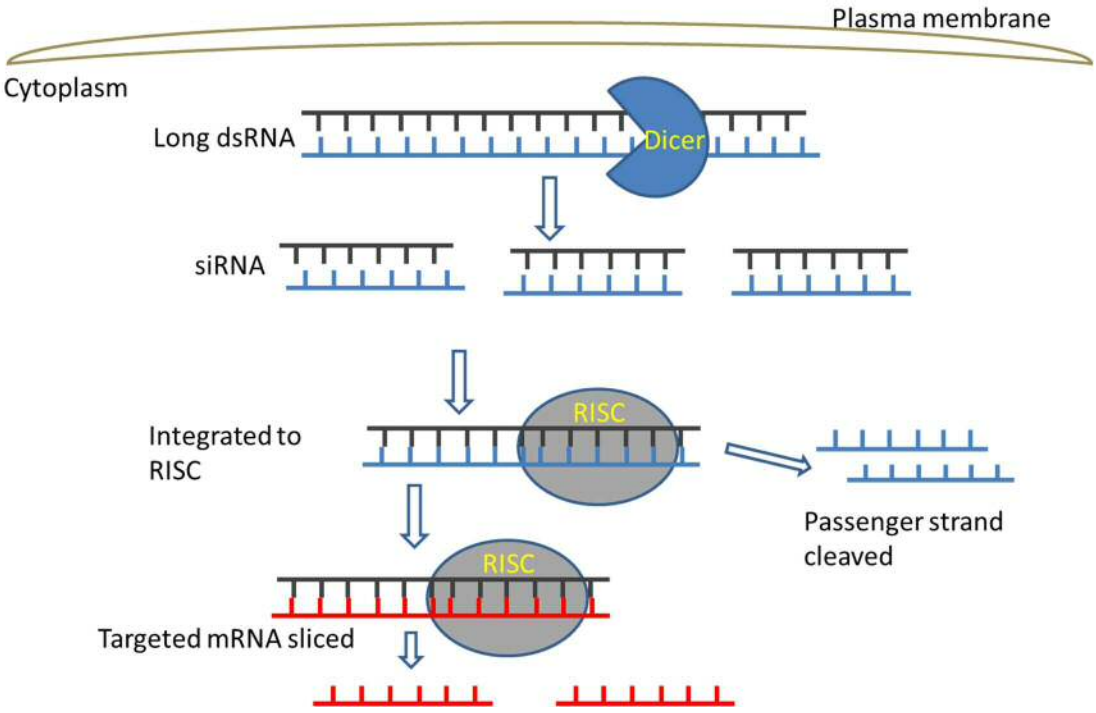

Figure 7 A diagram of the siRNA mediated RNAi pathway.

1.7 Aims and objectives

The main aim of this study is to investigate the interaction between UVA radiation with cultured human skin cells and possible involved proteins during this process. We will focus on NOX and Bach1 aimed to determine the role of these two proteins in the process of UVA induced skin damage respectively. To achieve this, we will examine:

1). The involvement of NOX in UVA induced ROS generation in cultured human skin cells in this process as well as the possible involved NOX subunits. NOX will be inhibited and UVA-induced ROS generation will be detected using flow cytometry. We will then detect the NOX activity upon UVA irradiation. Since NOX family have 7 protein members, we will also determine the possible involved NOX subunits. NOX1/4 protein will be mainly focused in this study and the expression of these two NOX proteins upon UVA irradiation will be detected by western blot.

2). If repressing Bach1 would enhance the protection of the HO-1 induction by UVA in cultured human skin cells. Bach1 will be repressed using RNA interfering technique and human skin cells cytotoxicity will be examined after UVA irradiation at various levels.

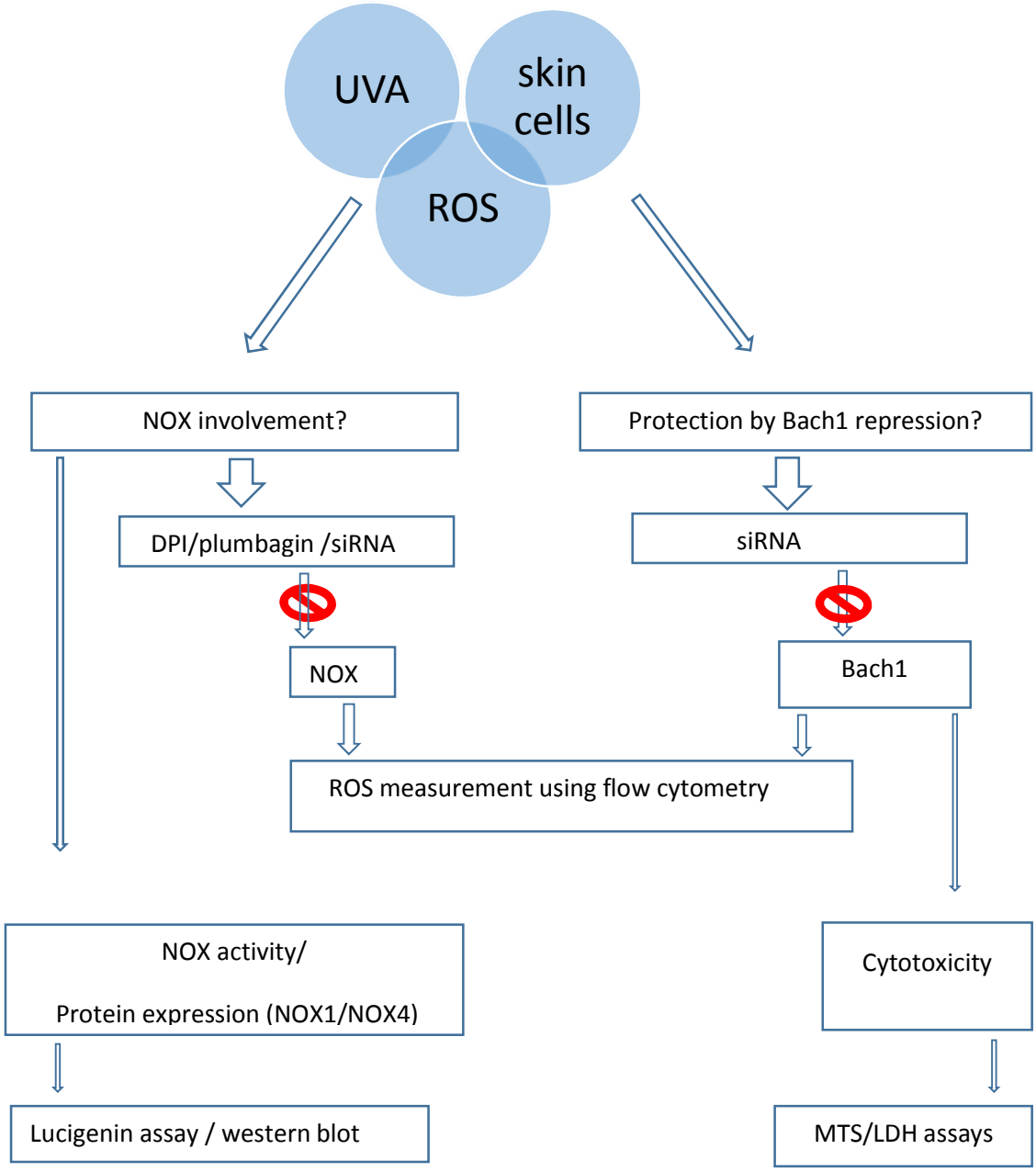

Scheme 2. A diagram of aims and objectives in this study.

Chapter 2 Materials and methods

2.1 Chemicals

All chemicals were purchased from Sigma-Aldrich Chemical (Poole, UK) unless specified otherwise.

Cell culture material used in this project were from Gibco (Invitrogen, UK) except foetal bovine serum (FBS) purchased from PAA Laboratories (Australia).

2.2 Cell culture

Human skin cell lines (FEK4 and HaCaT) used in this study were routinely cultured at 37°C and incubated with 5% CO_2 in a humidified atmosphere. $CuSO_4$ was used as an antibacterial within the incubator.

FEK4 cells were derived from human primary foreskin fibroblasts. Passages 9-16 were used since FEK4 fibroblasts are passage-dependent. EMEM (Eagle's modified minimum essential medium) was used for culturing FEK-4 cells. The medium was composed of 15% FBS (heat-inactivated at 56°C for 45 min before use), 0.25% sodium bicarbonate, 2 mM L-glutamine and 50 IU/ml each of penicillin/ streptomycin (P/S).

HaCaT cells were derived from a human spontaneously immortalised skin keratinocyte. The culture medium used for HaCaT cells was DMEM (high-glucose Dulbecco's modified Eagles medium) containing 10% FBS and 50 IU/ml each of penicillin/streptomycin (P/S).

2.3 Cell maintenance

FEK4 cells and HaCaT cells were centrifuged at 5,000 rpm for 5 min and the cell pellets were suspended (i.e. by pipetting up and down) in the culture medium (EMEM or DMEM) containing 10% DMSO and 20% FBS. Cells suspensions were then aliquoted in to the sterilized cryogenic storage vials. Cryogenic vials containing the cells were stored at -80°C overnight and then transferred to liquid nitrogen for long term storage.

When required for culture, the cells were rapidly thawed and placed in a 15 ml falcon tube containing 10 ml pre-warmed culture medium. After centrifugation, the cell pellet was then suspended in the culture medium (10 ml) and grown in a T75 cell culture flask.

2.4 UVA irradiation

A broad-spectrum 4 kW UVA lamp (Sellas, Germany) was used as a source of UVA radiation throughout this study. The irradiation times for corresponding UVA doses were calculated by measuring dose rate using a calibrated IL1700 radiometer (International Light, Newbury, MA).

Cells were seeded on to different dishes for irradiation experiments. On the day of treatment, conditioned medium was removed from each dish, cells were rinsed, replaced with PBS and then irradiated with UVA at required doses ranging from 50 to 500 kJ/m^2. Irradiation was conducted in a dark room with air-conditioning at 18°C in order to control temperature which will increase as a result of the UVA source. Following UVA irradiation, cells were then either analysed immediately or replaced with conditioned media for further incubation.

2.5 Chemical treatment

The compounds used in this study were added to the conditioned media from cells which had been grown to reach a certain confluence, and treatment was incubated with cells for indicated times from 10 min to 48h at the required final concentrations depending on the experimental requirement.

2.5.1 DPI treatment

Diphenylene iodonium (DPI) (D2929, Sigma) stock solution was prepared in DMSO (dimethyl sulphoxide) at a final concentration of 10 mM and aliquots were stored at -20°C until use. Conditioned medium was collected and DPI was diluted in the conditioned medium.

2.5.2 Plumbagin treatment

Plumbagin (P7262, Sigma) stock solution was prepared in DMSO at a final concentration of 10 mM and aliquots were stored at -20°C until use.

2.5.3 Hemin treatment

Hemin (iron ferric protoporphyrin IX) was dissolved in DMSO at a stock solution of 20 μM. Hemin was added to cells and incubated for 16 h before treatment.

2.6 siRNA transfection

RNA interference was used in this study to knock down targeted genes (Bach1, HO-1, NOX1 and NOX4). siRNAs for silencing of Bach1/NOX1/NOX4 were employed.

FEK-4 and HaCaT cells were seeded onto 3 cm plates in duplicate at a density of $8x10^4$ cells per plate. Concentrated siRNA and an equal amount of transfection reagent (RNAi Max, Invitrogen) were both diluted separately in 150 µl Opti-MEM, left at room temperature for 5 min, after which the siRNA was mixed with the transfection reagent. The mixture was incubated at room temperature for 30 min before being added to cells. The cells containing siRNAs were then incubated for 48 h. The siRNA sequences employed in this study are shown in Table 3.

Table 3 siRNA sequence used in this study.

siRNA	Sense	Antisense
NOX1A	ACAAUAGCCUUGAUUCUCAUGGUAA	UUACCAUGAGAAUCAAGGCUAUUGU
NOX1B	GCAAUAUUGUUGGUCAUGCAGCAUU	AAUGCUGCAUGACCAACAAUAUUGC
NOX4	GCCUCUACAUAUGCAAUAAtt	UUAUUGCAUAUGUAGAGGCtg
Bach1	GCCUUUGUCAGGUACAGACtt	GUCUGUACCUGACAAAGGCtt
HO-1	GGCCUUCUUUCUAGAGAGGtt	CCUCUCUAGAAAGAAGGCCtt

2.7 Cytotoxicity assay

The cytotoxicity was estimated using the cell proliferation assay (MTS assay), and cell membrane damage was detected by using the LDH assay.

2.7.1 MTS assay

MTS, 3-(4,5-dimethylthiazol-2-yl)-5-(3-carboxymethoxyphenyl)-2-(4-sulphophenyl)-2H-tetrazolium, inner salt, is a colourimetric assay which has been used widely in cell proliferations and cell viability measurement. It detects the ability of cellular mitochondrial dehydrogenase to convert the MTS into a coloured formazan product. The amount of formazan is directly proportional to the viable living cell number.

The enzymatic activity was measured using the CellTiter 96® AQueous One Solution Assay (Promega,UK)

For use, the MTS/SFM solution was freshly prepared by mixing MTS stock solution and SFM (serum free medium) (1:5) in a falcon tube to a final concentration of 0.5 mg/ml. After the indicated treatment, the medium was aspirated and the cells washed with PBS. Cells were then incubated with 100 µl MTS solution for 1.5 h. To determine the enzyme activity, 100 µl solutions from each sample was transferred in duplicate to a 96 well micro-titre plate and the absorbance was read by VERSAmax^{TM} (Molecular devices, California) at a wavelength of 490 nm wavelength. The absorbance was expressed as a percentage of enzyme activity.

2.7.2 LDH assay

The lactate dehydrogenase (LDH) assay can indicate membrane damage, since LDH activity released by damaged cells can be detected. The levels of

extracellular LDH were determined using the cytotoxicity detection kit for LDH (Roche Applied Science). After 4 h and 24 h incubation, LDH activity in both cells and cultured medium were measured according to the manufacturer's instructions. The percentage of LDH released was calculated from the values obtained. The release of LDH was determined by measuring the absorbance with a spectrophotometer plate reader at a wavelength of 490 nm.

LDH activity: Percentage LDH release= (LDH activity released / total LDH activity) x 100%

In this study, percentage LDH release was calculated using the following formula: Percentage LDH release = (LDH activity released in the cells / LDH activity in cells +LDH activity in medium) x 100%

2.8 ROS generation assay

ROS generation of UVA irradiated cells were detected using 5-(and-6)-chloromethyl-2',7'-dichlorodihydrofluorescein diacetate, acetyl ester (CM-H_2DCFDA) in a flow cytometry assay (C6828, Molecular Probes, Invitrogen): stock solution was prepared in DMSO at a final concentration of 5 nM. Aliquots were stored at -20°C until use.

2.8.1 Principle

CM-H_2DCFDA is a general indicator of intracellular ROS generation. On passive diffusion into cells, intracellular esterases will cleave the acetate groups. Meanwhile, intracellular glutathione and other thiols react with the thiol-reactive chloromethyl group. As a sequence, oxidation products generate fluorescence.

2.8.2 Procedure

FEK-4 and HaCaT cells were seeded onto 3 cm plates in duplicate for 3 nights. On the day of treatment, cells were incubated with DPI for 1h before UVA treatment as previously indicated. 5 μM CM-H_2DCFDA was mixed with PBS and incubated with cells for 25 min. The ROS generation in the cells were then detected by using flow cytometry.

For analysis of intracellular ROS generation, cells were treated with trypsin and re-suspended in FBS. The neutralized cells were centrifuged at 1,000 rpm for 5 min, washed twice using 0.1% BSA containing PBS and then centrifuged again (1,000 rpm, 5 min). Cells were then re-suspended in 2 μg/ml propidium iodide (PI).The collected cells were then transferred to a flow cytometer tube and analysed (10,000 or 50,000 events). The fluorescence intensity was quantified using a flow cytometer (Becton-Dickinson, Erembodegem, Belgium,

FACS Canto™) equipped with an argon ion laser (488 nm excitation), and a detector at 520 nm for fluorescence emission (see appendix for ROS for representative ROS generation data).

2.9 Flow cytometry (dual stain assay) apoptosis and necrosis assay

Cell death caused by apoptosis and necrosis was measured using the Annexin V-FITC (AV)/propidium iodide (PI) dual staining assay to distinguish the two cell death pathways. The protocols were carried out as described in the Annexin V-FITC detection kit (Roche).

2.9.1 Principle

Cell surface and plasma membrane are altered in the early stages of apoptosis. One major change is phosphatidylserine (PS) from the inner side being translocated to the outer layer side, thus PS is exposed to the external surface of the cell. As a calcium-dependent phospholipid-binding protein, Annexin-V FITC (AV) has a high affinity for PS which is only exposed to the cell surface; this compound can be used for detecting apoptotic cells.

When cells are exposed to extreme physiological conditions, necrosis occurs and the plasma membrane loses integrity and is then damaged. PI can enter the damaged cells by binding to the DNA; necrotic cells that lose membrane integrity can be stained with both PI and AV, therefore can be distinguished from apoptotic cells (Figure 8).

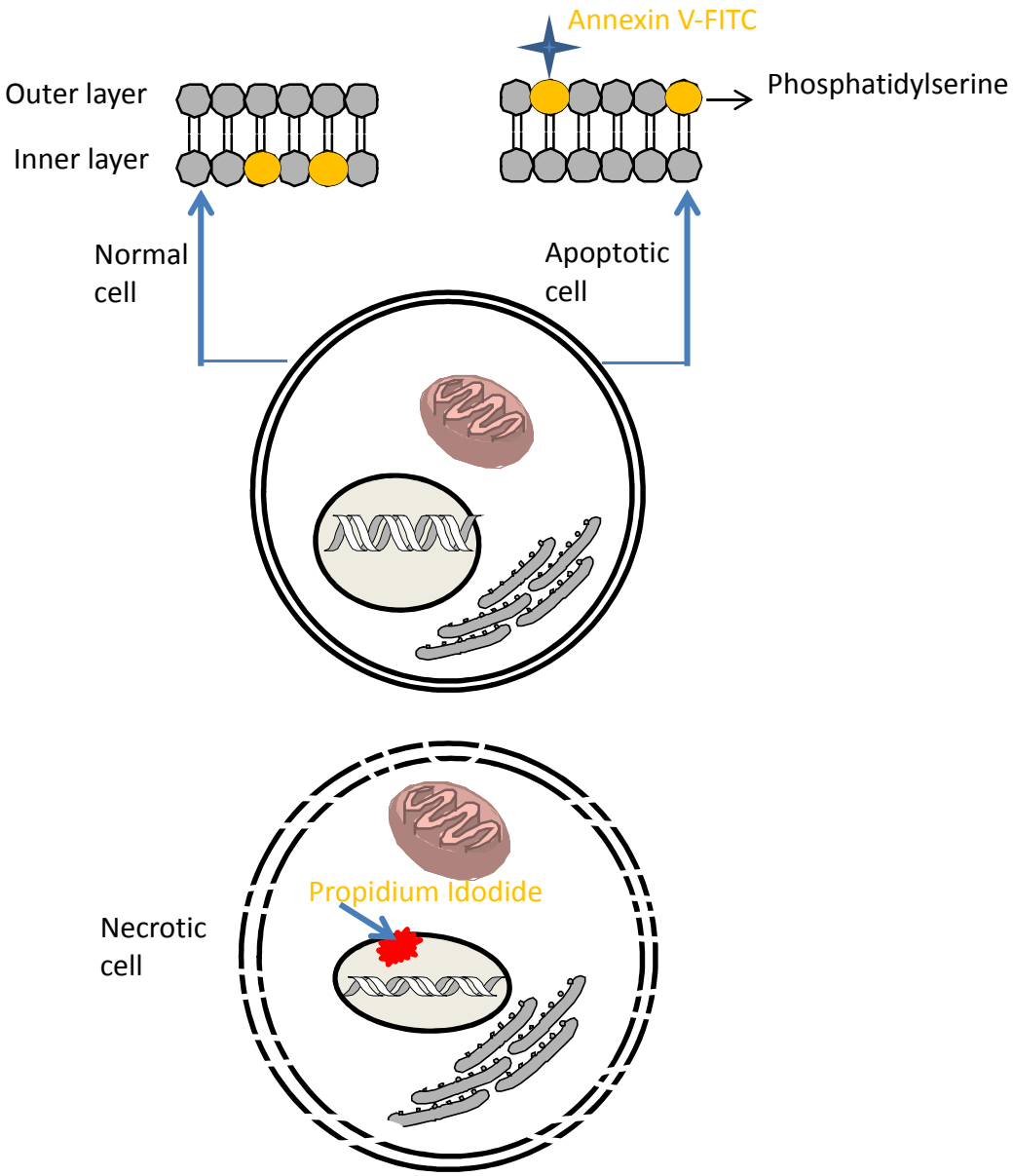

Figure 8 Mechanism of dual staining for necrotic and apoptotic cells. Dual staining by Annexin-V FITC and PI was used to identify necrosis and apoptosis. Necrotic cells are stained with both Annexin-V FITC and PI. Apoptosis are stained with PI alone.

2.9.2 Procedure

Cells were collected and washed with the incubation buffer (10 mM Hepes/NaOH, pH 7.4, 5 M NaCl, 100 mM $CaCl_2$). The cells with Annexin V dye (20 µl/ml) were incubated at room temperature under dark conditions for 20 min followed by 2 min incubation with PI (20 µg/ml).

2.10 Trypan blue assay

The cytotoxicity of diphenylene iodonium (DPI) on HaCaT and FEK-4 cells was tested using trypan blue dye. FEK-4 and HaCaT cells were seeded on a 6 cm dish with 6 ml 10% FBS containing DMEM (EMEM for FEK-4) for 3 days. Conditioned media was collected on the day of treatment; 2.5 ml of serial concentrations of DPI (0, 1, 2, 5, 10 and 20 µM) were added with conditioned media to the cells and incubated for 1 h. After treatment, cells were washed with PBS and replaced with saved conditioned media (3 ml per dish). Cells were incubated for 24 and 48 h and then the percentage of cell death was estimated counted by using trypan blue dye staining.

2.11 Total protein extraction

Following treatment, cells were detached with 0.25% trypsin and the pellet was collected by centrifugation at 13,000 rpm for 5 min. Supernatant was discarded and the cell pellets were suspended in 0.5 ml lysis buffer (KH_2PO4, 20 mM; ethylene-diaminetetraacetic acid (EDTA), 0.5 mM; PMSF, 0.1%; tablet inhibitor) (Roche) and then transferred to a 1.5 ml eppendorf tube and, sonicated for 14 seconds on ice (Rapidis 300, Ultrasonics, UK). After sonication, cell lysate was then centrifuged at 13,000 rpm for 5 min at 4ºC (Biofuge 13, Heraeus instrument). The supernatant that contained total protein was then collected and was either used for NOX enzymatic assay immediately

or flash-frozen on dry ice containing 100% methanol and stored at -80ºC for future use.

2.12 Quantification of protein concentration

Quantification of protein concentrations was measured by the Bio-Rad protein assay according to the method of Bradford (1976). The standard curve was generated by using bovine serum albumin (BSA, 1 mg/ml) at a final concentration of 0, 1, 2, 4, 6, 10, 15, 20 mg/ml. The total protein volume or BSA diluted in the same solvent of protein extraction of each well was 160 µl, 40 µl of Bio-rad protein reagent (Bio-rad, 500-0006) was then added to give a final volume of 200 µl. Each condition was performed in triplicate. The absorbance was read by VERSAmax^{TM} (Molecular Devices, California) with a 595 nm filter.

2.13 Sodium dodecyl sulphate polyacrylamide gel electrophoresis (SDS-PAGE)

A separating gel was prepared using a 10% resolving polyacrylamide gel solution composed of 30% acrylamide/bis, 0.5 M Tris-HCl, pH=6.8, 10% SDS , MilliQ H_2O, N,N,N',N'-tetramethylethylenediamine (TEMED) and 10% ammonium persulphate (APS). The gel solution was poured into an empty Bio-Rad gel casting system and then was allowed to form at room temperature for 1 h. MilliQ H_2O was added on top of the resolving gel in order to avoid any evaporation. The stacking gel solution was prepared using 4% polyacrylamide gel composed of 30% acrylamide/bis, 1.5 M Tris-HCl, pH=8.8, 10% SDS, MiliQ H_2O, TEMED and 10% APS. The stacking gel solution was then added on top of the resolving gel layer and was set for further 45 min.

Equal amounts of protein (10 µg) were diluted in a 5x sample buffer [300 mM Tris, 50% glycerol, 10% sodium dodecyl sulphate (SDS), 0.5% bromophenol blue, 0.05% β-mercaptoethanol] and then heated at 95 ºC for 5 min, and finally

loaded on to the SDS polyacrylamide gel. The electrophoresis was performed with 1x running buffer [25 mM Tris-HCl, 200 mM glycine, 0.1% w/v SDS] at 150 Volts for 1 h.

2.14 Western blot analysis

After electrophoresis, all proteins were then transferred to polyvinylidine difluoride (PVDF) membranes by using a tank blotting unit filled with transfer buffer (3% w/v tris, 14.4% w/v glycine, 20% methanol) at 14 V in a cold room overnight. Equal rates of transfer were confirmed by reversible staining with Ponceaus S. Blots were incubated with 3% BSA in Tris buffered saline with tween 20 (TBST) to block nonspecific binding at room temperature for 1h. The primary antibody was diluted at 1:200 and incubated with 3% BSA in TBST buffer at 4 ºC overnight. PVDF membranes were then washed in TBST buffer for 15 min, followed by 1 h incubation time with hypoxanthine-guanine phosphoribosyl-transferase (HPRT)-linked secondary antibody (1:5000) at room temperature on a rocking platform (Stuart Scientific) for 1 h. Enhanced Chemiluminescence was detected using x-ray film.

2.15 Confocal microscope cell imaging

Cells were seeded on a square glass cover slip at a density of $8x10^4$ per 3 cm dish to reach 70-80% confluence. siRNAs were then transfected into FEK4 and HaCaT cells and incubated for 48 h. After transfection, the cell culture media were aspirated from each well, and the cells were washed three times with PBS and fixed with 400 µl 4% paraformaldehyde in PBS for 10 min at room temperature. The fixed cells were permeabilised with 100% ice cold methanol for 2 min at -20ºC. After 2 min, methanol was aspirated and cells were then washed with PBS three times. The cell nucleus was then stained with 5 µg/ml final concentration of DAPI (4',6-diamidino-2-phenylindole, dihydrochloride) at room temperature for 20 min in the dark followed by three PBS washes. The coverslips were then removed from each well, left to dry, and then mounted on glass slides by using mounting medium (s3023, fluorescence Mounting medium, DAKO, UK) and left overnight to dry at room temperature in the dark. The cells were examined using a Carl Zeiss laser scanning microscope (LSM 510 META).

2.16 NADPH Oxidase activity assay

NADPH oxidase activity was detected by using the lucigenin assay.

2.16.1 Principle

Lucigenin (bis-N-methylacridinium dinitrate) (LC^{2+}) has been used as a luminescent indicator of superoxide production.

Addition of superoxide to the free radical gained with the reduction of lucigenin ($LC^{\cdot +}$), forms an unstable dioxetane, which in turn cleaves to produce N-methylacridone in the excited state and this is where the luminescence occurs. However, the reducing agents such as alkaline can also induce luminescence. Thus lucigenin is not specific to superoxide.

2.16.2 Procedure

Cells were seeded at a density of $8x10^4$ per 3 cm plates for 3 nights to reach a confluence of 80%. On the day of treatment, cells were irradiated with different UVA doses, and then cells were collected and centrifuged at 1,000 rpm for 5 min. Cells were re-suspended with 0.5 ml lysis buffer (KH_2PO4, 20mM; EDTA, 0.5 mM; PMSF, 0.1%; tablet inhibitor) (Roche) and then transferred to an eppendorf tube, sonicated for 14s on ice (Rapidis 300, Ultrasonics, UK). After sonication, cells were centrifuged at 13,000 rpm for 5 min at 4 ºC (Biofuge 13, Heraeus instrument). The supernatant was collected after the spin and the protein content was quantified by using the Bradford assay. 1 µg protein was added to the assay buffer containing 100 µM NADPH and 500 µM lucigenin. The assay buffer was then incubated in a water bath at 37 ºC for 10min then put on ice. The luminescence generated by superoxide anion was measured by using an illuminometer (TD20/20, Turner Biosystem).

2.17 Statistical analysis

Data are expressed as mean ± the standard error of the mean (SEM), and statistical significance of the results was determined by one-way analysis of variance followed by the student t-test, with statistical significance set at $p<0.05$.

Chapter 3. Results

Part I: Potential protection of human skin cells against cell damage/inactivation via UVA-induced HO-1

As mentioned in the introduction, protection against UVA-induced cellular damage in human skin cells is at least partially mediated by HO-1. A previous study (Raval et al., 2012) in this laboratory proved that Bach1 is involved in HO-1 induction in UVA irradiated FEK4 cells, and Bach1 inhibition increased the level of UVA-induced HO-1. Based on this study, we wanted to further examine whether Bach1 inhibition is involved in the protection process. In order to do this, the cell viability of UVA-irradiated FEK4 cells with siRNA of Bach1 (siBach1) pre-treatment was first of all checked by two cytotoxicity measuring assays with the potential to detect a role of Bach1 in protecting UVA-irradiated human skin fibroblasts: the MTS and LDH assays. We expected that there would be less cytotoxicity after UVA irradiation with siBach1 pre-treatment.

3.1 Silencing of Bach1 leads to no strong effect on cytotoxicity following UVA irradiation.

The dehydrogenase enzyme activity of FEK4 cells was determined 4h following UVA irradiation using the MTS assay. The absorbance is directly proportional to the enzyme activity. Unexpectedly, the Bach1 siRNA has a strong and significant effect on the un-irradiated control cells and appears to have affected enzymatic activity (Figure 9). UVA does result in significant reduction in enzymatic activity after 250 kJ/m^2 and 400 kJ/m^2 but there does not appear to be a significant difference between UVA treated cells with or without scrambled (sb) or Bach1 targeted siRNAs.

In view of the inconclusive results 4h after irradiation, dehydrogenase enzymatic activity of FEK4 cells was also determined 24h following UVA irradiation using the MTS assay with and without treatment with Bach1 siRNA.

A higher concentration (20 nM) of siRNAs as well as a higher UVA dose was used in this experiment. The enzyme activity was reduced in a dose-dependent manner following UVA irradiation, with significant reduction at the 500 kJ/m^2 dose level; however, silencing of Bach1 had no effect on the cell viability (Figure 10). The results described in this section so far indicate that although Bach1 appears to be involved in UVA-induction of HO-1, this protein does not seem to protect against UVA induced cellular damage in human skin fibroblasts.

However, it is possible that in contrast to the results (Tyrrell and Pidoux, 1988) seen using inactivation of colony-forming activity as a viability measurement, UVA reduced viability as measured by the MTS assay is not redox dependent (i.e. cellular oxidative damage induced by UVA is not detected by the MTS assay). To further understand this, we next performed glutathione depletion in FEK4 cells and measured reduced viability using the MTS assay following UVA irradiation.

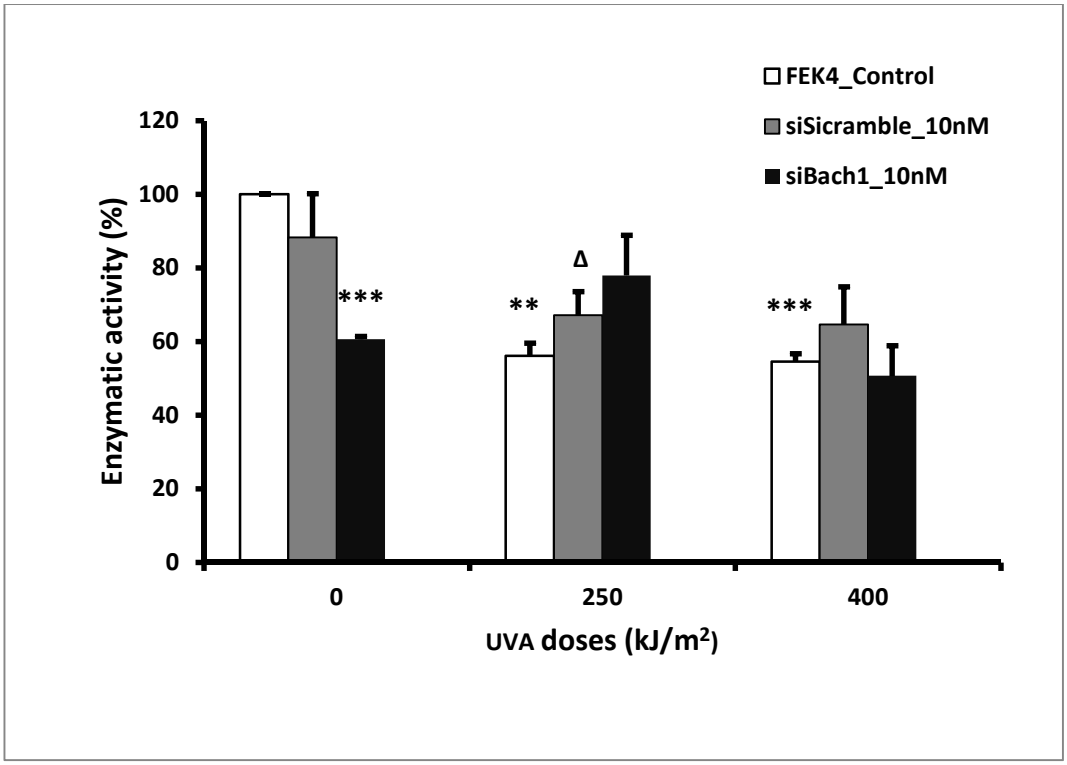

Figure 9 MTS assay of FEK-4 cells pre-treated with siBach1 (4h) following UVA irradiation with doses of 250 and 400 kJ/m^2 of UVA. FEK-4 cells were transfected with or without siBach1 and seeded onto 24 well plates 48h before UVA irradiation as described in Materials and Methods. The MTS assay was performed after 4h incubation. The values of untreated cells were set to 100% and other values were normalized as a percentage of this control. Data shown are mean ± SEM (n=3).

** $p<0.01$, *** $p<0.001$ significant difference when compared to untreated FEK control cells.

Δ $p<0.05$ significant difference from UVA irradiated control cells.

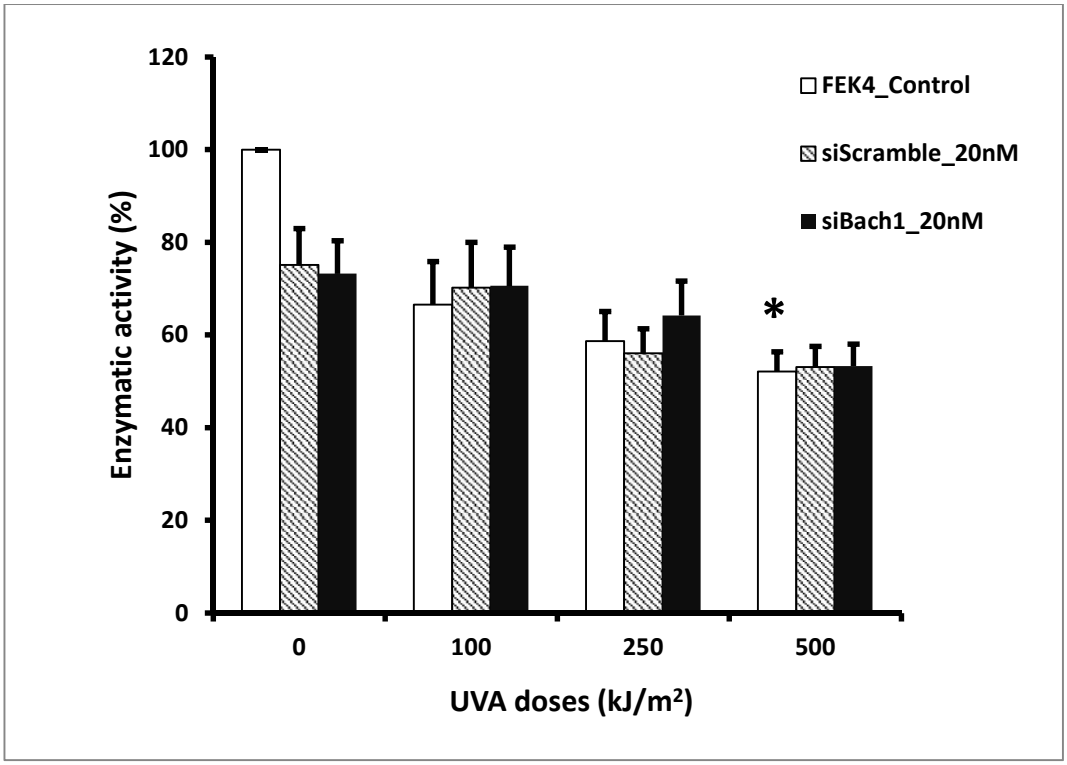

Figure 10 MTS assay of FEK-4 cells pre-treated with or without siBach1 for 48h and measurements taken 24h following UVA irradiation at a series of doses (n=3). FEK-4 cells transfected with/without siBach1 were seeded onto the 24 well plates 48h before UVA irradiation. The MTS assay was performed after 24h incubation. Data shown represents mean values ± SEM.

* $p<0.05$ significant difference from untreated control cells.

3.2 Glutathione depletion of FEK4 cells by treatment with BSO results in a higher cytotoxicity following UVA irradiation.

It has been proven that there is a direct correlation between the levels of sensitivity to UVA and cellular GSH content (Tyrrell and Pidoux, 1988) and that endogenous glutathione protects skin fibroblasts against UVA-induced cell damage (Tyrrell and Pidoux, 1986). Earlier studies had shown that depletion of cellular glutathione levels in UVA irradiated human skin cells led to lethal damage including the damage induced by oxidative stress. The reduced cell viability induced by this damage has been measured and confirmed by colony forming assay, but it is unknown whether this lethal damage can be detected by the MTS assay. To answer this question, we performed the same treatment in FEK4 cells (i.e. UVA irradiate FEK4 cells following glutathione depletion), and the MTS assay was used for measuring the cell viability.

FEK4 cells were pre-treated with D,L-buthionine-S,R-sulphoximine (BSO) for glutathione depletion and the reduction in viability following UVA irradiation was measured using the MTS assay. The results in Figure.11 show the inactivation of FEK4 cells as a function of UVA dose. Notably, after 100 and 150 kJ/m^2 UVA, the viability in glutathione depleted cells was significantly reduced compared with untreated cells. This result is consistent with previous findings (Lautier et al., 1992) that upon UVA irradiation, there was an inactivation of colony forming ability in glutathione depleted cells compared to non-depleted cells.

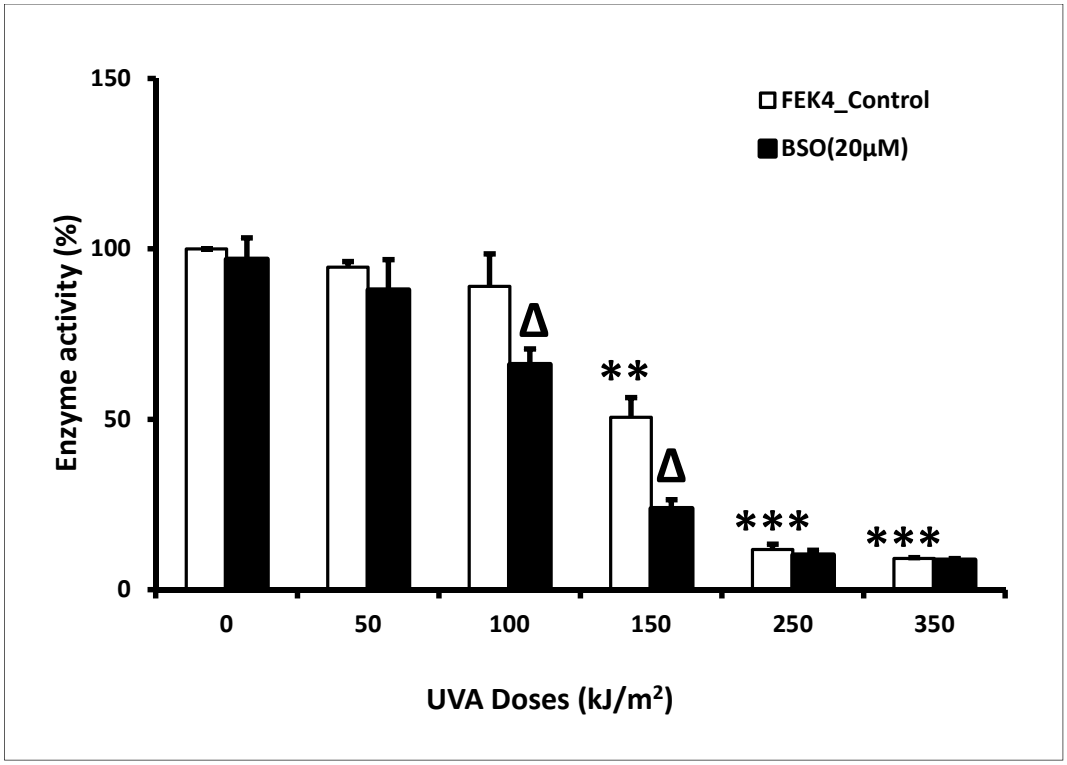

Figure 11 MTS assay to measure inactivation of cultured skin fibroblasts by UVA irradiation with and without pre-treatment with BSO. BSO (20 µM) was added to FEK-4 cells 18h before UVA treatment. The MTS assay was carried out as described (Materials and Methods). All data points are mean values from three independent experiments and are shown as mean ± SEM. The Student t-test was used to evaluate the statistical significance ($p<0.05$) of each data point.

* ($p<0.05$), ** ($p<0.01$), *** ($p<0.001$) when compared to non-irradiated control cells.

Δ $p<0.05$ when compared to UVA-irradiated control cells.

Since this result showed that the change in response to UVA as a result of glutathione depletion could also be measured by the MTS assay, we conclude that UVA-induced oxidative damage is detectable by the MTS assay. The results in Figure 11 using the MTS assay will therefore also reflect the oxidative damage sector. Taken together, the results of Bach1 inhibition experiments from this section provide evidence that silencing of Bach1 does not influence the viability of FEK4 cells (i.e. protect) following UVA damage.

UVA-induced cellular damage generally initiates with lipid peroxidation which consequently leads to membrane damage. In view of the above results concerning cell viability in Bach1 inhibited FEK4 cells (as measured by the MTS assay), we speculated whether Bach1 inhibition could protect FEK4 cells against UVA-induced damage at the membrane level. Thus, membrane damage as measured by the LDH assay was employed next in UVA-irradiated FEK4 cells in this study to determine if silencing of Bach1 could protect the cells against UVA-induced membrane damage.

3.3 Silencing of Bach1 does not result in lower membrane damage in FEK4 cells

LDH released as a result of membrane damage to cells following UVA irradiation was measured using the LDH assay as described in Materials and Methods with and without pre-treatment with siBach1. The results in Figure 12 showed a higher LDH release from UVA irradiated FEK4 cells compared with the non-irradiated control cells. The level of LDH release is 3 fold that of non-irradiated control cells after 250 kJ/m^2 UVA irradiation, and then slightly declined at 400 kJ/m^2. With siBach1 pre-treatment, the UVA-induced LDH release level was strong in UVA irradiated (250 kJ/m^2) cells. Surprisingly, the cells treated with scrambled siRNA (sisb) also lowered the level of UVA-induced LDH release at both UVA doses. sisb RNA has no significant effect on the LDH release level in unirradiated FEK4 cells. This result revealed that, although siBach1 treatment decreased the higher level of LDH release following UVA irradiation, and therefore appears to protect FEK4 cells from UVA induced membrane damage, this is an artefact since the sisb treated control cells show similar effects.

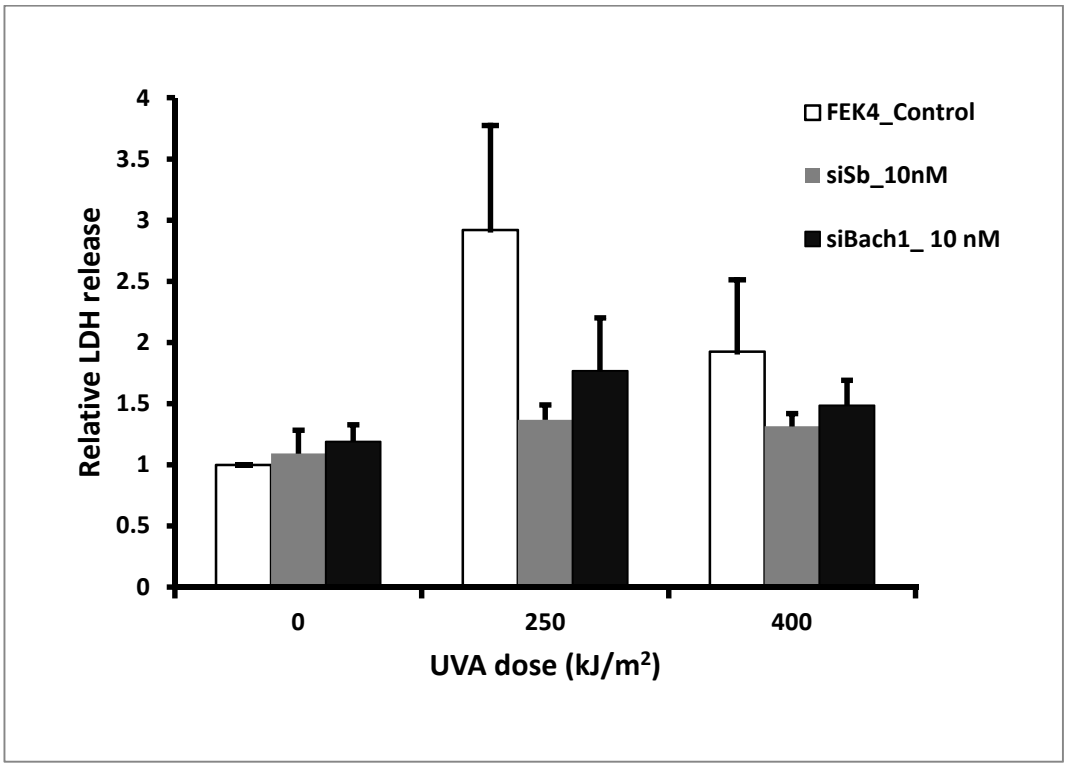

Figure 12 LDH release in FEK4 cells with or without siBach1 (for 48h) treatment 4h following UVA irradiation at two doses (250 and 400 kJ/m^2). The relative levels of LDH release were calculated as the proportion of LDH activity released from cells in the total LDH activity (LDH activity released from cells + LDH activity released from medium). The value of FEK4 control cells was set to 1, and all the other values were normalized to this value. Data shown are mean ± SEM (n=3). Paired student t test was used for analysis of statistical significance.

Based on the data shown in Figures 9-12, the siBach1 treatment neither increased the UVA inactivated FEK4 cellular viability as measured by the MTS assay nor protected the cells against UVA–induced membrane damage as measured by the LDH assay. The results therefore indicate that Bach1 inhibition has no protective effect against UVA-induced cellular damage, although it increases HO-1 induction. Nevertheless, it is also possible that the Bach1 inhibition is not sufficient to protect against UVA-induced damage at the level of viability or at the membrane damage level, but may be involved in a protective pathway at a more sensitive level, for example: ROS generation. To further explore this, ROS generation was then measured in FEK4 cells with siBach1 treatment followed by UVA irradiation.

3.4 Effect of siBach1/siHO-1 on ROS generation after UVA irradiation

Bach1 binds to the HO-1 gene promoter and suppresses HO-1 gene expression (Sun et al., 2002). Okada and co-workers (Okada et al., 2010) have shown that in keratinocytes, lowering of Bach1 levels led to a higher level of HO-1 gene expression following H_2O_2 treatment, but did not lower the ROS generation by H_2O_2. The ROS level was higher in Bach1 depleted keratinocytes. On the other hand, when keratinocytes overexpressed Bach1, the HO-1 induction was completely abolished following H_2O_2 treatment, and the ROS level induced by H_2O_2 was enhanced compared with control cells (Okada et al., 2010).

Since induction of HO-1 is believed to protect against oxidative stress, we questioned whether depletion of Bach1 protein in FEK4 cells could reduce UVA-induced ROS generation. In order to examine the role of Bach1 in the process of UVA-induced ROS generation, cells were treated with siBach1 RNA 48 h before UVA treatment. Flow cytometry analysis was employed in this study using the ROS dye CM-H_2DCFDA; the fluorescence intensity was analysed using flow cytometry (Materials and Methods).

Curiously, the results (Figure 13A) showed more ROS generation in UVA irradiated cells that had been pre-treated with siBach1 RNA than in control cells. sisb RNA pre-treatment of FEK4 cells has less effect on UVA irradiated ROS generation, particularly at 200kJ/m^2.

Since the Bach1 gene depletion increased ROS generation in UVA treated skin fibroblasts, we next examined if HO-1 gene knock-down would influence the UVA-induced ROS generation pathway. HO-1 was targeted using HO-1 siRNA in FEK4 cells and the ROS generation after UVA irradiation was measured by flow cytometry. Since previous experiments (Zhong et al., 2010) from this laboratory had shown that siHO-1 RNA did decrease the HO-1

protein expression level, the same siHO-1 RNA was employed in the current study for siHO-1 RNA treatments. The results (Figure 13B) revealed that siHO-1 RNA pre-treated FEK4 cells exhibited slightly diminished ROS generation after UVA compared with the cells not treated with siRNA. However, the scrambled siRNA pre-treated cells also showed diminished ROS generation, so that there is no difference between sisb and siHO-1 treated cells.

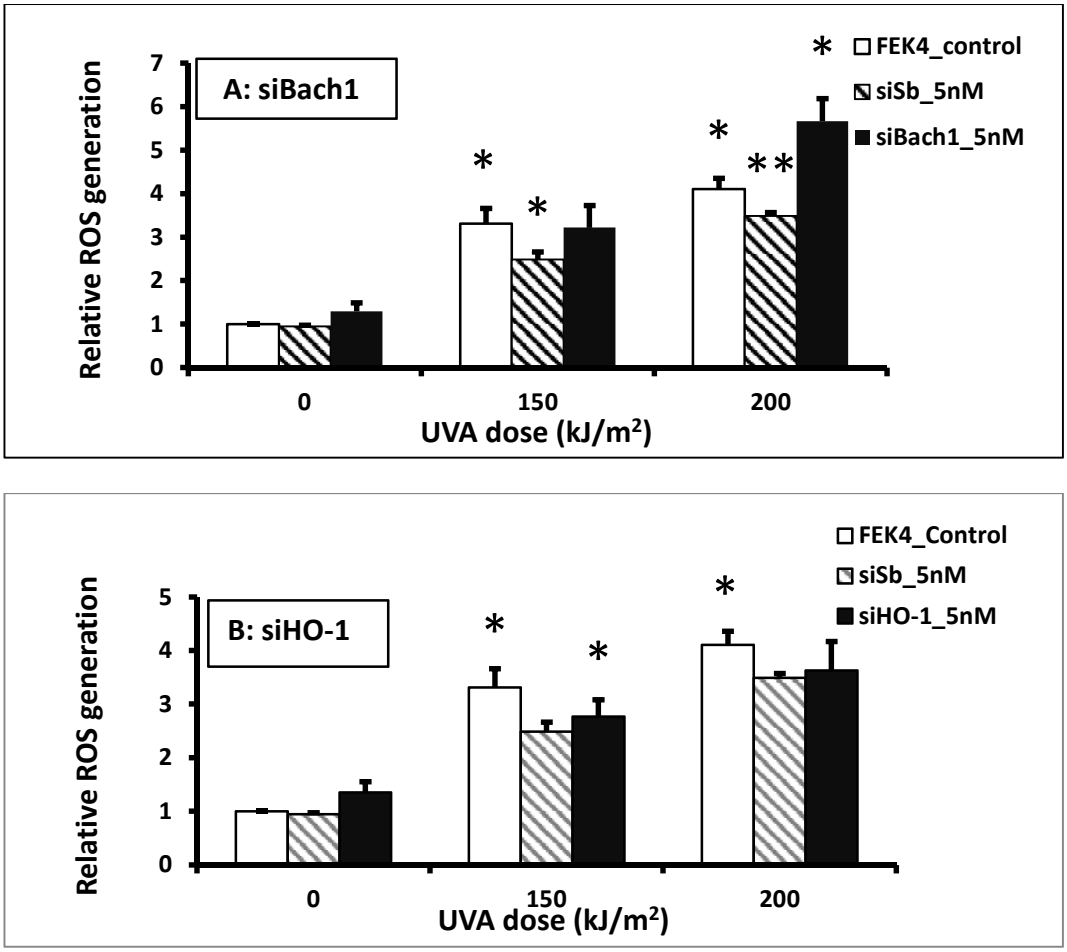

Figure 13 Effects of siRNA silencing of either Bach1 or HO-1 on ROS generation following UVA irradiation in FEK4 cells. A: Modulation of ROS generation in FEK4 cells with and without siBach1 pre-treatment. B: Modulation of ROS generation in FEK4 cells with and without siHO-1 pre-treatment. Values represent mean ± SEM (n=3). The siRNA for either Bach1 or HO-1 was transfected into FEK4 cells which were incubated for 48 h before UVA irradiation. ROS generation was detected using a fluorescent dye (CM-H_2DCFDA) with flow cytometry. The data are shown as the fold change in ROS generation relative to non-irradiated FEK4 control cells. The value of ROS intensity for untreated FEK4 cells was set to 1 and all the other values were normalized to this control value. The student t test was used to evaluate the statistical significance of each data point.

*$p<0.05$, **$p<0.01$ significance level when compared to untreated control cells.

Based on the results shown in Figure 13, silencing of Bach1 increased ROS generation especially at a higher UVA dose (200 kJ/m^2), whereas silencing of HO-1 did not significantly alter the ROS level. We conclude that reduction of HO-1 does not have much influence on the level of ROS generation in FEK4 cells following UVA treatment. However, depletion of the Bach1 gene increased ROS generation levels.

HO-1 has generally been considered as having antioxidant activity, but there is evidence that it may be pro-oxidant in some circumstances (Kvam et al., 2000; Li and Stocker, 2009), and possibly as a result of release of low-molecular-mass iron (Kvam et al., 2000; Lamb et al., 1999). Free labile iron is the major Fenton catalyst and can lead to generation of ROS and enhance lipid peroxidation (Dennery et al., 1997). A previous study (Kvam et al., 2000) from this laboratory found that increased HO-1 activity increased the free labile iron level in HO-1 overexpressed cells which consequently led to a stronger sensitivity to UVA radiation. Therefore, a possible explanation for the increase in ROS when the HO-1 levels are enhanced by Bach1 depletion is that the increase in HO-1 leads to the release of iron.

It is evident that oxidative stress induced p53-related senescence is regulated by Bach1 in murine embryonic fibroblasts (Dohi et al., 2008); in view of this evidence, another possible explanation for our result is that Bach1-regulated other genes involved in the process of increasing UVA-induced ROS generation.

In summary, initially, since the reduction of Bach1 is the key to increasing HO-1 induction, the main hypothesis of this study is that Bach1 would be involved in HO-1 mediated events. Thus, we predicted that knocking down of Bach1 would lead to enhanced protection against skin cell damage via UVA induce HO-1 induction. However, the results obtained from this section revealed that reducing Bach1 increased HO-1 induction, but that there is no enhancement of protective effects against UVA-induced cell damage at either the membrane damage or cell viability level. The glutathione depletion experiments result provide the evidence that viability as measured by MTS assay included the

oxidative damage sector and therefore leads to the conclusion that Bach1 reduction is insufficient to enhance protection against cell damage by UVA irradiation via the HO-1 induction pathway (i.e. it is independent of the oxidative pathway). The results also indicate the HO-1 reduction does not influence ROS generation by UVA irradiation.

Taken together, these findings provide evidence that Bach1 inhibition is involved in the response to UVA events (i.e. HO-1 induction, ROS generation) but is not involved in protecting skin fibroblasts against UVA-induced cell damage.

In this part, we hypothesised that as a key factor in HO-1 regulation, Bach1 would be involved in HO-1 mediated events (i.e. knocking out Bach1 will enhance the protection of UVA-induced cellular damage). Therefore, we performed a series of experiments with Bach1 knock down treatment in UVA irradiated cells aimed to prove whether Bach1 inhibition would enhance the protection. However, all the data gained from this part showed us that Bach1 inhibition is not protective against UVA-induced cytotoxicity in human skin fibroblasts. As the UVA-mediated HO-1 induction appears to protect against cellular damage by a different pathway, we considered it important to find out the cellular source of UVA-induced damage. Since excessive ROS generation has been considered the major reason for damage, the source of UVA-induced ROS generation became our next research target. As a major source of ROS formation, NADPH oxidase has been extensively studied recently and there is evidence to show that NADPH oxidase (NOX) is the major source of UVA-induced ROS generation in cultured human keratinocytes (Valencia and Kochevar, 2008). Thus, the involvement of NOX in UVA-mediated ROS generation in human skin cells is the main purpose of the experiments that follow.

Part II: The Role of NADPH oxidase (NOX) in the response of human skin cells to UVA irradiation –ROS generation

In this part, we hypothesized that NOX may be involved in the response of UVA-mediated ROS generation and that NOX would be activated in human skin cells in response to ROS induction by UVA irradiation. We therefore predict that induction of ROS will be inhibited by NOX inhibition. To investigate this, we performed experiments that included an investigation of the ROS generation following NOX inhibition in UVA-irradiated human skin cells as measured by flow cytometry. NOX activity following UVA treatment has been measured by the lucigenin assay to further understand the role of NOX in the process of UVA-mediated ROS generation.

3.5 Comparisons of ROS generation in skin cells after UVA irradiation

In order to investigate whether NOX is involved in the process of UVA-mediated ROS generation, the first step was to determine the influence of NOX on the ROS induction by UVA. ROS generation was detected in primary human skin fibroblasts (FEK4) as well as human immortalized keratinocytes (HaCaT) using flow cytometry analysis with CM-H_2DCFDA dye as described in Materials and Methods. UVA irradiation generated significant induction of intracellular ROS in both these two types of skin cell lines but to different levels.

The ROS induction was measured after UVA irradiation in FEK4 cells as well as keratinocytes (Figure 14). Following UVA treatment, fluorescence intensity of ROS induction in FEK4 cells increased in a UVA dose dependent manner (Figure 14A). The fold change of ROS generation as measured by fluorescence intensity over non-irradiated FEK4 cells was by 2.5 fold at 150 kJ/m^2 and by 3.5 fold at 200 kJ/m^2. A similar trend occurs in HaCaT cells (Figure 14B); ROS generation increased up to nearly 3 fold over non-irradiated cells after 150 kJ/m^2 but declined slightly at 200 kJ/m^2. This decline may be due to damage to proteins that generate ROS by higher doses of UVA

irradiation. These results are consistent with the previous results observed for ROS generation after UVA irradiation in human skin tissue (Ou-Yang et al., 2004; Tyrrell, 2012). The results shown in Figure 15 showed a much larger induction of ROS in skin fibroblasts (FEK4 cells) compared with skin keratinocytes (HaCaT cells).

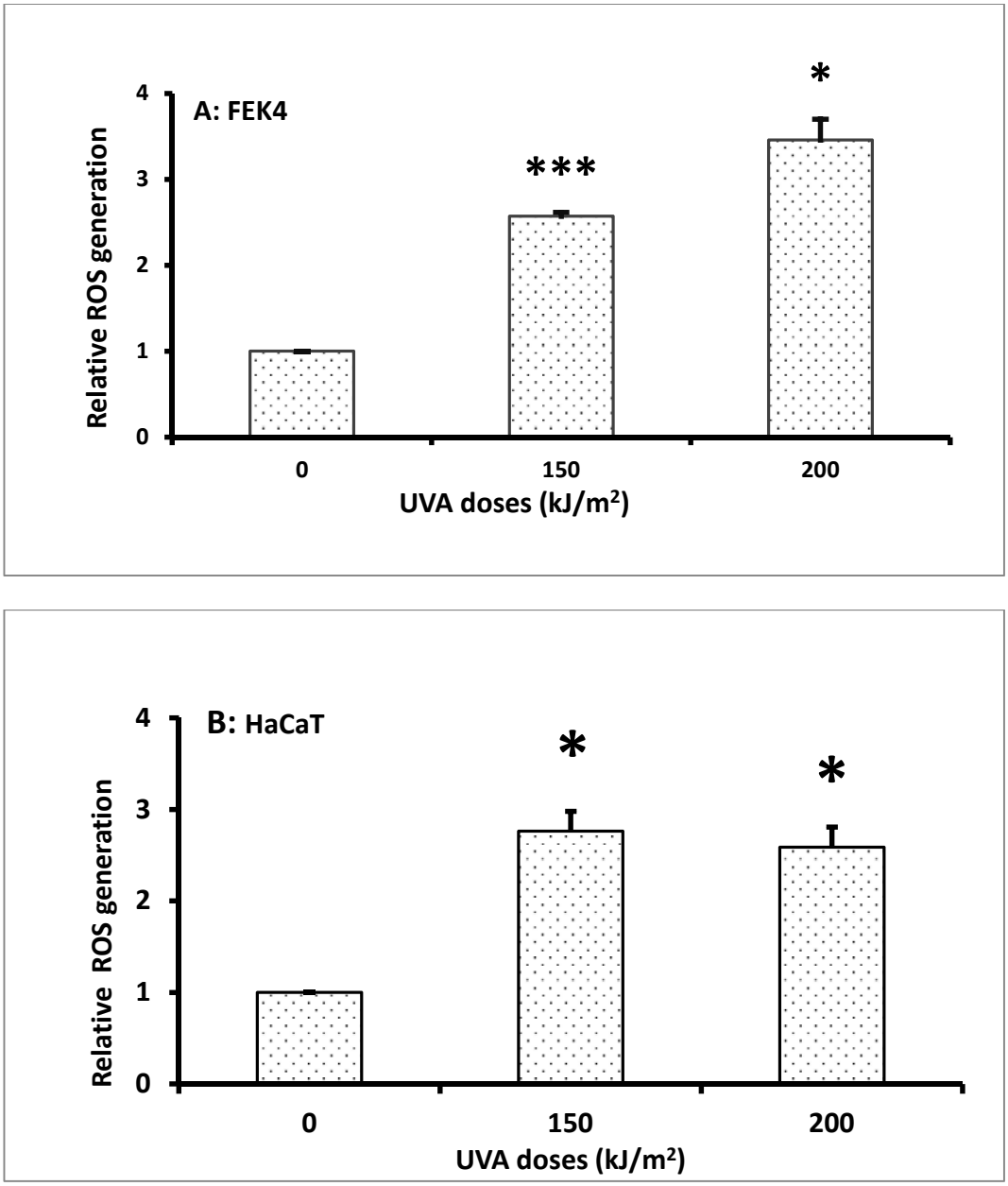

Figure 14 A: ROS generation after UVA irradiation of FEK4 cells. B: ROS generation after UVA irradiation of HaCaT cells. ROS generation was measured by flow cytometry after 25 min incubation with a derivative of the fluorescein ROS dye (CM-H_2DCFDA) as described in Materials and Methods. The results of relative ROS fluorescent intensity were expressed as the fold change relative to normalized control FEK4 cells and HaCaT cells (mean ± SEM). Statistics were carried out using the student t-test (n=3).

* $p<0.05$, *** $p<0.001$ significance level when compared with the control un-irradiated cells.

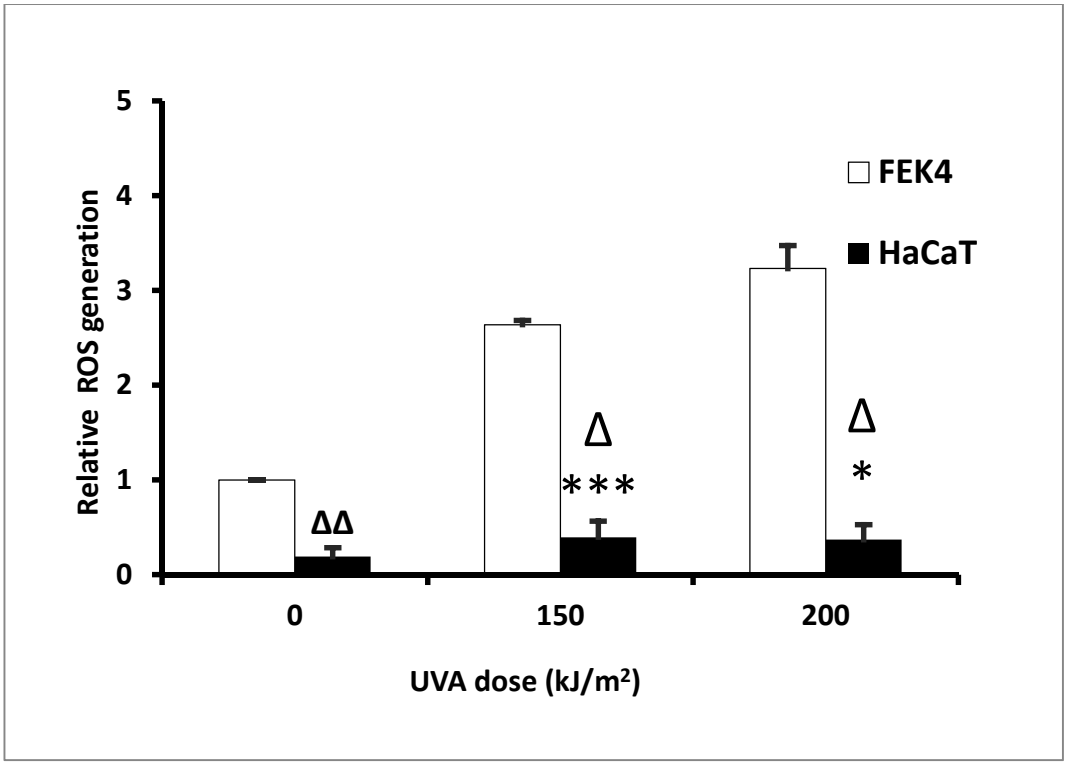

Figure 15 A direct comparison of ROS generation in FEK4 cells (□) and HaCaT (■) cells. ROS generation was measured by flow cytometry after 25 min incubation with a derivative of the fluorescein ROS dye (CM-H_2DCFDA) as described in Materials and Methods. The results of relative ROS fluorescent intensity were expressed as the fold change relative to normalized control FEK4 cells. The value (mean ± SEM) of ROS intensity for untreated FEK4 cells was set to 1 and all the other values were expressed relative to this value. The student t test was used to evaluate the statistical significance of each data point.

*P<0.05, ***p<0.001 when compared to UVA treated FEK4 cells.

Δ P< 0.05, ΔΔ p<0.01 when compared to untreated FEK4 control cells.

In summary, UVA irradiation of human skin cells results in dose-dependent ROS induction and differs between FEK4 cells and HaCaT cells. The basal level of ROS in FEK4 cells is significantly higher than that in HaCaT cells; UVA irradiation also leads to significantly stronger ROS induction in FEK4 fibroblasts compared with HaCaT cells.

The NOX activity after UVA irradiation was examined in the following section in order to further investigate if NOX is involved in UVA-mediated ROS generation as well as to determine the relative importance of NOX subunits (i.e. NOX1 and NOX4).

3.6 A comparison of UVA activated NOX activity in cultured skin cells following UVA irradiation

NOX activation was observed in human keratinocytes (Valencia and Kochevar, 2008). We have now examined whether NOX is also activated in cultured human skin fibroblasts, and compared the result with those obtained in HaCaT cells (immortalized keratinocytes). The modulation of NOX activity in skin cells following UVA treatment was determined in this section.

Firstly, we determined the dose response as well as the time response of the appearance of NOX activity after UVA irradiation of cultured human skin fibroblasts. The results in Figure 16 show that in skin fibroblasts (FEK4 cells), NOX activity was activated as a function of dose (Figure 16A) and time (Figure 16B) after UVA treatment. The results indicate that a substantial NOX activity is apparent when measurement is done as soon after irradiation as possible. A 3-fold increase in activity was seen within 5 min and the activity declined slightly over the next 30 min. The response of NOX activity to changes in UVA dose in HaCaT cells was also determined in this study, and NOX activity was observed after 150 kJ/m^2 UVA treatment (Figure 17). This activity increased with increase in UVA dose.

The results in Figure 18 are a comparison of NOX activity between FEK4 cells and HaCaT cells. NOX was strongly activated in FEK4 cells in a dose dependent manner at doses up to 150 kJ/m^2. From 200 kJ/m^2, the pattern of dose response to UVA activation was quite different between fibroblasts and immortalized keratinocytes. In fibroblasts, NOX activity started to drop down to 3 fold compared to control cells. For HaCaT cells, little NOX activation was observed at doses less than 150 kJ/m^2 and the highest activation (7 fold compared to control) was observed at 200 kJ/m^2. This result demonstrated that NOX is activated following UVA irradiation to different extents in different skin cell types.

The results in this section showed that NOX is activated following UVA irradiation in both FEK4 and HaCaT cells. The potential contribution of different subunits of NOX in both cell types was then investigated.

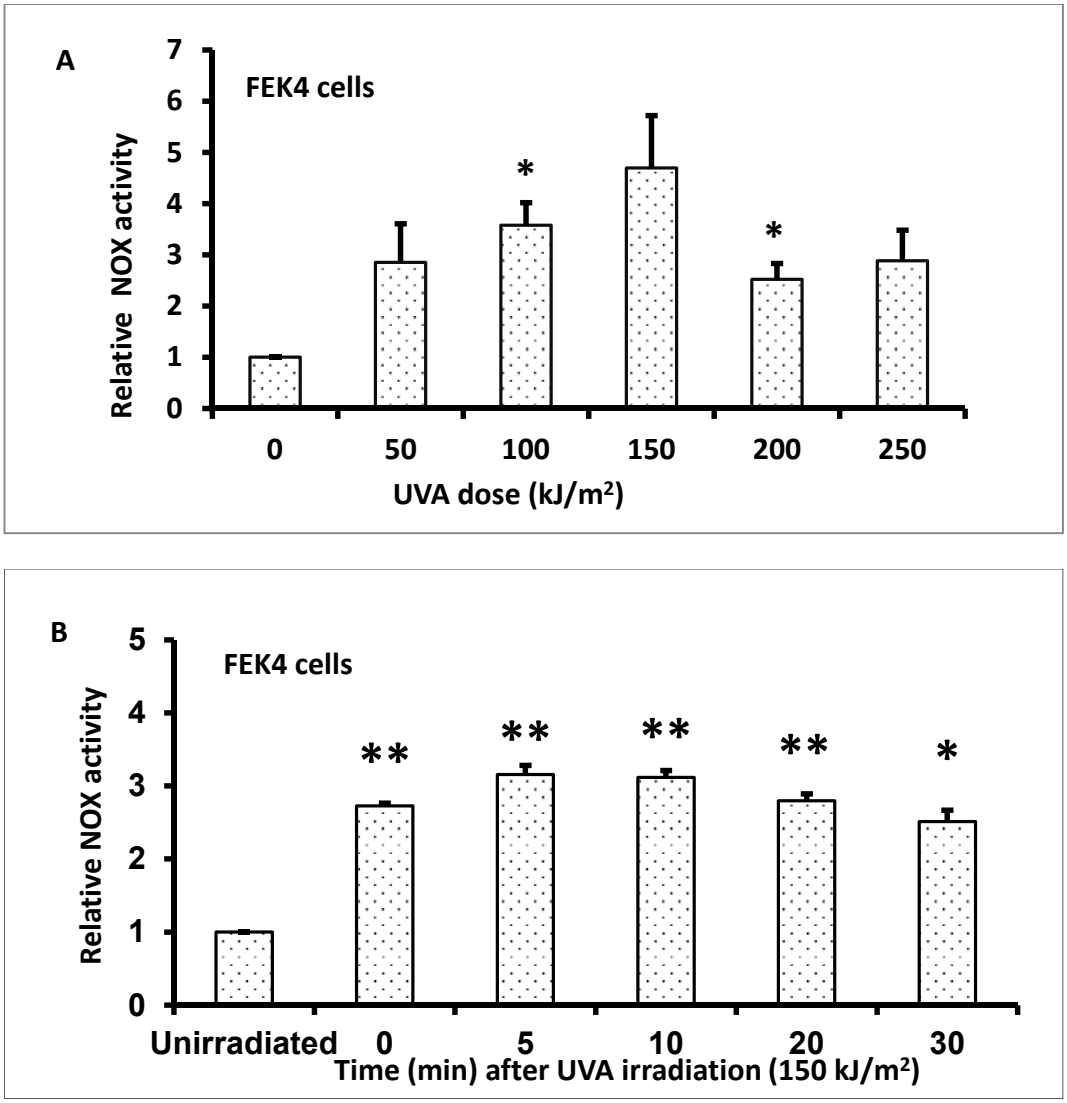

Figure 16 A: The dose response of NOX activation following UVA treatment of FEK4 cells. B: The time-dependent response of NOX activation after UVA irradiation of FEK4 cells. FEK4 cell lysates were incubated with lucigenin and NADPH for 10 min and superoxide generation was determined by measuring photoemission (using an illuminometer). Values in the bar represent the relative light emission. The Data shown are mean ± SEM (n=3). The value of NOX activity for untreated FEK4 cells was set to 1; other values were normalized to this value. The student t test was used for statistical significance of each data point. Data shown are mean ± SEM (n=3-4).

*$p<0.05$ when compared with unirradiated FEK4 control cells.

*$p<0.05$, **$p<0.01$ when compared with un-irradiated FEK4 control cells.

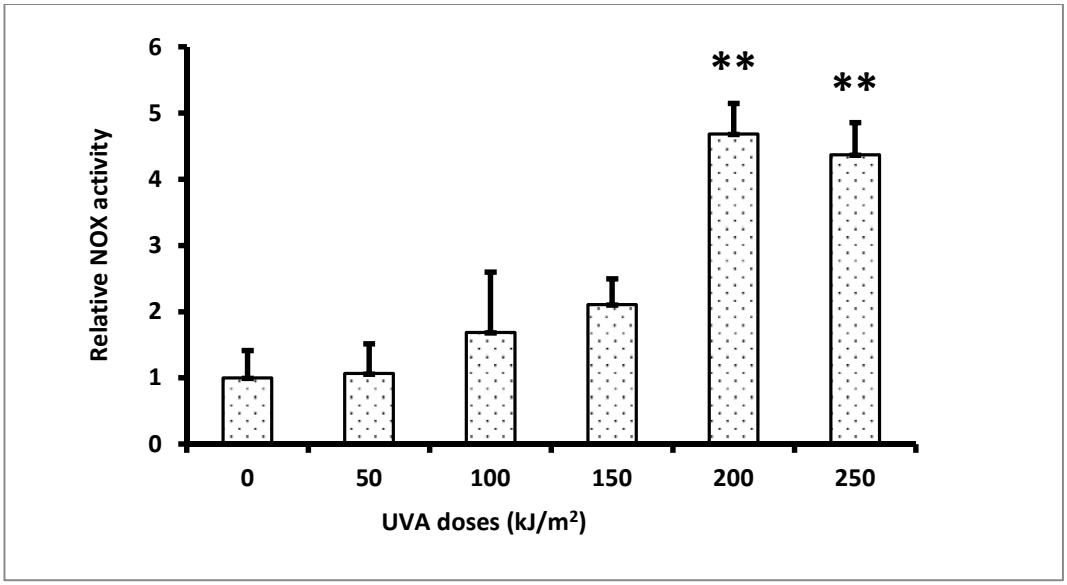

Figure 17 Dose response of NOX activation following UVA irradiation of HaCaT cells over a range of doses; HaCaT cell lysates were incubated with lucigenin and NADPH for 10 min and super oxide generation was determined from photoemission levels using an illuminometer. Data shown are mean ± SEM (n=3) relative to controlled HaCaT cells. The student t test was used for statistical significance of each data point.

** $p<0.01$ when compared with unirradiated HaCaT control cells

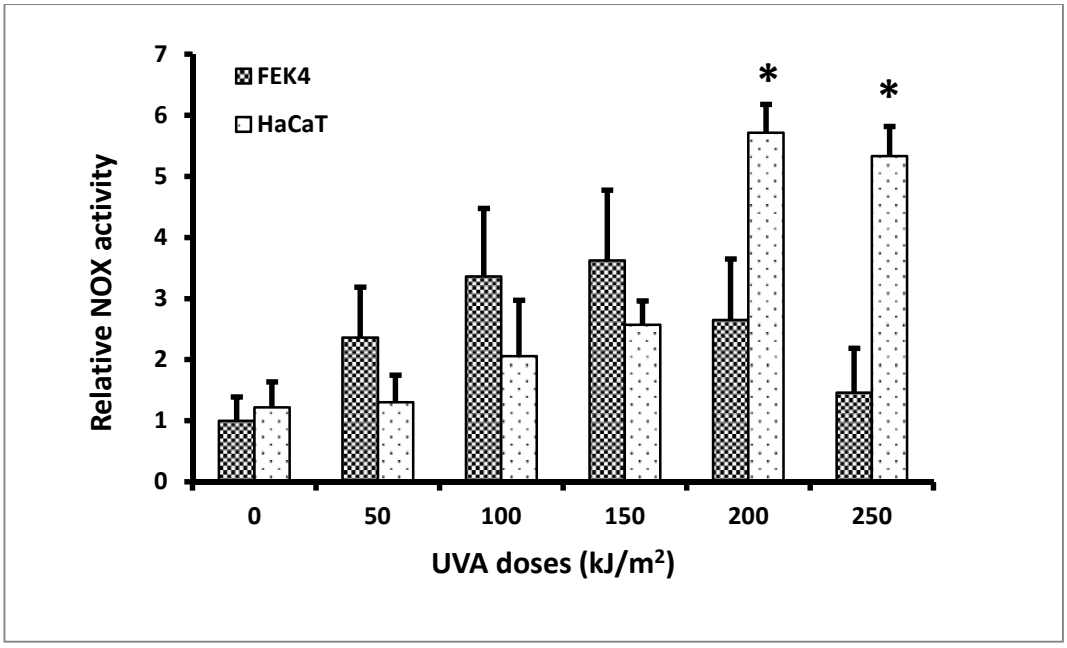

Figure 18 A comparison of UVA activation of NOX activity in FEK4 and HaCaT cells. The value for the FEK4 control cells without UVA irradiation was set to 1 and other values were expressed relative to this value. Data shown are mean ± SEM (n=3). The student t test was used to determine statistical significance of each data point.

*p<0.05 when compared with UVA irradiated FEK4 cells.

3.7 A comparison of UVA activation of NOX proteins (NOX1 and NOX4) in cultured skin cells following UVA irradiation

The results described above show that NOX is activated by UVA irradiation in both skin cell lines used although with different dose-dependencies. Considering that the NOX family includes 7 classes of proteins, we next sought to identify which NOX family members were involved in the response in each cell type. The proteins potentially involved in this response were investigated next in this study in order to further answer the question as to whether NOX is involved in the UVA-mediated ROS response. From the literature, we predicted that NOX1 and NOX4 are most likely to be involved in the UVA activation of NOX. We therefore, studied the appearance of both NOX1 and NOX4 subunits after UVA irradiation in both skin cell lines using western blots. The result (Figure 19 and Figure 20) showed that both NOX1 and NOX4 protein were involved in the activation but to different extents.

The results (Figure 19) revealed that basal levels of NOX1 protein expression are 3 fold greater in HaCaT cells than in fibroblasts. Following UVA irradiation of FEK4 cells, NOX1 protein was up-regulated up to 1.5 fold (100 kJ/m^2) compared with control cells. Meanwhile, in HaCaT cells, NOX1 expression did not change much upon UVA treatment. These results indicate that NOX1 contributed more to NOX activation in UVA-induced FEK4 cells.

The NOX4 subunit has also been extensively studied relative to the other family members. The activation of NOX4 in fibroblasts has been related to oxidative stress (Goyal et al., 2005; Schroder et al., 2012). So it was logical to examine NOX4 expression in cultured human skin cells following UVA irradiation. The results shown in (Figure 20) are consistent with the possibility that NOX4 contributes to NOX activation in HaCaT cells, but not in FEK4 cells.

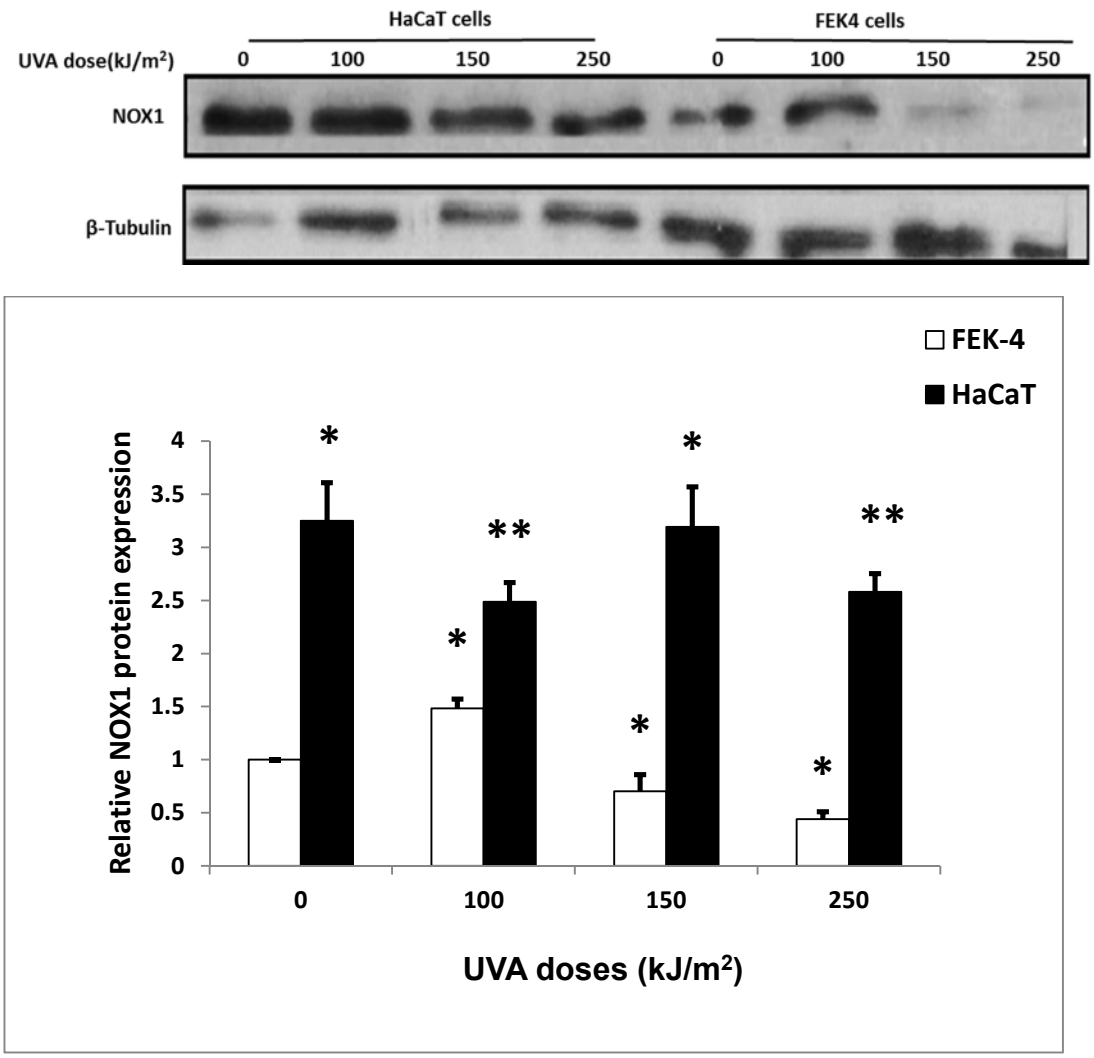

Figure 19 A comparison of NOX1 protein expression in two skin cell types (FEK4 and HaCaT) after UVA irradiation. NOX1 protein expression in skin cells was measured by western blot as described in Materials and Methods. Values in the column represent the optical density of each band as detected by chemiluminescence and analysed using ImageJ. The results are shown as the mean ± SEM (n=3). The value for untreated FEK4 control cells was set to 1 and other values were expressed relative to this value. The student t test was used to determine the statistical significance of each data point.

*p<0.05 when compare to untreated FEK4 cells.

** p<0.01 when compared to untreated FEK4 cells.

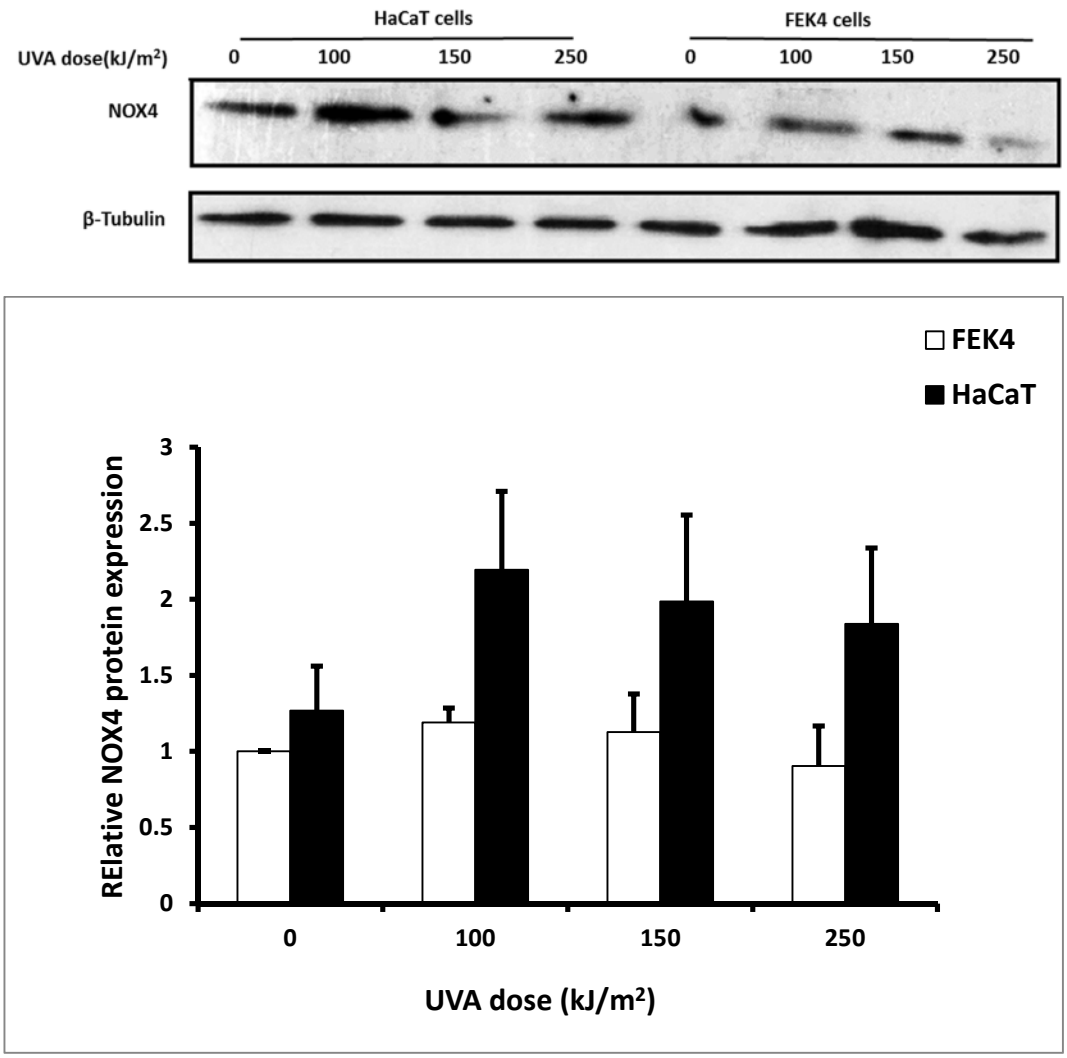

Figure 20 A comparison of NOX4 protein expression in two skin cell types (FEK4 and HaCaT) after UVA irradiation. NOX4 protein expression in skin cells was measured by western blot as described in Materials and Methods. Values in the column represent the optical density as detected by chemiluminescence and analysed using ImageJ. The results are shown as the mean ± SEM (n=3). The value for untreated FEK4 control cells was set to 1 and other values were expressed relative to this value. The student t test was used to determine the statistical significance of each data point.

Basal level of NOX4 protein expression was not significantly different between the two skin cell types. However, following UVA radiation treatment, NOX4 expression in HaCaT cells was up-regulated 2 fold compared with FEK4 cells. These results indicate that NOX4 contributes more to NOX activation in UVA-irradiated HaCaT cells than in UVA-irradiated fibroblasts.

In summary, NOX1 and NOX4 protein expression are up-regulated to different extents in these two skin cells lines, but NOX1 and NOX4 subunits are clearly both involved in the UVA-induced NOX activation process.

To further investigate whether NOX is involved in the process of UVA-induced ROS generation, NOX inhibition experiments were carried out using NOX inhibitors (diphenylene iodonium, plumbagin and siRNAs for NOX1 and NOX4). In this way we could determine the effect of inhibition of NOX on UVA-induced ROS generation.

3.8 Effects of NOX inhibitors on UVA-mediated ROS generation.

As mentioned in the introduction, diphenylene iodonium (DPI) has been widely used as a general NOX inhibitor and plumbagin has been used as a NOX4 inhibitor. Therefore, DPI is employed in this study for general NOX inhibition and plumbagin was initially used for inhibiting NOX4. Inhibiting NOX using DPI abolished the UVA-induced ROS generation.

However, treatment with plumbagin led to more complex effects and siRNAs for both NOX1 and NOX4 were also employed in this study in order to achieve more specific inhibitory effects.

Effect of DPI pre-treatment on UVA-mediated ROS generation in skin cells

Valencia and Kochevar (2008) have shown that DPI pre-treatment of skin keratinocytes decreased UVA-induced ROS generation event at the lowest (1 μM) DPI concentration used. This concentration was used for the remaining experiments. We have found that DPI pre-treatment also reduced UVA-induced ROS generation in skin fibroblasts, a result consistent with NOX involvement in UVA-induced ROS generation in fibroblasts.

NOX was inhibited using DPI and the inhibitory effect on ROS generation in cultured human skin fibroblasts (FEK4 cells) was then determined by flow cytometry. The results (Figure 21) showed that in DPI pre-treated FEK4 cells, UVA induced ROS generation was completely prevented even at the lowest DPI concentration (1 μM). After 250 kJ/m^2, ROS were induced to 2 fold higher levels than unirradiated control cells. With DPI pre-treatment, at concentrations as low as 1 μM, the ROS generation by UVA was diminished to basal level. The same effect was found in the cells with the higher concentrations (i.e. 5, 10 and 20 μM) employed in this study. The UVA-induced ROS level dropped slightly below the basal level at 20 μM. The maximum concentration used (20 μM) only slightly affected the basal ROS level of un-

irradiated cells. In addition, interestingly, we found that ROS generation was cell confluency dependent (with or without DPI treatment) following UVA irradiation of skin fibroblasts.

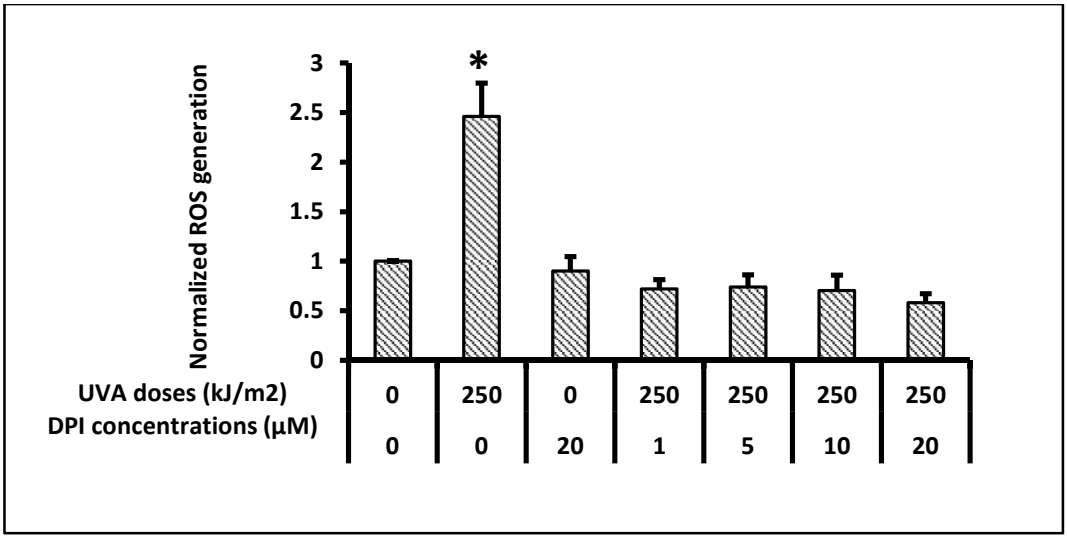

Figure 21 ROS generation in UVA irradiated FEK4 cells following pre-treatment with DPI. FEK4 cells were pre-treated with different concentrations of DPI for 1 h before UVA treatment. ROS generation was measured by Flow cytometry after 25 min incubation with a derivative of the fluorescein ROS dye (CM-H_2DCFDA) as described in Materials and Methods. The values represent mean ± SEM (n=3). The value of ROS intensity for untreated FEK4 cells was set to 1; all the other values were expressed relative to this control.

*$p<0.05$ when compare to untreated FEK4 cells.

A skin cell confluency effect on UVA-induced ROS generation (with or without NOX inhibition)

During this study, we also found an interesting phenomenon concerning a confluency effect on ROS generation in skin fibroblasts treated with UVA (with or without DPI pre-treatment). The results show that the level of ROS generation following UVA irradiation of skin fibroblast is confluency dependent.

FEK4 cells were seeded at two different starting numbers in 3 cm dishes on the same day before UVA treatment to reach a different density. The results (Figure 22) showed that ROS were induced by UVA treatment at both confluences. However, irradiation of cells with 100 kJ/m^2 UVA at the higher confluence generated less ROS than UVA irradiation at the lower confluence but the effect was the opposite at 200 kJ/m^2.

Notably, with the DPI treatment in subconfluent cells (i.e. 50%), the ROS induction increased with increase in UVA dose (Figure 23). On the day of treatment, the subconfluent FEK4 cells were treated with or without DPI followed by UVA irradiation. The results showed that in FEK4 cells pre-treated with DPI at a lower density (Figure 23), the increase in ROS induction by UVA is higher than in the non-DPI pre-treated FEK4 cells. Consistent with the results at lower density, FEK4 cells are more sensitive to UVA–induced ROS generation; one possible explanation for this is that DPI enhances the sensitivity to ROS generation when the cells are under sensitive conditions. There is evidence for DPI induced ROS generation at higher concentrations (5 μM) and longer durations (1h) in human promyelocytic leukaemia cells (Li et al., 2003b).

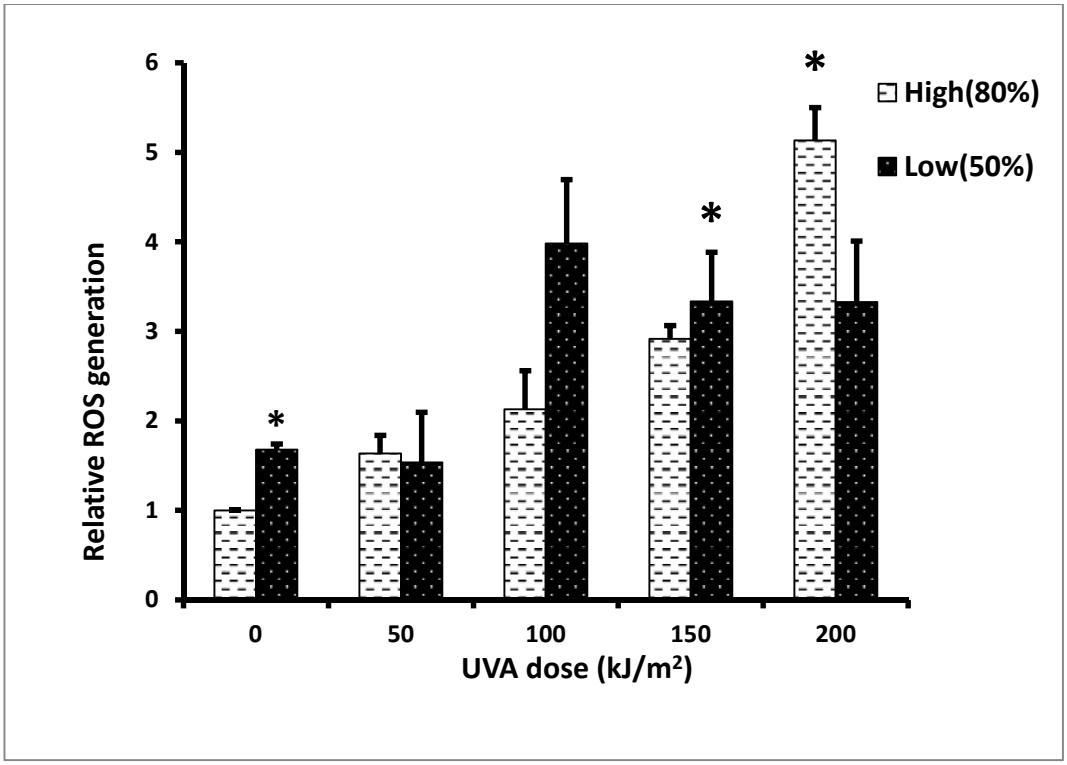

Figure 22 The effect of confluence on ROS induction after UVA irradiation of FEK4 cells. ROS generation was measured by flow cytometry after 25 min incubation with a derivative of the fluorescein ROS dye (CM-H_2DCFDA) as described in Materials and Methods. Values represent mean ± SEM. The data are shown as the relative change in ROS generation relative to non-irradiated FEK control cells grown to the higher density (80%). The value of ROS generation for untreated FEK4 cells (80% density) was set to 1 and all the other values were expressed relative to this value. The Student t test was used to evaluate the statistical significance of each data point.

*$p<0.05$ when compared to higher density of FEK4 cells.

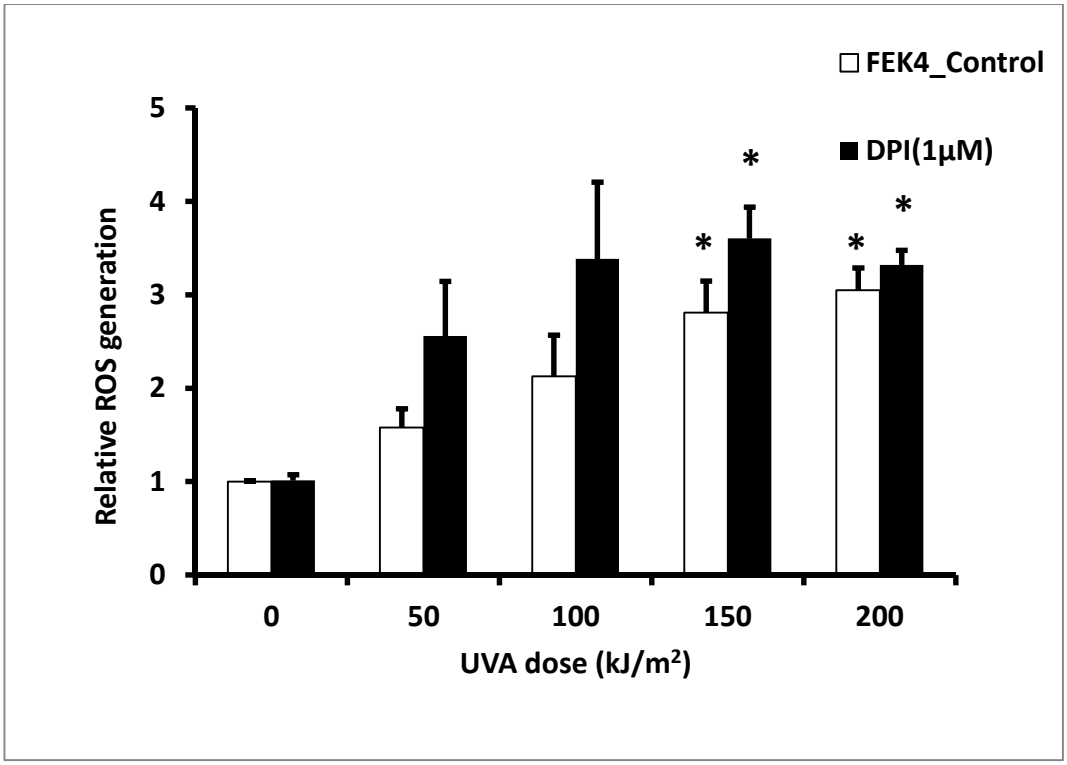

Figure 23 ROS generation after UVA irradiation of FEK4 cells at the lower density (50%) with DPI (1 µM) pre-treatment. The values represent mean ± SEM (n=3). ROS generation was measured by flow cytometry after 25 min incubation with a derivative of the fluorescein ROS dye (CM-H_2DCFDA) as described in Materials and Methods. The value of ROS generation for untreated FEK4 cells (50% density) was set to 1 and all the other values were expressed relative to this value. The Student t test was used to evaluate the statistical significance of each data point.

*$p<0.05$ when compared to untreated control cell.

In summary, a general NOX inhibitor (DPI) decreased UVA-induced ROS generation in FEK4 cells. As NOX inhibition using the general inhibitor DPI abolished the UVA-induced ROS, it demonstrated that NOX may also be involved in the UVA-mediated ROS generation in skin fibroblasts. Since UVA-induced ROS generation is also inhibited by the NOX inhibitor DPI in cultured human skin fibroblasts, we questioned which NOX family protein may contribute to this process. As the earlier results of this study showed that both NOX1 and NOX4 contribute to UVA-induced NOX activation, we focused on these two NOX proteins to determine if they are involved in UVA-induced ROS generation. The effect of the NOX4 inhibitor (plumbagin) on ROS generation in FEK4 cells treated with UVA was first measured by flow cytometry.

Inhibiting effects of NOX4 inhibitor (plumbagin) pre-treatment on UVA-mediated ROS generation in skin.

Among the 7 NOX classes of proteins, NOX1 and NOX4 have been the most widely studied subunits in relation to ROS events so far. According to previous studies (Valencia and Kochevar, 2008), NOX1 was considered as a major source of ROS generation following UVA irradiation of skin keratinocytes; NOX4 has been shown to be involved in the ROS generating events in human dermal fibroblasts (Rossary et al., 2007). Based on these findings, the role of NOX1 and NOX4 subunits in UVA-mediated ROS generation was determined. We inhibited NOX4 using plumbagin in cultured human skin cells to determine NOX4 involvement in UVA-induced ROS generation. The results in plumbagin pre-treated skin cells that were treated with UVA irradiation were complex.

Skin cells were pre-treated with plumbagin and then UVA irradiated. The cells were then incubated with CM-H_2DCFDA and ROS generation was measured. Surprisingly, there is a significant induction of ROS generation in both plumbagin pre-treated non-irradiated FEK4 cells (Figure 24) and HaCaT (Figure 25) cells. Nevertheless, plumbagin considerably reduced the UVA-induced ROS induction in both skin cell lines upon UVA treatment.

In FEK4 cells (Figure 24), ROS induction was observed as expected after UVA treatment in non-plumbagin treated cells compared to control cells. However, in non-irradiated plumbagin pre-treated cells, substantive ROS generation was induced by the plumbagin pre-treatment alone. Nevertheless, with UVA treatment, ROS induction by UVA was considerably reduced to below basal levels. Similarly, in HaCaT cells (Figure 25), ROS induction was again observed in non-plumbagin treated cells compared to control cells. In un-irradiated HaCaT cells, plumbagin strongly induced ROS generation even at the lowest concentration (1 µM). This result established that plumbagin alone induced ROS in skin cells although to different extents. The results indicate that although plumbagin is inhibiting ROS generation by UVA, it also induced

ROS generation by itself, which will confound interpretation. In order to further explore this phenomenon, ROS generation in non-irradiated skin cells treated with plumbagin as well as the reduction of UVA-induced ROS by plumbagin was examined using flow cytometry.

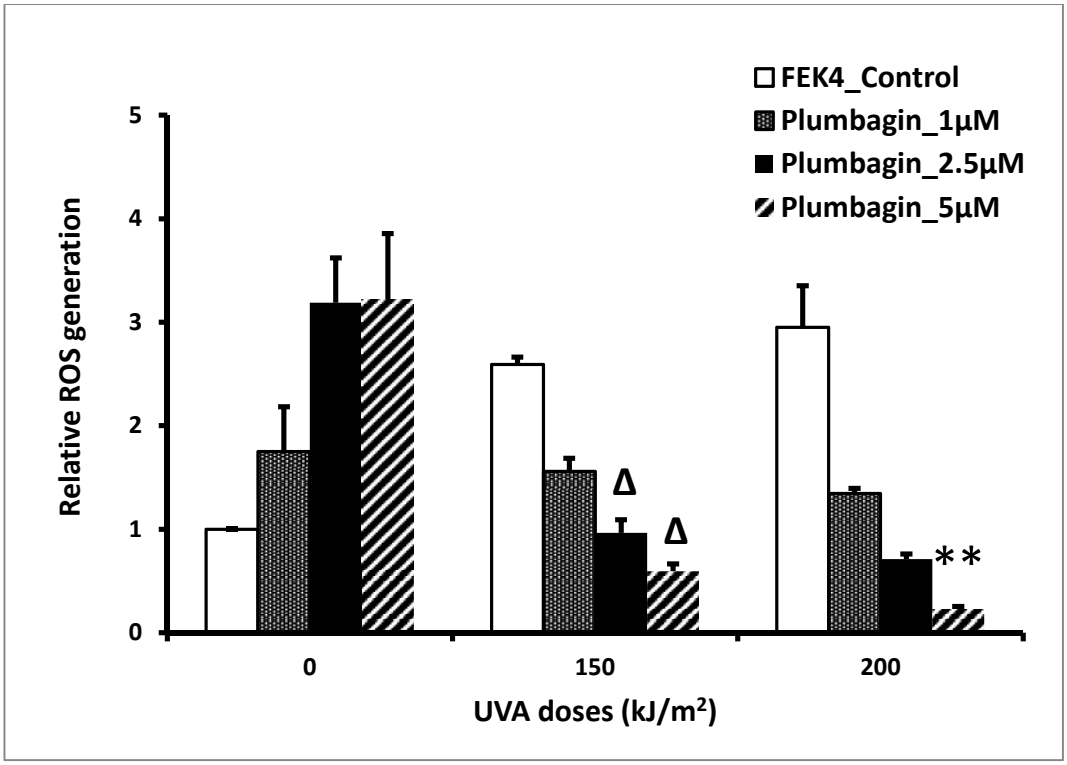

Figure 24 ROS generation after UVA irradiation of FEK4 cells with and without plumbagin pre-treatment. FEK4 cells were pre-treated with and without plumbagin for 10 min followed by UVA irradiation. ROS generation was measured by flow cytometry after 25 min incubation with a derivative of the fluorescein ROS dye (CM-H_2DCFDA)The values of ROS fluorescent intensity were expressed relative to control FEK4 cells Data are shown as the mean ± SEM (n=3). Statistical analysis was performed by the Student t test.

** $p < 0.01$ when compared with untreated FEK4 control cells.

Δ $p < 0.05$when compared with UVA irradiated cells.

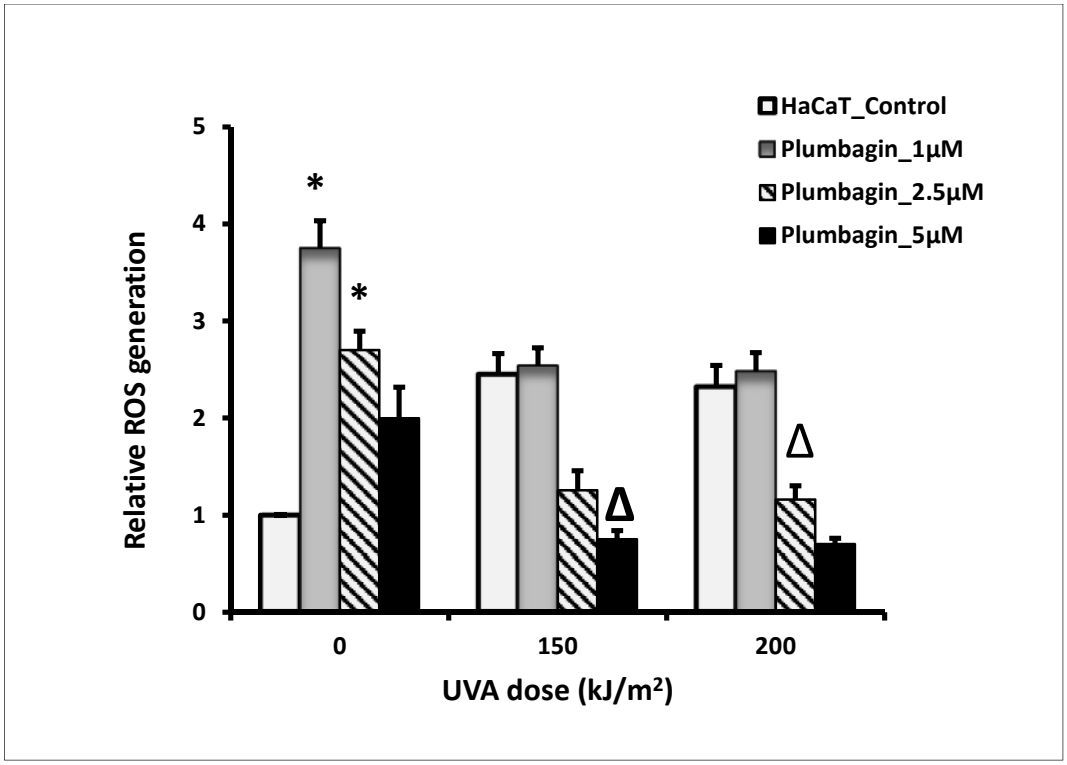

Figure 25 ROS generation after UVA irradiation of HaCaT cells with and without plumbagin pre-treatment. HaCaT cells were pre-treated with and without plumbagin for 10 min followed by UVA irradiation. ROS generation was measured by flow cytometry after 25 min incubation with a derivative of the fluorescein ROS dye (CM-H_2DCFDA). The results of ROS fluorescent intensity were expressed relative to control HaCaT cells. Data are shown as mean ± SEM (n=3). Statistical analysis was performed by the student t-test.

* $p < 0.05$ significant difference when compared with untreated FEK4 control cells.

Δ $p<0.05$ significant difference when compared with UVA irradiated cells.

Analysis of apoptosis and necrosis in UVA irradiated cells which have been pre-treated with plumbagin

Plumbagin treatment of cells results in a complex response with an expected effect on UVA activation of ROS. Plumbagin treated skin cells induced ROS generation in the absence of UVA treatment so that the analysis of the effect of pre-treatment with plumbagin or UVA induced ROS is more complicated. In order to find out whether plumbagin induced ROS leads to skin cell damage, the level of skin cell death (i.e. apoptosis and necrosis) was analysed by dual stain flow cytometry.

Apoptosis and necrosis are two pathways of cell death. Apoptosis often starts with cell membrane damage but with membrane integrity maintained, necrosis starts with loss of the membrane integrity. Dual staining with annexin V-FITC (AV) and propidium idodide (PI) were employed in this study to distinguish apoptotic from necrotic cells. As a nuclear binding dye, PI stains the nuclei of those cells that have lost their membrane integrity as a result of undergoing necrosis. As a protein dye, AV will bind to externalized phosphatidylserine when cells are in the early stage of apoptosis.

Human cultured skin cells were pre-treated with plumbagin followed by UVA irradiation (150 kJ/m^2); cells were then collected and stained with AV and PI for flow cytometry analysis. The results shown (Figure 26-29) represent the analysis of cell death by flow cytometry. The results are presented in two ways (dot plot graphs and data charts). Apoptotic and necrotic cell death are observed in FEK4 cells and HaCaT cells following plumbagin treatment both with and without UVA irradiation.

FEK4 cells undergo increased necrosis after 2.5 μM plumbagin treatments alone whereas the apoptotic population is decreased (Figure 27). A lower concentration of plumbagin (1 μM) as well as UVA treatment increases necrosis of FEK4 cells. This necrosis increased further at higher concentrations of plumbagin (2.5 μM) pre-treatment; however, UVA induced apoptosis almost disappeared after 2.5 μM pre-treatment (Figure 27). Similarly,

in HaCaT cells (Figure 29), plumbagin pre-treatment alone led to increased necrosis (up to 59.2%) at higher plumbagin concentration (2.5 μM). At a lower concentration of plumbagin (1 μM) and with UVA treatment, the necrosis increased up to 77.3%. This necrosis dramatically increased further to 94.3% at a higher concentration of plumbagin (2.5 μM). Similar to FEK4 cells, the apoptosis almost disappeared after 2.5 μM pre-treatment (Figure 29).

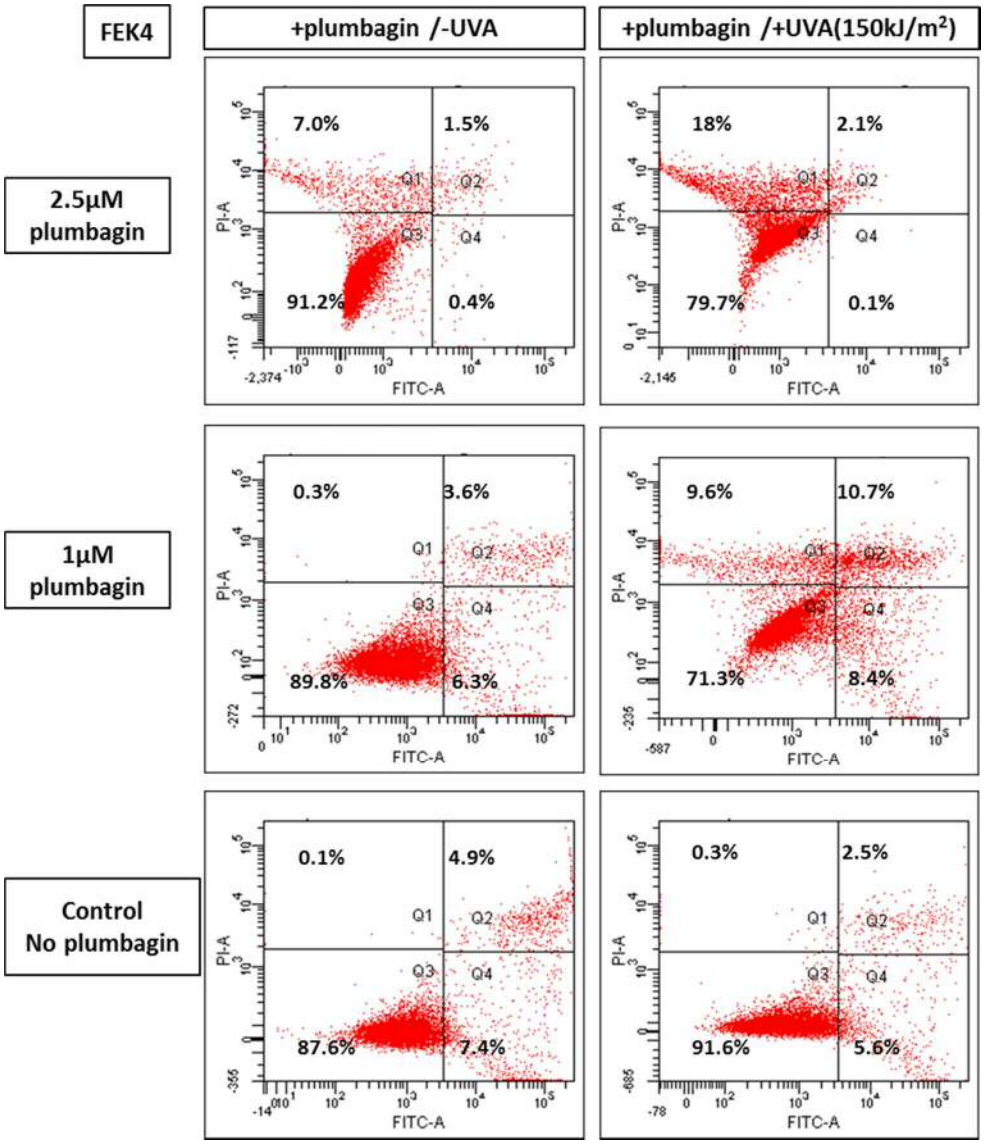

Figure 26 Flow cytometry analyses of plumbagin pre-treated FEK4 cells with and without UVA irradiation. FEK4 cells were pre-treated with and without plumbagin for 10 min followed by UVA irradiation (right column). FEK4 cells were dual stained with PI and AV before measurement. The percentage of apoptotic and necrotic cell death was scored by flow cytometry. The plots represent the fluorescence intensity of individual cells in the cell population. Numbers shown are the percentage of cells in each quadrant. In this study (n=1), PI positive (Q1) and AV positive cells (Q2) were considered necrotic cells; PI negative but AV positive cells were considered apoptotic cells (Q4). Both PI and AV negative cells were considered Live cells (Q3). PI-Area (PI-A) represent the PI fluorescence intensity.

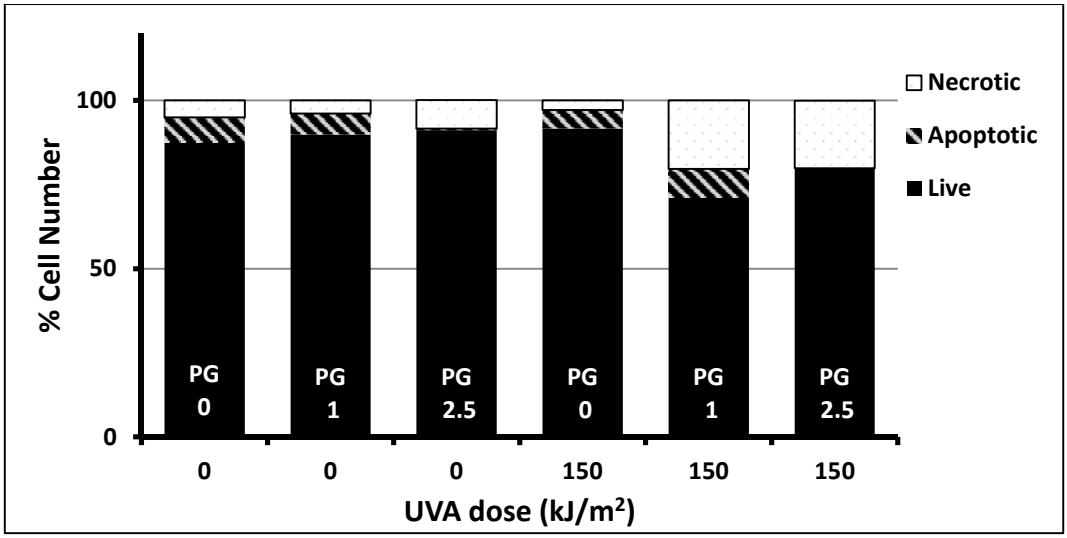

Figure 27 Flow cytometry analyses of plumbagin pre-treated FEK4 cells with and without UVA irradiation. The bars show the percentage of apoptotic and necrotic cells induced 4 h after UVA irradiation following plumbagin pre-treatment of FEK4 cells. Data shown are as a percentage of total cells under each condition (n=1). Plumbagin (PG) concentration (μM) is indicated in each bar.

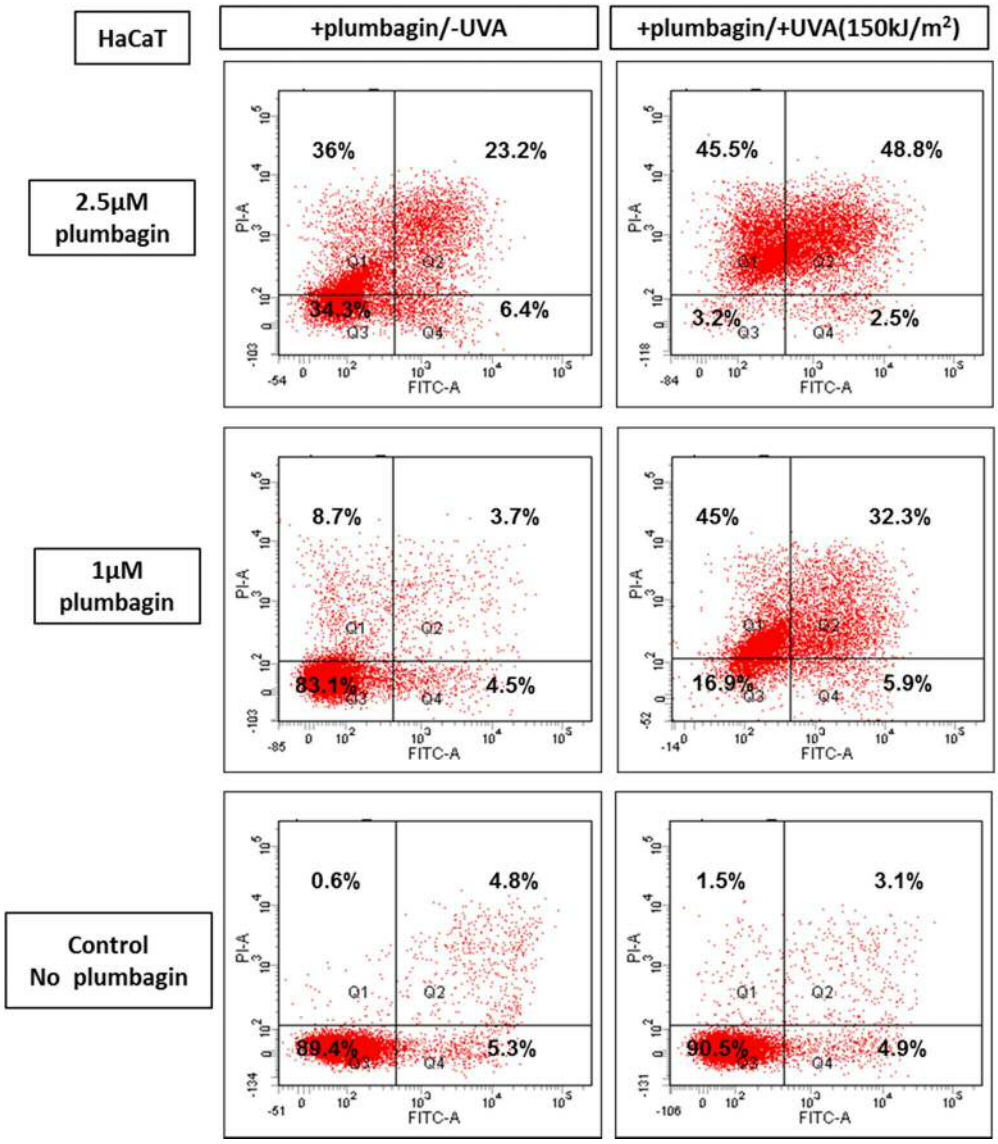

Figure 28 Flow cytometry analyses of plumbagin pre-treated HaCaT cells with and without UVA irradiation. HaCaT cells were pre-treated with and without plumbagin for 10 min incubation followed by UVA irradiation (right column). FEK4 cells were dual stained with PI and AV before measurement. The percentage of apoptotic and necrotic cell death was scored by flow cytometry. The fluorescence intensity of individual cells in the population is plotted. Numbers shown are the percentage of cells in each quadrant. In this study (n=1), PI positive (Q1) and AV positive cells (Q2) were considered as necrotic cells; PI negative but AV positive cells were considered apoptotic cells(Q4). Both PI and AV negative cells were considered live cells (Q3). PI-Area (PI-A) represent the PI fluorescence intensity.

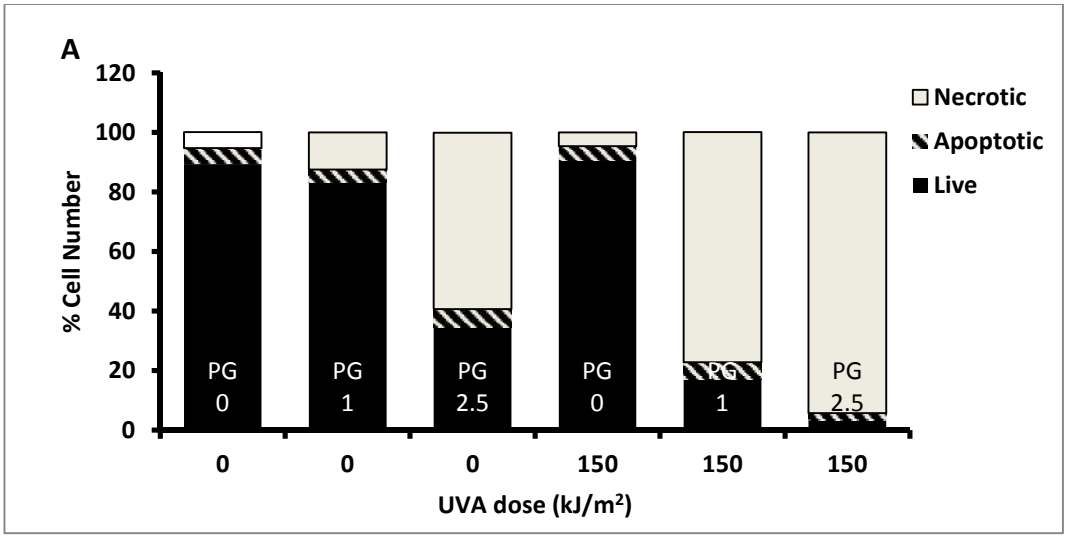

Figure 29 Flow cytometry analyses of plumbagin pre-treated HaCaT cells with and without UVA irradiation (n=1). The bars show the percentage of apoptotic and necrotic cells induced 4 h after UVA irradiation following plumbagin pre-treatment of HaCaT cells. Data shown are as a percentage of total cells under each condition. Plumbagin (PG) concentration (μM) is indicated in each bar.

To summarise, in skin fibroblasts, plumbagin alone induced ROS generation and led to necrosis. Plumbagin abolished UVA generated ROS and led to further necrosis. In HaCaT cells (as in FEK4), plumbagin strongly induced ROS generation at a lower concentration (1 μM) leading to necrosis. With UVA treatment, although plumbagin decreased the ROS generation, this reduction led to a stronger cell death. Thus, these results revealed that although plumbagin largely abolished UVA-induced ROS generation even under basal level, this reduction resulted in necrosis.

The results obtained in the plumbagin treatment experiments demonstrate a toxic effect of plumbagin on UVA irradiated skin cells. They also showed that plumbagin decreased ROS induction by UVA irradiation and that this was unrelated to a protective effect.

In this section, we provide evidence that a general inhibitor of NOX inhibits UVA-induced ROS generation. We hypothesised that NOX4 may contribute to this process, so that plumbagin treatment which would inhibit NOX4 would abolish the UVA-mediated ROS generation. However, the results of NOX4 inhibition using plumbagin show effects of the drug itself which confounded interpretation. Based on these results and to further investigate the NOX subunits involved, small interfering RNA (siRNA) were employed for targeting NOX1 and NOX4 to achieve more specific NOX inhibitory effects.

3.9 Effect of NOX1/NOX4 gene knockdown on ROS generation after UVA irradiation of skin cells.

Since both NOX1 and NOX4 protein expression are up-regulated in both skin cell types, the specific role of NOX1 and NOX4 protein in the process of UVA induced ROS generation was investigated using siRNA to knock down expression of each of the genes. First of all, the efficiency of knocking down each of the genes was examined in cultured skin cells using various parameters.

Efficiency of siRNA knocking down of NOX1 and NOX4

Human cultured skin cells were seeded and transfected with siRNAs, and then incubated for 48 h. The efficiency of the knock down using siRNAs for NOX1 and NOX4 in cultured human skin cells (FEK4 and HaCaT) were detected at various levels which are: cellular level as measured by confocal imaging, protein expression level as measured by western blot and NOX enzymatic activity level as measured by NOX activity assay. The results showed high siRNA delivery efficiency at different levels in both skin cell types (Figure 30-34).

As shown in Figure 30, the efficiency of siRNA delivery into cells was measured by confocal imaging; the results showed that the siRNAs were successfully delivered into both FEK4 cells and HaCaT cells using the siRNA transfection method employed in this study (as described in Material and Methods). The fluorescent tagged sisb RNA was observed to localize inside the cells 48 h after transfection.

The efficiency of siRNA in changing NOX activity level and protein level were also checked in this study and the results obtained are shown in Figure 31-34. In FEK4 cells, the NOX activity reduced to almost half of the untreated control

cell level after treatment of FEK4 cells with a mixture of siNOX1 + siNOX4 (48 h) RNAs (Figure 31). We chose the 48 h incubation time for the remaining study. Treatment with siNOX1 or siNOX4 RNA individually already decreased NOX1 or NOX4 activity by 50% compared with the untreated control FEK4 cells (Figure 32). Treatment with siNOX1 reduced the NOX1 protein expression level to 70% of the level in untreated cells (Figure 32A). Treatment with siNOX4 reduced the NOX4 protein expression level to 50% of the level in untreated cells (Figure 32B).

In HaCaT cells, the NOX activity was reduced by more than half of the untreated control cells after treatment with siNOX1 alone and siNOX4 treatment reduced the NOX activity to around 40% of untreated control cell levels (Figure 32B). This suggests that NOX1 and NOX4 contribute to NOX activity in HaCaT cells. Interestingly, neither siNOX1 nor siNOX4 significantly reduced the NOX1 or NOX4 protein expression levels (Figure 34). Silencing NOX1 and NOX4 genes may have different effects at the protein level and activity level.

In summary, the results in this section showed that siRNA can be delivered successfully into skin cells using the transfection method employed in this study. Transfection of siNOX1 or siNOX4 RNAs using a similar methodology results in a large reduction of the activity and protein expression levels of NOX1 and NOX4, respectively. These results demonstrate the efficiency of the knock down approach in inhibiting the targeted subunits.

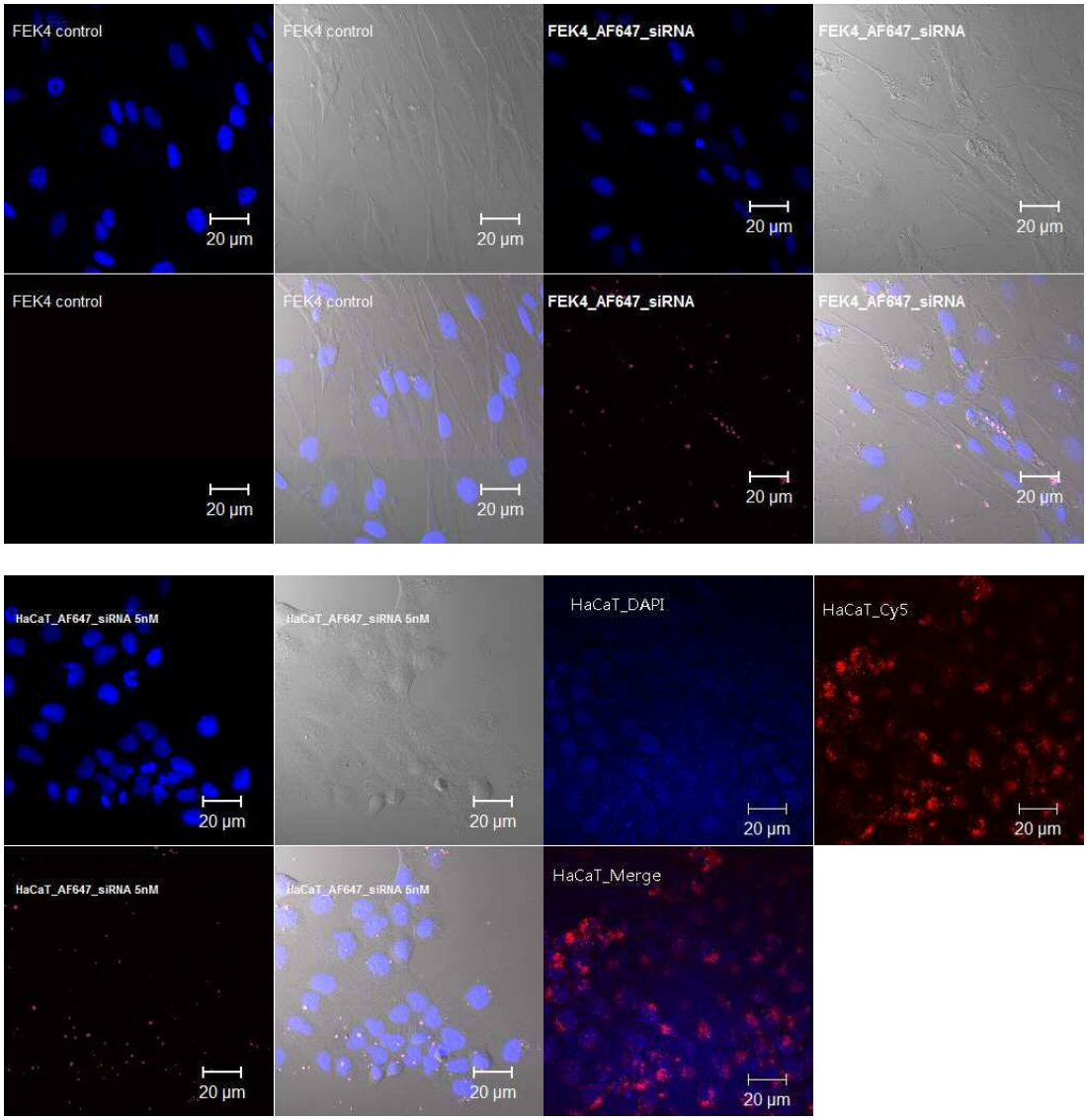

Figure 30 Confocal microscopy cell imaging of siRNA delivery in skin cells. A: siRNA delivery in FEK4 cells. A: siRNA delivery in HaCaT cells. Alexa Fluor 647 or Cy5 labelled scrambled siRNA (5 nM) were transfected into FEK4 and HaCaT cells and incubated for 48 h; cells were then fixed and stained with DAPI nuclear stain after mounting on microscope slides. The confocal images were captured with an x60 oil lens of a Zeiss META 510 confocal microscope as described in Material and Methods. The fluorescent intensity detected in the confocal imaging shows siRNAs localized within the FEK4 and HaCaT cells. Blue is nuclear stained by DAPI, red is either Alexa Fluor 647 or Cy5 labelled siRNA.

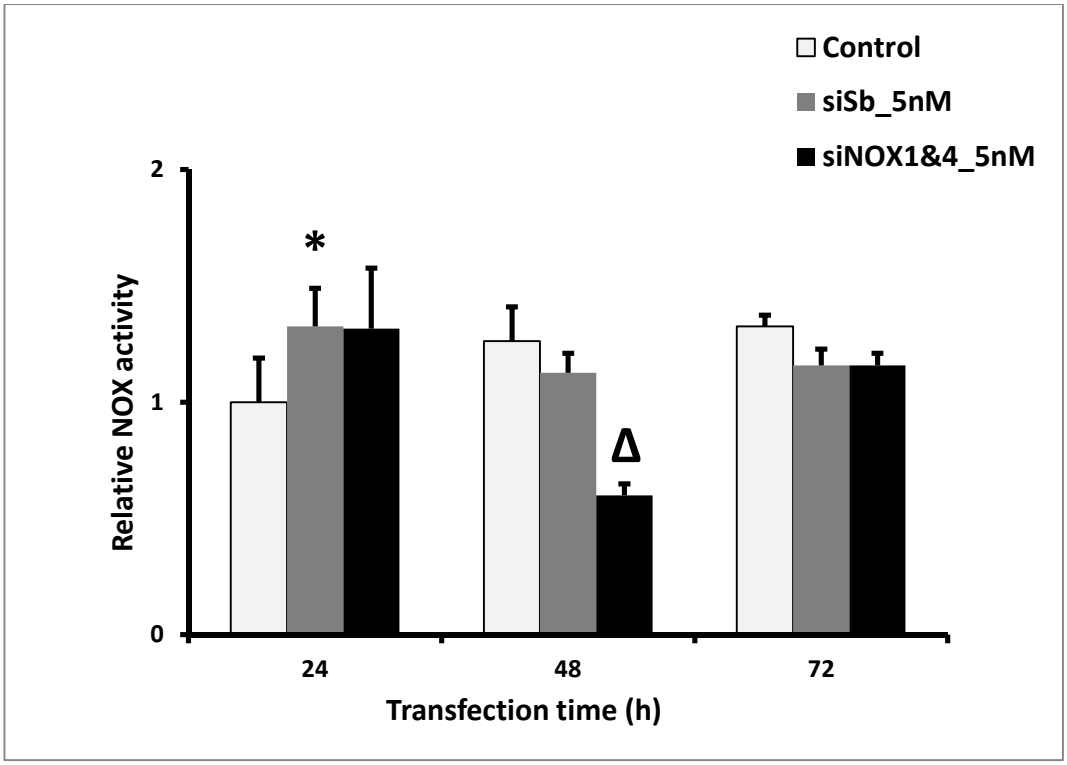

Figure 31 The effect on NOX activity of adding a mixture of NOX1 and NOX4 siRNA to FEK4 cells as a function of transfection time. A mixture of siRNAs (5 nM) for NOX1 and NOX4 were transfected into FEK4 cells and incubated for the indicated times (24, 48 and 72 h). NOX activity was then determined using the lucigenin assay as described in 2.11. Values in the bar represent the relative NOX activity with respect to untreated FEK4 cells. Data shown are mean ± SEM (n=3). The student t test was used for analysis of statistical significance of each data point.

* $p<0.05$ significant difference from no siRNA treated FEK4 control cells.

Δ $p<0.05$ significant difference from scrambled siRNA treated FEK4 cells.

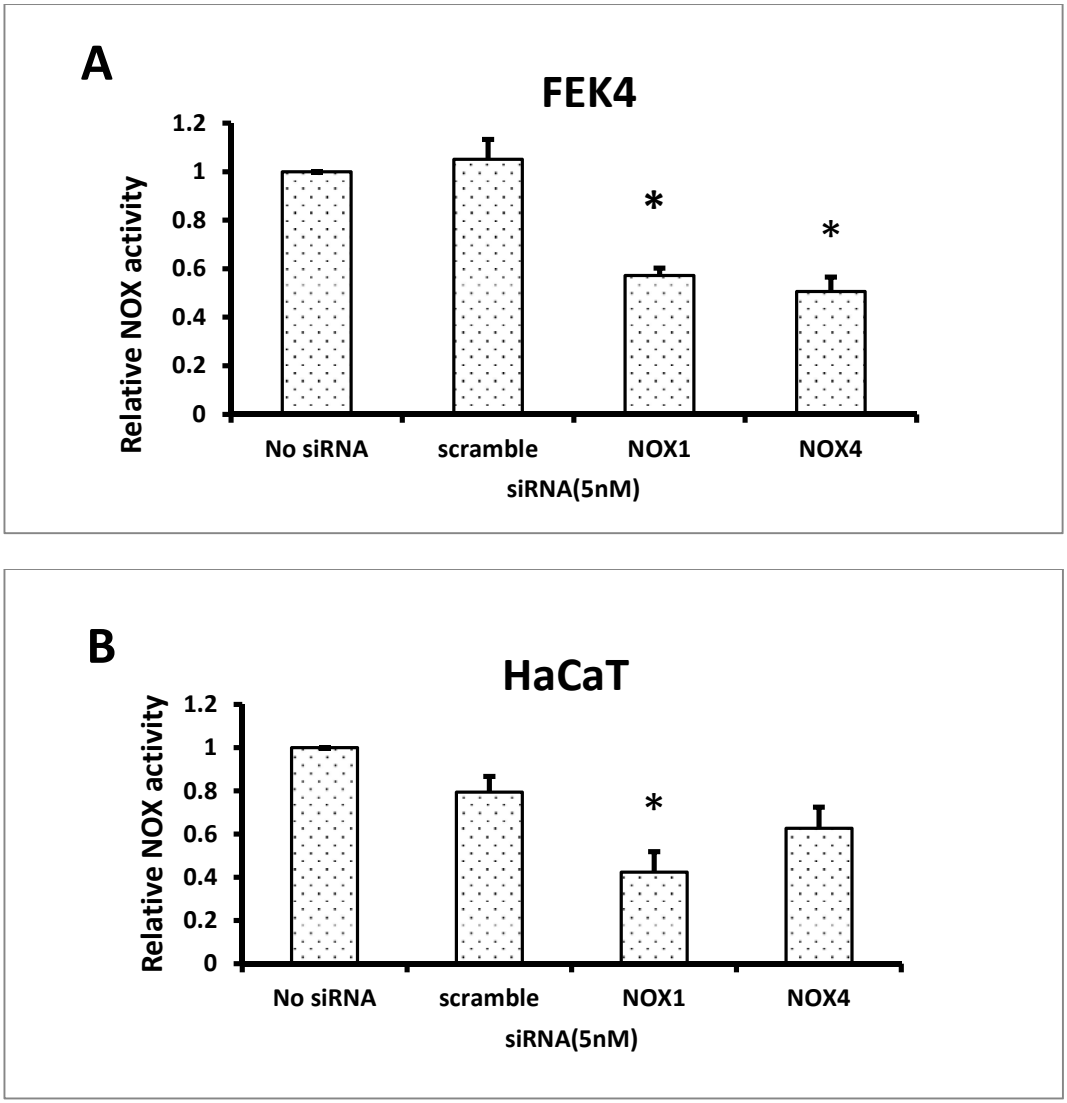

Figure 32 The effect of adding NOX1 or NOX4 siRNAs on the NOX activity of cultured skin cells. A): siNOX1 or siNOX4 effect on NOX activity in FEK4 cells. B): siNOX1 or siNOX4 effect on NOX activity of HaCaT cells. siRNAs for NOX1 or NOX4 were transfected into cells and incubated for 48 h. NOX activity was then determined using the lucigenin assay as described in Materials and Methods. Values in the bar represent the NOX activity relative to the untreated control cells (set to 1). Data shown are mean ± SEM (n=3). Other values were normalized to this value. The student t test was used for the analysis of statistical significance of each data point.

* $p<0.05$ significant difference when compared to untreated control.

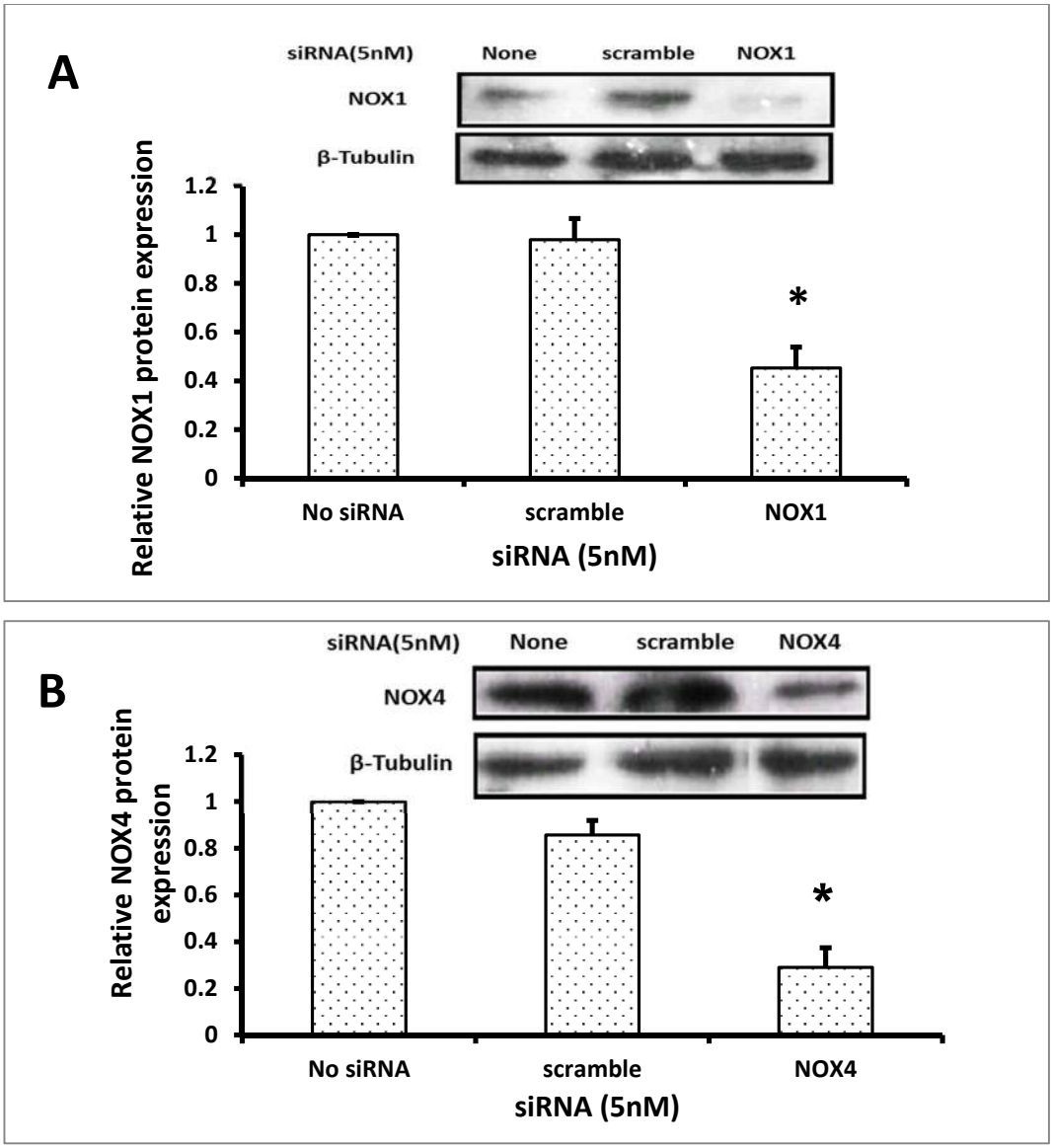

Figure 33 The effect of siNOX1 or siNOX4 on NOX1 and NOX4 protein expression in FEK4 cells. A: siNOX1 effect on NOX1 protein expression of FEK4 cells. B: siNOX4 effect on NOX4 protein expression of FEK4 cells. siRNAs for NOX1 or NOX4 were transfected into FEK4 cells and incubated for 48 h. The NOX protein expression of each sample was determined by western blot. Values in the column represent the optical density as detected by chemiluminescence and analysed using ImageJ software. The results are shown as mean ± SEM (n=3). The values of protein expression are shown relative to the control. The student t test was used for analysis of statistical significance of each data point.

* $p<0.05$ significant difference when compared to untreated control.

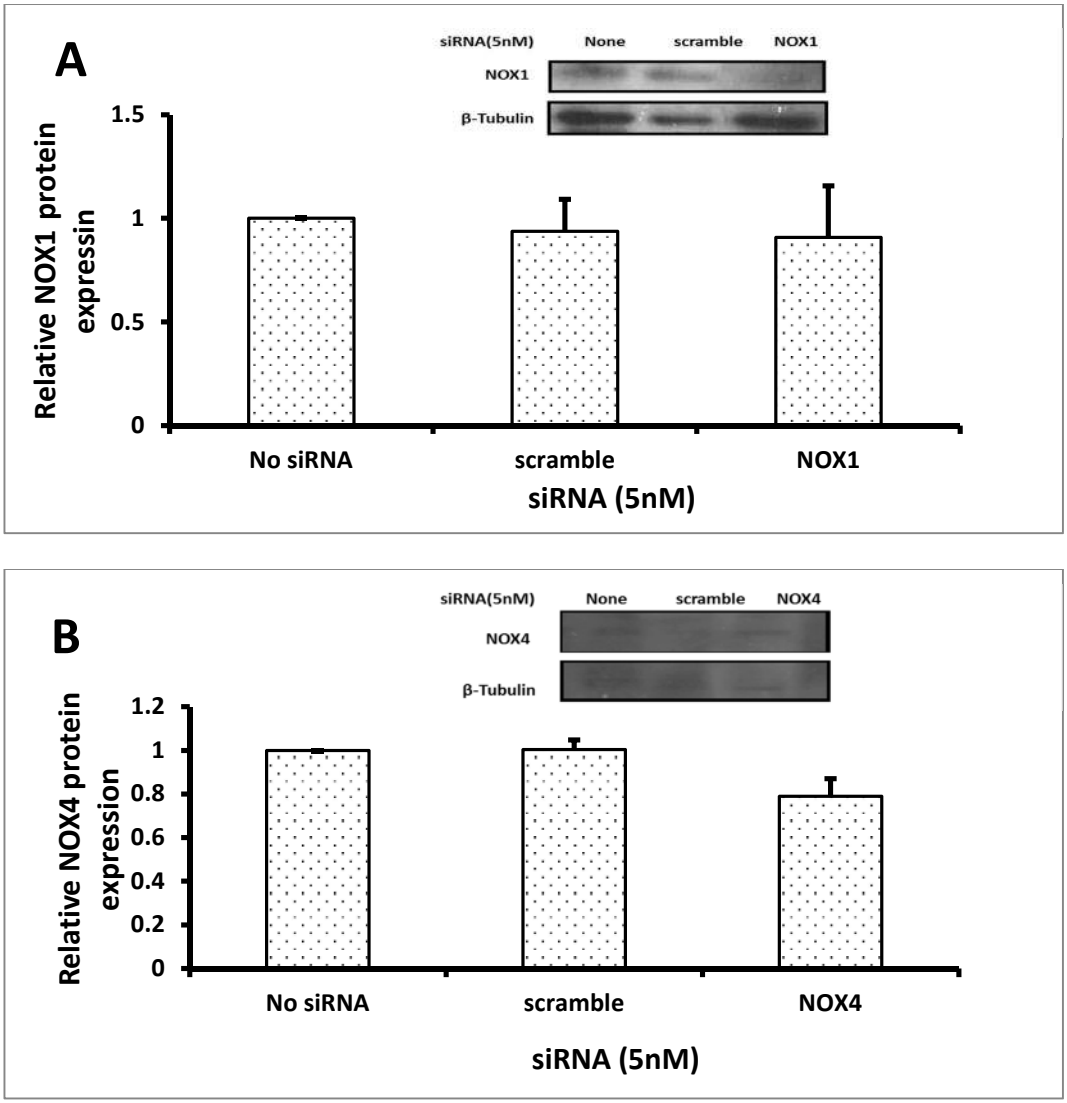

Figure 34 The effect of siNOX1 or siNOX4 on NOX1 and NOX4 protein expression in HaCaT cells. A: siNOX1 effect on NOX1 protein expression of HaCaT cells. B: siNOX4 effect on NOX4 protein expression of HaCaT cells. siRNAs for NOX1 or NOX4 was transfected into HaCaT cells and incubated for 48 h. The NOX protein expression of each sample was determined by western blot. Values in the column represent the optical density as detected by chemiluminescence and analysed using ImageJ software. The results are shown as mean ± SEM (n=3). The values of protein expression are shown relative to the control. The student t test was used for analysis of statistical significance of each data point.

* $p<0.05$ significant difference when compared to untreated control.

Effect of siNOX on ROS generation after UVA irradiation.

Based on the results of the siRNA transfection experiments, skin fibroblasts were treated with siNOX1 or siNOX4 and the ROS generated by UVA irradiation were detected by flow cytometry. The results (Figure 35 and Figure 36) did not show any modification of ROS level following treatment with siNOX1 RNA, siNOX4 RNA or both in siRNA pre-treated FEK4 cells.

As shown in Figure 35, although the transfection regent alone decreased ROS induction at a higher UVA dose (250 kJ/m^2), the results showed further ROS reduction when the siRNA treatment was with the individual siRNA (i.e. siNOX1 or siNOX4). However, the reduction was also observed with scrambled siRNA treatment, and it is not very different from the effect of the targeted siRNA. Similarly, when the siRNA treatment was with the combined siRNA of NOX1 and NOX4 (Figure 36), UVA-induced ROS generation was reduced, but the same reduction was also observed after scrambled siRNA treatment.

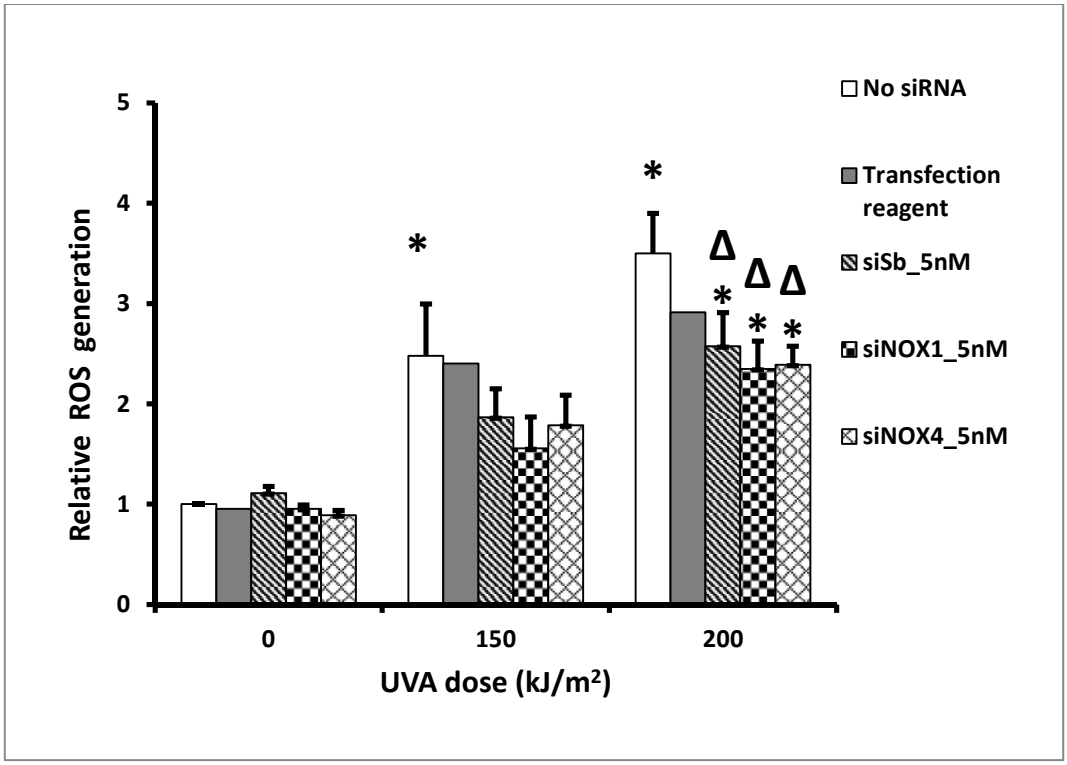

Figure 35 The effect of NOX gene silencing on ROS generation by UVA irradiation of human FEK4 cells. siRNAs (for either NOX1 or NOX4) were added into FEK4 cells with transfection reagent according to the manufacturer 's protocol, incubated for 48 h following UVA irradiation and then ROS generation was detected by flow cytometry. Data shown are mean ± SEM of three independent experiments. Values for ROS generation are expressed relative to untreated FEK4 cells. The student t test was used to evaluate the statistical significance of each data point.

*$p<0.05$ when compared to untreated control cells.

$\Delta p<0.05$ when compared to UVA irradiated cells.

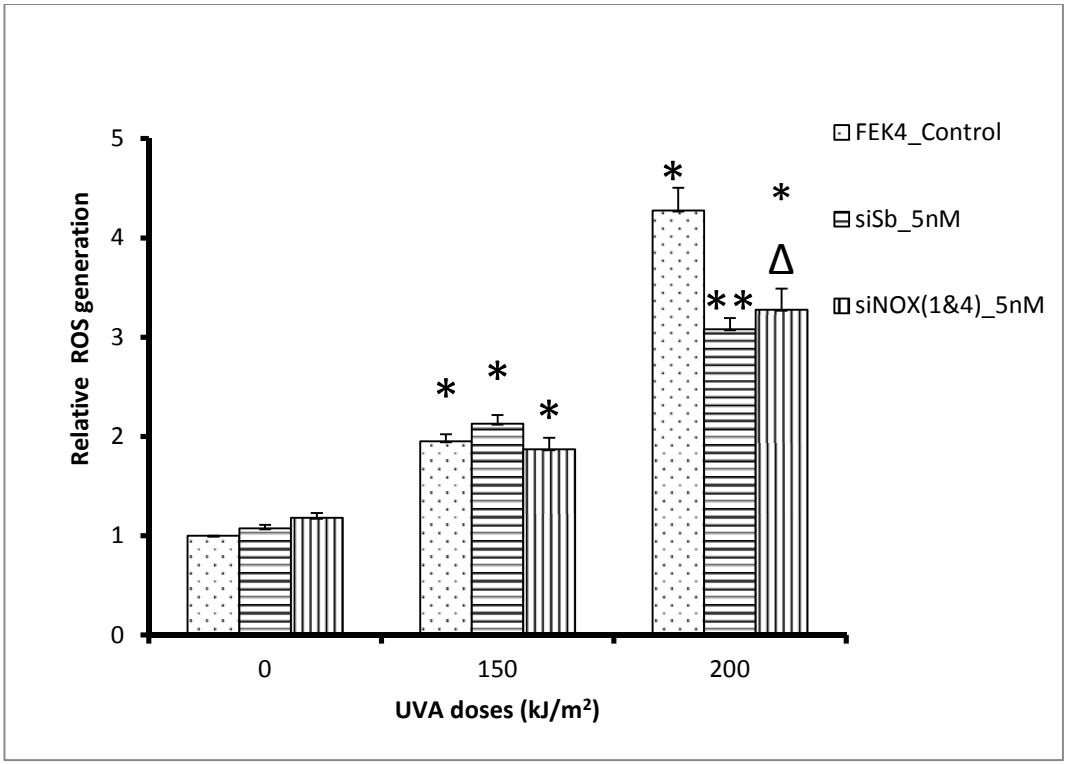

Figure 36 The effect of NOX gene silencing (NOX1 and NOX4) on ROS generation by UVA irradiation of human FEK4 cells. A mixture of siRNA (for NOX1 and NOX4) was transfected into FEK4 cells, incubated for 48 h before UVA irradiation and ROS generation detection by flow cytometry. Data shown are mean ± SEM of three independent experiments. Values for ROS generation are expressed relative to untreated FEK4 cells. The student t test was used to evaluate the statistical significance of each data point.

*$p<0.05$ when compared to untreated control cells.

** $p< 0.01$ when compared with untreated FEK4 control cells

$\Delta p<0.05$ when compared to UVA irradiated cells.

Apparently, although both siNOX1 RNA and siNOX4 RNA treatment had decreased the NOX1 and NOX4 protein expression level as described in the previous section, NOX1 or NOX4 gene knock down does not alter the UVA-mediated ROS generation after UVA irradiation in cultured human skin fibroblasts. These results are therefore in sharp contrast to the results seen in epidermal keratinocytes by Valencia and Kochevar (2008) who observed an almost 50% reduction in UVA-induced ROS using NOX1 siRNA treatment.

In summary, although the siNOX1 and siNOX4 RNAs both reduced NOX activity in FEK4 cells as well as the protein expression level, this treatment does not inhibit UVA-induced ROS generation. One possible explanation may be the confounding effect of scrambled siRNA, but there is also a possibility that the NOX1 and NOX4 proteins are both involved in the UVA-induced NOX activation, but that this is not sufficient to supress the UVA-induced ROS generation since the other NOX family proteins may be involved.

3.10 The effect of HO-1 knocking-down on NOX activity in cultured human skin keratinocytes after UVA irradiation.

Finally, as mentioned in the introduction, there is evidence for the interaction of HO-1 with NOX. Therefore, based on the results obtained in this study, it is reasonable to propose that there will be interdependence between HO-1 and NOX following UVA irradiation. To further understand this, HO-1 was silenced using siHO-1 RNA treatment of HaCaT cells; NOX activity was measured after UVA irradiation, and the results (Figure 37) demonstrated that inhibiting HO-1 decreased NOX activity after UVA irradiation.

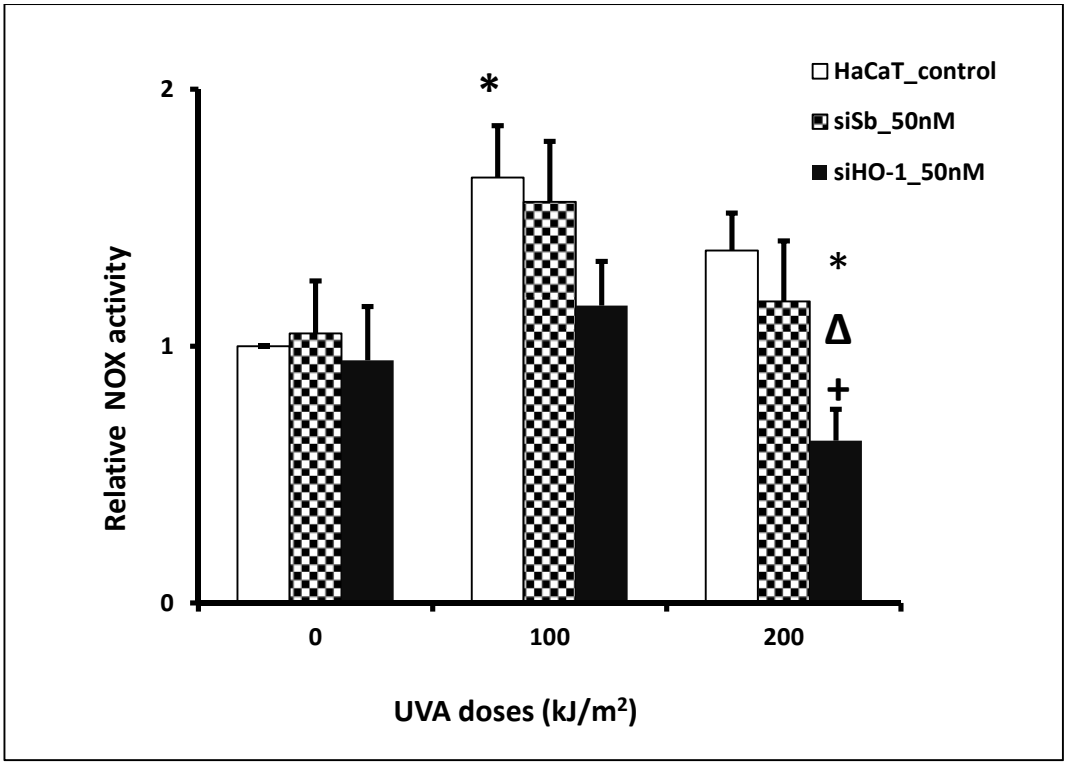

Figure 37 The effect of silencing HO-1 on the activation of NOX activity by UVA irradiation of HaCaT cells. HaCaT cells were pre-treated with siHO-1 and incubated for 48 h before UVA irradiation. Cells were then lysed and the total protein was collected for the NOX activity assay. Values in the bar represent the NOX activity relative to unirradiated, untreated control. The value of untreated HaCaT cell was set to 1; other values were normalized to this value. All values are shown as mean ± SEM (n=3). The student t test was used to evaluate the statistical significance of each data point.

*$p<0.05$ when compared to untreated control cells.

$\Delta p<0.05$ when compared to UVA irradiated cells.

+$p<0.05$ when compared to siscrambled (sisb) RNA treated cells.

Lower NOX activity was observed in HO-1 depleted HaCaT cells that were subsequently treated with UVA irradiation (Figure 37). After 100 kJ/m^2, the sisb RNA slightly decreased the NOX activity as compared with untreated cells, but a further reduction of NOX activity was observed with siHO-1 treatment compared with untreated cells. At a higher UVA dose, the sisb RNA decreased the NOX activity but the siHO-1 RNA treatment decreased further the activity compared to scrambled siRNA treatment.

Induction of NOX1 gene expression by bilirubin was observed in lipopolysaccharide (LPS) activated cells (Weinberger et al., 2013). This provided evidence for the interaction between bilirubin and NOX1 gene activation. This finding could be a possible explanation for the results we have seen in this study i.e. the reduced NOX activity may be due to the lack of one of the HO-1 degradation products (bilirubin) in HO-1 depleted HaCaT cells.

Chapter 4 Discussions and conclusions

HO-1 induction is well known to protect cells against UVA damage and Bach1 is involved in the negative regulation of the HO-1 gene (Raval et al., 2012). Following on from these studies, we proposed that Bach1 inhibition would increase UVA-induced HO-1 and thereby enhance the protection of skin cells against UVA damage. FEK4 cells and HaCaT cells were chosen as the skin cell models in this study. However, the results from our experiments using Bach1 depletion in cultured FEK4 cells showed that there was no significant protection in Bach1 depleted skin fibroblasts compared with control cells. We then tested whether Bach1 inhibition could protect skin cells against UVA damage at the more sensitive ROS level, and we hypothesised that Bach1 inhibition would reduce UVA-induced ROS damage. However, the results indicated that there is a rather higher ROS induction upon UVA treatment at higher UVA doses in Bach1 depleted cells. Based on the results of these Bach1 depletion experiments, we conclude that Bach1 inhibition has no protective role in the process of UVA-induced skin damage, at least for the parameters that we tested. This led us to consider in more depth the mechanism underlying ROS induction in UVA-irradiated skin cells. We studied NADPH oxidase (NOX) for the rest of this study since it is considered as a major source of ROS generation and we hypothesised that it would be the major source of UVA-induced ROS generation.

4.1 Role of Bach1 in protecting against UVA-induced skin cell damage

According to previous research (Raval et al., 2012; Raval., 2008), “Bach1 could act as a negative regulatory protein” in the process of UVA-induced HO-1 up-regulation. This study further investigated whether the inhibition of Bach1 and the consequent increase in HO-1 would alter the UVA-mediated ROS response and skin cell damage. We hypothesized that inhibitory Bach1 would enhance HO-1 induction and thereby enhance protection against UVA damage in cultured human skin fibroblasts. Bach1 inhibition was achieved by silencing Bach1 using specific siRNA and the cell viability in response to UVA irradiation was examined to determine whether Bach1 inhibition would protect against cellular damage.

However the results showed very little protection against cytotoxicity in Bach1 depleted skin fibroblasts compared with control cells (as measured by the MTS assay). Although an oxygen-dependent lethal effect of UVA damage had been identified by colony forming ability assays in FEK4 fibroblasts, we considered it possible that the MTS assay did not pick up this effect. Thus, we performed glutathione depletion experiments and tested UVA dose-dependent reduction in MTS activity in control cells and the ones depleted of glutathione. This study provided evidence that the MTS assay is able to detect the UVA-induced oxidative damage effect. We therefore conclude that Bach1 inhibition effects on skin cells lead to no protective effect against UVA-induced cytotoxicity. We next questioned whether inhibiting Bach1 would lessen UVA-induced ROS generation and we investigated this further in human skin fibroblasts.

4.2 Bach1/HO-1 involvement in UVA-induced ROS generation

To examine the effect of Bach1 inhibition on UVA-induced ROS generation, we examined UVA-induced ROS generation after inhibition of both Bach1 and HO-1. Consistent with the results described in the previous section, silencing Bach1 does not reduce UVA-induced ROS generation in skin fibroblasts; rather it increased ROS induction level at higher UVA dose. In addition to being involved in the oxidative stress response, Bach1 was recently found to be involved in cell cycle proliferation and apoptosis. The increase in ROS generation by Bach1 depletion may be due to other Bach1 mediated cellular events. Interestingly, silencing of HO-1 has little effect on UVA-induced ROS generation. Thus, although we have clearly inhibited Bach1 this is not sufficient to protect skin cells against UVA damage and has no effect on ROS generation. This also implies that the protective role of HO-1 induction after UVA treatment is independent of the UVA-induced ROS response.

4.3 NOX involvement in UVA induced ROS generation

Despite our prediction, it is evident that Bach1 inhibition does not protect skin cells against UVA induced damage. UVA generation of ROS appears to be a complex process that does not involve Bach1 or HO-1. This led us to investigate the role of NOX in UVA-induced ROS generation in cultured human skin cells. NOX activation occurrence has been proven in vitro under various stimuli; for example, treatment of angiotensin II in endothelial cells induces NOX activation (Cai et al., 2003). To examine whether NOX is involved in the process of UVA-induced ROS generation, we tested the response of NOX activity to UVA irradiation and the results demonstrated NOX activation occurs, although to different extents, in both FEK4 and HaCaT cells. It is interesting to note that NOX activation has been observed in human dermal fibroblasts following treatment with very long fatty acid (Dhaunsi et al., 2005).

We next investigated the effect of NOX inhibition on UVA-induced ROS generation. This study firstly showed that inhibiting NOX using the general NOX inhibitor DPI decreased ROS induction in human skin fibroblasts. A similar result was found in UVB irradiated human dermal fibroblasts (Lim et al., 2013). A study in rat mast cells has shown that DPI abolished UVA-induced ROS generation (Zhou et al., 2009).

In addition, ROS generation in skin fibroblasts was found to be cell confluency dependent. UVA radiation generates ROS to a higher extent in more confluent skin fibroblasts. We obtained evidence that the effect of DPI treatment on UVA-induced ROS generation is confluence dependent and that a low confluence level would increase ROS generation following UVA irradiation. Evidence from another laboratory has shown DPI treatment can induce ROS generation and consequently lead to cellular apoptosis in the human promyelocytic leukemia cell line, HL-60 (Li et al., 2003a). Studies in neurons in vitro found that NOX-derived ROS induction is involved in neuronal death under various conditions such as ketamine (Behrens et al., 2007) and stroke (i.e. reoxygenation) (Sorce and Krause, 2009). NOX inhibition by apocynin reversed these effects.

4.4 The contribution of NOX1/NOX4 subunits

In order to further understand which NOX subunit contributed to UVA-induced ROS generation, NOX1 and NOX4 were chosen in this study since they are the most widely studied and previous evidence has strongly indicated that they are involved in the ROS generating system.

As mentioned in the introduction, it is evident that NOX4 activity was increased by docosahexaenoic acid (DHA) in human dermal fibroblasts and DHA-induced ROS generation was abolished by both silencing NOX4 and chemical inhibition of NOX4 (i.e. plumbagin treatment) (Rossary et al., 2007). Similarly, in this study, we observed that basal levels of NOX activity were decreased to different extents with siNOX1 RNA and siNOX4 RNA treatment in both FEK4

and HaCaT cells. Following UVA irradiation, we tested protein expression levels in both FEK4 and HaCaT cells and the results showed that the expression of NOX1 and NOX4 proteins was up-regulated to different extents. This result indicated that these two NOX isoforms are both involved in the UVA-induced NOX activation process, although they contribute to different extents to protein expression levels and enzymatic activity levels. We also noted in this study that at basal level, overall NOX activity appears similar in between FEK4 cells and HaCaT cells. However the level of expression of NOX1 protein is higher in HaCaT cells than in FEK4 cells, whereas NOX4 protein is expressed to a similar extent in both cell lines. This result implies that other NOX proteins in addition to NOX4 may account for the NOX activity in HaCaT cells. A recent study has shown that ROS generation via the NOX2 activation pathway is involved in the wound healing process of HaCaT cells (Bui et al., 2014).

There is evidence that silencing of either NOX1 or NOX4 isoforms can eliminate ROS induction by co-treatment with hapatocyte growth factor (HGF) and TGF-β1 in HaCaT cells (Nam et al., 2010). In contrast with this result, NOX1 and NOX4 subunits were found to have only a limited contribution to UVA-induced ROS generation, suggesting the involvement of other NOX subunits in this process.

In this study, the inhibitory effect of plumbagin was initially employed to inhibit NOX4 subunits, but the results revealed an unexpected role of plumbagin as a redox active molecule in addition to being a NOX4 inhibitor. We discovered that although plumbagin-treatment of skin cells alone strongly reduced UVA-induced ROS generation levels, the compound alone strongly increased ROS generation in skin cells. We have detected cell death in skin cells (pre-treated with plumbagin) and the results confirmed increased apoptotic and necrosis. However, plumbagin completely abolished ROS generation by UVA irradiation. There is evidence that in human melanoma cells, plumbagin induces apoptosis via the generation of ROS (Wang et al., 2008). Powolny and Singh

(2008) also reported that plumbagin results in apoptosis through ROS generation in human prostate cancer cells. Thus, the decrease in ROS generation that we have observed may be due to the oxidising damage by plumbagin. In view of the confounding effects of such chemical inhibition, more specific gene knock down by siRNA targeting NOX1 and NOX4 was carried out as described in the previous section.

In summary, this study has confirmed that NOX1 and NOX4 subunits both contribute to NOX total activity, and may influence on ROS generation following UVA irradiation in cultured human skin fibroblasts. However, additional subunits of NOX enzymes should also be employed for future study. Different NOX isoforms have been reported to be related to ROS-mediated events. NOX2-derived ROS was found to be involved in cell survival in the heart (Rosc-Schluter et al., 2012). NOX3-derived ROS may contribute to hearing loss (Banfi et al., 2004a). NOX5-derived ROS was found to be involved in the vasculature process in endothelial cells (BelAiba et al., 2007). A recent study has shown that in human normal keratinocytes, DUOX1-based ROS production was induced by IL-4 and IL-3 treatment (Hirakawa et al., 2011). All these studies provided evidence that there are other NOX isoforms involved in the ROS mediated events. UVA-induced ROS generation may involve one or more NOX proteins other than NOX1 and NOX4.

4.5 The relationship between HO-1 and NOX

HO-1 induction has been shown to interact with NOX in different conditions; inhibition of NOX1 enzymatic activity has been shown to decrease HO-1 expression in chronic myelogenous leukaemia cells (Singh et al., 2012). NOX has been shown to be involved in the upstream up-regulation of HO-1 expression by arsenite in HaCaT cells (Cooper et al., 2009). Based on these findings, the relationship between HO-1 and NOX was also investigated in this study. We predicted that silencing of HO-1 would increase UVA-induced NOX

activity in HaCaT cells; the results however showed reduced NOX activity. Although silencing of HO-1 decreased UVA activation of NOX in skin keratinocytes in this study, the result clearly confirmed that HO-1 is involved in NOX activation upon UVA treatment. Although we expected that silencing of HO-1 would promote NOX activation, the results may emphasize the pro-oxidant effect of HO-1, and one of the products of HO-1 degradation may also induce cellular damage. A previous study from our laboratory has demonstrated that HO-1 overexpression transitionally hyposensitized cells to UVA-induced cellular damage as a consequence of the release of iron (Kvam et al., 2000). This may be a reason why HO-1 inhibition decreases NOX activity following UVA treatment in skin keratinocytes, a mechanism which meant further study.

4.6 Conclusions

In conclusion, this study has examined the role of Bach1 in UVA-induced HO-1 induction as well as ROS generation in human skin cells. Our results revealed that Bach1 depletion is not sufficient to enhance the protective pathway mediated by UVA-induced HO-1.

Furthermore, we tested the importance role of NOX in UVA-induced ROS generation. The results confirmed that UVA activates NOX in human skin cells and that inhibiting NOX activation decreases UVA-induced ROS. Nevertheless, targeting specific NOX subunits (NOX1/NOX4) did not modify ROS generation after UVA treatment.

Future work should be done to investigate the effect of other NOX subunits. Although less is known about the role of NOX2/3/5 in human skin cells, published evidence that these subunits take part in ROS-mediated events encourages an investigation of the role of these NOX proteins in the process of UVA-induced ROS generation in human skin cells. The contribution of NOX1 and NOX4 to UVA-induced ROS generation in HaCaT cells was not performed further in this study due to technical difficulties and merits further study. Little is known about the function of DUOX1/2, but evidence that DUOX1 contributes the ROS production in HaCaT cells under certain stimuli supports the investigation of DUOX1 as a possible candidate for UVA-induced ROS generation in HaCaT cells. Our study shown that NOX-derived ROS are a major source of UVA-induced ROS generation in cultured human skin cells and therefore that inhibiting the activate sites of the appropriate subunits provide a potential target for prevention of UVA-induced skin damage.

Since HO-1 is found to interact with NOX activity in the process of UVA activated NOX, the relationship between HO-1 and NOX also merits further investigation as one of the potential protective pathways against UVA-induced cellular damage. For example, it would be of value to investigate whether NOX activation is upstream of UVA-induced HO-1 induction and this would be of

value in understanding the mechanism of antioxidant properties of UVA-induced HO-1. This can be studied as a potential antioxidant mechanism pathway of UVA-induced HO-1 in cultured human skin cells in the future.

Chapter 5 References

Ambasta RK, Kumar P, Griendling KK, Schmidt HH, Busse R and Brandes RP (2004) Direct interaction of the novel Nox proteins with p22phox is required for the formation of a functionally active NADPH oxidase. *The Journal of biological chemistry* **279**:45935-45941.

Ameziane-El-Hassani R, Morand S, Boucher JL, Frapart YM, Apostolou D, Agnandji D, Gnidehou S, Ohayon R, Noel-Hudson MS, Francon J, Lalaoui K, Virion A and Dupuy C (2005) Dual oxidase-2 has an intrinsic Ca^{2+}-dependent H_2O_2-generating activity. *The Journal of biological chemistry* **280**:30046-30054.

Applegate LA, Luscher P and Tyrrell RM (1991) Induction of heme oxygenase: a general response to oxidant stress in cultured mammalian cells. *Cancer Research* **51**:974-978.

Aroun A, Zhong JL, Tyrrell RM and Pourzand C (2012) Iron, oxidative stress and the example of solar ultraviolet A radiation. *Photochemical & photobiological sciences : Official journal of the European Photochemistry Association and the European Society for Photobiology* **11**:118-134.

Bánfi B, Maturana A, Jaconi S, Arnaudeau S, Laforge T, Sinha B, Ligeti E, Demaurex N and Krause K-H (2000) A Mammalian H+ Channel Generated Through Alternative Splicing of the NADPH Oxidase Homolog NOH-1. *Science* **287**:138-142.

Balla G, Jacob HS, Eaton JW, Belcher JD and Vercellotti GM (1991) Hemin - a Possible Physiological Mediator of Low-Density-Lipoprotein Oxidation and Endothelial Injury. *Arterioscler Thromb* **11**:1700-1711.

Balla J, Jacob HS, Balla G, Nath K, Eaton JW and Vercellotti GM (1993) Endothelial-Cell Heme Uptake from Heme-Proteins - Induction of Sensitization and Desensitization to Oxidant Damage. *Proceedings of the National Academy of Sciences of the United States of America* **90**:9285-9289.

Banfi B, Malgrange B, Knisz J, Steger K, Dubois-Dauphin M and Krause KH (2004a) NOX3, a superoxide-generating NADPH oxidase of the inner ear. *The Journal of biological chemistry* **279**:46065-46072.

Banfi B, Molnar G, Maturana A, Steger K, Hegedus B, Demaurex N and Krause KH (2001) A Ca(2+)-activated NADPH oxidase in testis, spleen, and lymph nodes. *The Journal of biological chemistry* **276**:37594-37601.

Banfi B, Tirone F, Durussel I, Knisz J, Moskwa P, Molnar GZ, Krause KH and Cox JA (2004b) Mechanism of Ca^{2+} activation of the NADPH oxidase 5 (NOX5). *The Journal of biological chemistry* **279**:18583-18591.

Beak SM, Lee YS and Kim JA (2004) NADPH oxidase and cyclooxygenase mediate the ultraviolet B-induced generation of reactive oxygen species and activation of nuclear factor-kappaB in HaCaT human keratinocytes. *Biochimie* **86**:425-429.

Bedard K and Krause K-H (2007) The NOX Family of ROS-Generating NADPH Oxidases: Physiology and Pathophysiology. *Physiological Reviews* **87**:245-313.

Behrens MM, Ali SS, Dao DN, Lucero J, Shekhtman G, Quick KL and Dugan LL (2007) Ketamine-induced loss of phenotype of fast-spiking interneurons is mediated by NADPH-oxidase. *Science* **318**:1645-1647.

BelAiba RS, Djordjevic T, Petry A, Diemer K, Bonello S, Banfi B, Hess J, Pogrebniak A, Bickel C and Gorlach A (2007) NOX5 variants are

functionally active in endothelial cells. *Free radical biology & medicine* **42**:446-459.

Bickers DR and Athar M (2006) Oxidative stress in the pathogenesis of skin disease. *The Journal of investigative dermatology* **126**:2565-2575.

Booth DM, Mukherjee R, Sutton R and Criddle DN (2011) Calcium and reactive oxygen species in acute pancreatitis: friend or foe? *Antioxidants & redox signaling* **15**:2683-2698.

Boveris A, Oshino N and Chance B (1972) The cellular production of hydrogen peroxide. *Biochemical Journal (1972) 128, 617-630* **128**:617-630.

Brar SS, Kennedy TP, Sturrock AB, Huecksteadt TP, Quinn MT, Whorton AR and Hoidal JR (2002) An NAD(P)H oxidase regulates growth and transcription in melanoma cells. *American journal of physiology Cell physiology* **282**:C1212-1224.

Breen AP and Murphy JA (1995) Reactions of oxyl radicals with DNA. *Free radical biology & medicine* **18**:1033-1077.

Brieger K, Schiavone S, Miller FJ, Jr. and Krause KH (2012) Reactive oxygen species: from health to disease. *Swiss medical weekly* **142**:w13659.

Briganti S and Picardo M (2003) Antioxidant activity, lipid peroxidation and skin diseases. What's new. *Journal of the european academy of dermatology and venereology : JEADV* **17**:663-669.

Brouard S, Otterbein LE, Anrather J, Tobiasch E, Bach FH, Choi AM and Soares MP (2000) Carbon monoxide generated by heme oxygenase 1 suppresses endothelial cell apoptosis. *Journal of experimental medicine* **192**:1015-1026.

Brown DI and Griendling KK (2009) Nox proteins in signal transduction. *Free radical biology & medicine* **47**:1239-1253.

Bui NT, Ho MT, Kim YM, Lim Y and Cho M (2014) Flavonoids promoting HaCaT migration: II. Molecular mechanism of 4',6,7-trimethoxyisoflavone via NOX2 activation. *Phytomedicine : international journal of phytotherapy and phytopharmacology* **21**:570-577.

Burritt JB, Busse SC, Gizachew D, Siemsen DW, Quinn MT, Bond CW, Dratz EA and Jesaitis AJ (1998) Antibody imprint of a membrane protein surface. Phagocyte flavocytochrome b. *The Journal of biological chemistry* **273**:24847-24852.

Cai H, Griendling KK and Harrison DG (2003) The vascular NAD(P)H oxidases as therapeutic targets in cardiovascular diseases. *Trends in pharmacological sciences* **24**:471-478.

Caterina JJ, Donze D, Sun CW, Ciavatta DJ and Townes TM (1994) Cloning and functional characterization of LCR-F1: a bZIP transcription factor that activates erythroid-specific, human globin gene expression. *Nucleic Acids Research* **22**:2383-2391.

Celleno L and Tamburi F (2009) Chapter 1 - Structure and Function of the Skin, in *Nutritional Cosmetics* (Tabor A and Blair RM eds), William Andrew Publishing, Boston. p^pp 3-45.

Chamulitrat W, Stremmel W, Kawahara T, Rokutan K, Fujii H, Wingler K, Schmidt HH and Schmidt R (2004) A constitutive NADPH oxidase-like system containing gp91phox homologs in human keratinocytes. *The Journal of investigative dermatology* **122**:1000-1009.

Chan JY, Han XL and Kan YW (1993) Cloning of Nrf1, an NF-E2-related transcription factor, by genetic selection in yeast. *Proceedings of the National Academy of Sciences of the United States of America* **90**:11371-11375.

Cheeseman KH and Slater TF (1993) An introduction to free radical biochemistry. *British Medical Bulletin* **49**:481-493.

Cheng G, Cao Z, Xu X, van Meir EG and Lambeth JD (2001) Homologs of gp91phox: cloning and tissue expression of Nox3, Nox4, and Nox5. *Gene* **269**:131-140.

Cooper KL, Liu KJ and Hudson LG (2009) Enhanced ROS production and redox signaling with combined arsenite and UVA exposure: contribution of NADPH oxidase. *Free radical biology & medicine* **47**:381-388.

Datla SR, Dusting GJ, Mori TA, Taylor CJ, Croft KD and Jiang F (2007) Induction of heme oxygenase-1 in vivo suppresses NADPH oxidase derived oxidative stress. *Hypertension* **50**:636-642.

DeLeo FR, Burritt JB, Yu L, Jesaitis AJ, Dinauer MC and Nauseef WM (2000) Processing and maturation of flavocytochrome b558 include incorporation of heme as a prerequisite for heterodimer assembly. *The Journal of biological chemistry* **275**:13986-13993.

Dennery PA, Sridhar KJ, Lee CS, Wong HE, Shokoohi V, Rodgers PA and Spitz DR (1997) Heme Oxygenase-mediated Resistance to Oxygen Toxicity in Hamster Fibroblasts. *Journal of biological chemistry* **272**:14937-14942.

Denu JM and Tanner KG (1998) Specific and reversible inactivation of protein tyrosine phosphatases by hydrogen peroxide: evidence for a sulfenic acid intermediate and implications for redox regulation. *Biochemistry* **37**:5633-5642.

Dhaunsi GS, Kaur J, Alsaeid K, Turner RB and Bitar MS (2005) Very long chain fatty acids activate NADPH oxidase in human dermal fibroblasts. *Cell biochemistry and function* **23**:65-68.

Dhaunsi GS, Paintlia MK, Kaur J and Turner RB (2004) NADPH oxidase in human lung fibroblasts. *Journal of biomedical science* **11**:617-622.

Dohi Y, Ikura T, Hoshikawa Y, Katoh Y, Ota K, Nakanome A, Muto A, Omura S, Ohta T, Ito A, Yoshida M, Noda T and Igarashi K (2008) Bach1 inhibits oxidative stress-induced cellular senescence by impeding p53 function on chromatin. *Nature structural & molecular biology* **15**:1246-1254.

Drummond GR, Selemidis S, Griendling KK and Sobey CG (2011) Combating oxidative stress in vascular disease: NADPH oxidases as therapeutic targets. *Nature reviews drug discovery* **10**:453-471.

Dupuy C, Ohayon R, Valent A, Noel-Hudson MS, Deme D and Virion A (1999) Purification of a novel flavoprotein involved in the thyroid NADPH oxidase. Cloning of the porcine and human cdnas. *The Journal of biological chemistry* **274**:37265-37269.

Ehrlich K, Viirlaid S, Mahlapuu R, Saar K, Kullisaar T, Zilmer M, Langel U and Soomets U (2007) Design, synthesis and properties of novel powerful antioxidants, glutathione analogues. *Free radical research* **41**:779-787.

Elbashir SM, Harborth J, Lendeckel W, Yalcin A, Weber K and Tuschl T (2001) Duplexes of 21-nucleotide RNAs mediate RNA interference in cultured mammalian cells. *Nature* **411**:494-498.

Ellmark SH, Dusting GJ, Fui MN, Guzzo-Pernell N and Drummond GR (2005) The contribution of Nox4 to NADPH oxidase activity in mouse vascular smooth muscle. *Cardiovascular research* **65**:495-504.

Evans ND, Oreffo ROC, Healy E, Thurner PJ and Man YH (2013) Epithelial mechanobiology, skin wound healing, and the stem cell niche. *Journal of the Mechanical Behavior of Biomedical Materials* **28**:397-409.

Fire A, Xu S, Montgomery MK, Kostas SA, Driver SE and Mello CC (1998) Potent and specific genetic interference by double-stranded RNA in Caenorhabditis elegans. *Nature* **391**:806-811.

Fitzpatrick AM, Jones DP and Brown LA (2012) Glutathione redox control of asthma: from molecular mechanisms to therapeutic opportunities. *Antioxidants & redox signaling* **17**:375-408.

Fukuto JM, Carrington SJ, Tantillo DJ, Harrison JG, Ignarro LJ, Freeman BA, Chen A and Wink DA (2012) Small molecule signaling agents: the integrated chemistry and biochemistry of nitrogen oxides, oxides of carbon, dioxygen, hydrogen sulfide, and their derived species. *Chemical research in toxicology* **25**:769-793.

Galano A and Alvarez-Idaboy JR (2011) Glutathione: mechanism and kinetics of its non-enzymatic defense action against free radicals. *RSC Advances* **1**:1763-1771.

Geiszt M, Kopp JB, Varnai P and Leto TL (2000) Identification of renox, an NAD(P)H oxidase in kidney. *Proceedings of the National Academy of Sciences of the United States of America* **97**:8010-8014.

Godic A, Poljsak B, Adamic M and Dahmane R (2014) The Role of Antioxidants in Skin Cancer Prevention and Treatment. **2014**:860479.

Gomes EC, Silva AN and de Oliveira MR (2012) Oxidants, antioxidants, and the beneficial roles of exercise-induced production of reactive species. *Oxidative medicine and cellular longevity* **2012**:756132.

Goossens V, Grooten J, De Vos K and Fiers W (1995) Direct evidence for tumor necrosis factor-induced mitochondrial reactive oxygen intermediates and their involvement in cytotoxicity. *Proceedings of the National Academy of Sciences of the United States of America* **92**:8115-8119.

Goyal P, Weissmann N, Rose F, Grimminger F, Schafers HJ, Seeger W and Hanze J (2005) Identification of novel Nox4 splice variants with impact on ROS levels in A549 cells. *Biochemical and biophysical research communications* **329**:32-39.

Griendling KK, Minieri CA, Ollerenshaw JD and Alexander RW (1994) Angiotensin II stimulates NADH and NADPH oxidase activity in cultured vascular smooth muscle cells. *Circulation Research* **74**:1141-1148.

Guerin P, El Mouatassim S and Menezo Y (2001) Oxidative stress and protection against reactive oxygen species in the pre-implantation embryo and its surroundings. *Human reproduction update* **7**:175-189.

Gutteridge JM, Rowley DA, Halliwell B, Cooper DF and Heeley DM (1985a) Copper and iron complexes catalytic for oxygen radical reactions in sweat from human athletes. *Clinica chimica acta; international journal of clinical chemistry* **145**:267-273.

Gutteridge JMC, Rowley DA, Halliwell B, Cooper DF and Heeley DM (1985b) Copper and iron complexes catalytic for oxygen radical reactions in sweat from human athletes. *Clinica Chimica Acta* **145**:267-273.

B. Halliwell and J. M. C. Gutteridge (1999) *Free Radicals in Biology and Medicine*, Oxford University Press, Oxford, UK, 3rd edition.

Harman D (1956) Aging: a theory based on free radical and radiation chemistry. *Journal of gerontology* **11**:298-300.

Harper RW, Xu C, Eiserich JP, Chen Y, Kao CY, Thai P, Setiadi H and Wu R (2005) Differential regulation of dual NADPH oxidases/peroxidases, Duox1 and Duox2, by Th1 and Th2 cytokines in respiratory tract epithelium. *Federation of European Biochemical Societies letters* **579**:4911-4917.

Hill-Kapturczak N, Sikorski E, Voakes C, Garcia J, Nick HS and Agarwal A (2003) An internal enhancer regulates heme- and cadmium-mediated induction of human heme oxygenase-1. *American Journal of Physiology-Renal Physiology* **285**:F515-F523.

Hirakawa S, Saito R, Ohara H, Okuyama R and Aiba S (2011) Dual oxidase 1 induced by Th2 cytokines promotes STAT6 phosphorylation via oxidative inactivation of protein tyrosine phosphatase 1B in human epidermal keratinocytes. *Journal of immunology (Baltimore, Md : 1950)* **186**:4762-4770.

Hockberger PE (2002) A History of Ultraviolet Photobiology for Humans, Animals and Microorganisms. *Photochemistry and Photobiology* **76**:561-579.

Holmgren A (1985) Thioredoxin. *Annual review of biochemistry* **54**:237-271.

Honig LS and Rosenberg RN (2000) Apoptosis and neurologic disease. *The American Journal of Medicine* **108**:317-330.

Hu T, Ramachandrarao SP, Siva S, Valancius C, Zhu Y, Mahadev K, Toh I, Goldstein BJ, Woolkalis M and Sharma K (2005) Reactive oxygen species production via NADPH oxidase mediates TGF-beta-induced cytoskeletal alterations in endothelial cells. *American journal of physiology Renal physiology* **289**:F816-825.

Jacobson MD (1996) Reactive oxygen species and programmed cell death. *Trends in Biochemical Sciences* **21**:83-86.

Johnson WM, Wilson-Delfosse AL and Mieyal JJ (2012) Dysregulation of glutathione homeostasis in neurodegenerative diseases. *Nutrients* **4**:1399-1440.

Jones DP (2008) Radical-free biology of oxidative stress. *American Journal of Physiology-Cell Physiology* **295**:C849-C868.

Kaide JI, Zhang F, Wei Y, Jiang H, Yu C, Wang WH, Balazy M, Abraham NG and Nasjletti A (2001) Carbon monoxide of vascular origin attenuates the sensitivity of renal arterial vessels to vasoconstrictors. *The Journal of clinical investigation* **107**:1163-1171.

Kanitakis J (2002) Anatomy, histology and immunohistochemistry of normal human skin. *European journal of dermatology : EJD* **12**:390-399; quiz 400-391.

Katsuyama M, Matsuno K and Yabe-Nishimura C (2012) Physiological roles of NOX/NADPH oxidase, the superoxide-generating enzyme. *Journal of clinical biochemistry and nutrition* **50**:9-22.

Kawahara T, Ritsick D, Cheng G and Lambeth JD (2005) Point mutations in the proline-rich region of p22phox are dominant inhibitors of Nox1- and Nox2-dependent reactive oxygen generation. *The Journal of biological chemistry* **280**:31859-31869.

Kehrer JP (1993) Free radicals as mediators of tissue injury and disease. *Critical reviews in toxicology* **23**:21-48.

Kevin J. Trouba HKH, Rupesh P. Amin, and Dori R (2002). Germolec Oxidative Stress and Its Role in Skin Disease. *Antioxidants & Redox Signaling* **4(4)**: 665-673.

Keyse SM and Tyrrell RM (1987) Both near ultraviolet radiation and the oxidizing agent hydrogen peroxide Induce a 32-kDa tress protein in normal human skin fibroblasts. *Journal of biological chemistry* **262**:14821-14825.

Keyse SM and Tyrrell RM (1989) Heme oxygenase is the major 32-kDa stress protein induced in human skin fibroblasts by UVA radiation, hydrogen peroxide, and sodium arsenite. *Proceedings of the National Academy of Sciences of the United States of America* **86**:99-103.

Khan AA and Quigley JG (2011) Control of intracellular heme levels: heme transporters and heme oxygenases. *Biochimica et biophysica acta* **1813**:668-682.

Kielbassa C, Roza L and Epe B (1997) Wavelength dependence of oxidative DNA damage induced by UV and visible light. *Carcinogenesis* **18**:811-816.

Kikuchi H, Hikage M, Miyashita H and Fukumoto M (2000) NADPH oxidase subunit, gp91(phox) homologue, preferentially expressed in human colon epithelial cells. *Gene* **254**:237-243.

Kleikers PM, Wingler K, Hermans JJR, Diebold I, Altenhöfer S, Radermacher KA, Janssen B, Görlach A and Schmidt HHHW (2012) NADPH oxidases as a source of oxidative stress and molecular target in ischemia/reperfusion injury. *Journal of molecular medicine* **90**:1391-1406.

Kodama M (1988) [Role of active oxygen species in carcinogenesis]. *Tanpakushitsu kakusan koso Protein, nucleic acid, enzyme* **33**:3136-3143.

Kohen R (1999) Skin antioxidants: their role in aging and in oxidative stress--new approaches for their evaluation. *Biomedicine & pharmacotherapy* **53**:181-192.

Kondo K, Ishigaki Y, Gao J, Yamada T, Imai J, Sawada S, Muto A, Oka Y, Igarashi K and Katagiri H (2013) Bach1 deficiency protects pancreatic beta-cells from oxidative stress injury. *American journal of physiology Endocrinology and metabolism* **305**:E641-648.

Kutty RK, Kutty G, Rodriguez IR, Chader GJ and Wiggert B (1994) Chromosomal localization of the human Heme oxygenase genes: heme oxygenase-1 (HMOX1) maps to chromosome 22q12 and heme

oxygenase-2 (HMOX2) maps to chromosome 16p13.3. *Genomics* **20**:513-516.

Kvam E, Hejmadi V, Ryter S, Pourzand C and Tyrrell RM (2000) Heme oxygenase activity causes transient hypersensitivity to oxidative ultraviolet A radiation that depends on release of iron from heme. *Free Radical Biology and Medicine* **28**:1191-1196.

Kvam E, Noel A, Basu-Modak S and Tyrrell RM (1999a) Cyclooxygenase dependent release of heme from microsomal hemeproteins correlates with induction of heme oxygenase 1 transcription in human fibroblasts. *Free radical biology & medicine* **26**:511-517.

Kvam E, Noel A, Basu-Modak S and Tyrrell RM (1999b) Cyclooxygenase dependent release of heme from microsomal hemeproteins correlates with induction of heme oxygenase -1 transcription in human fibroblasts. *Free radical biology & medicine* **26**:511-517.

Lamb NJ, Quinlan GJ, Mumby S, Evans TW and Gutteridge JM (1999) Haem oxygenase shows pro-oxidant activity in microsomal and cellular systems: implications for the release of low-molecular-mass iron. *The Biochemical journal* **344 Pt 1**:153-158.

Laude K, Cai H, Fink B, Hoch N, Weber DS, McCann L, Kojda G, Fukai T, Schmidt HH, Dikalov S, Ramasamy S, Gamez G, Griendling KK and Harrison DG (2005) Hemodynamic and biochemical adaptations to vascular smooth muscle overexpression of p22phox in mice. *American journal of physiology Heart and circulatory physiology* **288**:H7-12.

Lautier D, Luscher P and Tyrrell RM (1992) Endogenous glutathione levels modulate both constitutive and UVA radiation/hydrogen peroxide inducible expression of the human heme oxygenase gene. *Carcinogenesis* **13**:227-232.

Leto TL, Adams AG and de Mendez I (1994) Assembly of the phagocyte NADPH oxidase: binding of Src homology 3 domains to proline-rich targets. *Proceedings of the National Academy of Sciences of the United States of America* **91**:10650-10654.

Li C and Stocker R (2009) Heme oxygenase and iron: from bacteria to humans. *Redox report : communications in free radical research* **14**:95-101.

Li N, Ragheb K, Lawler G, Sturgis J, Rajwa B, Melendez JA and Robinson JP (2003a) DPI induces mitochondrial superoxide-mediated apoptosis. *Free radical biology & medicine* **34**:465-477.

Li N, Ragheb K, Lawler G, Sturgis J, Rajwa B, Melendez JA and Robinson JP (2003b) DPI induces mitochondrial superoxide-mediated apoptosis. *Free radical biology & medicine* **34**:465-477.

Lim TG, Jung SK, Kim JE, Kim Y, Lee HJ, Jang TS and Lee KW (2013) NADPH oxidase is a novel target of delphinidin for the inhibition of UVB-induced MMP-1 expression in human dermal fibroblasts. *Experimental dermatology* **22**:428-430.

Liu GS, Peshavariya H, Higuchi M, Brewer AC, Chang CW, Chan EC and Dusting GJ (2012) Microphthalmia-associated transcription factor modulates expression of NADPH oxidase type 4: a negative regulator of melanogenesis. *Free radical biology & medicine* **52**:1835-1843.

Loughlin DT and Artlett CM (2010) Precursor of advanced glycation end products mediates ER-stress-induced caspase-3 activation of human dermal fibroblasts through NAD(P)H oxidase 4. *PloS one* **5**:e11093.

Luna L, Johnsen O, Skartlien AH, Pedeutour F, Turc-Carel C, Prydz H and Kolsto AB (1994) Molecular cloning of a putative novel human bZIP transcription factor on chromosome 17q22. *Genomics* **22**:553-562.

Maines MD, Trakshel GM and Kutty RK (1986) Characterization of two constitutive forms of rat liver microsomal heme oxygenase. Only one molecular species of the enzyme is inducible. *The Journal of biological chemistry* **261**:411-419.

Martyn KD, Frederick LM, von Loehneysen K, Dinauer MC and Knaus UG (2006) Functional analysis of Nox4 reveals unique characteristics compared to other NADPH oxidases. *Cellular signalling* **18**:69-82.

Masaki H (2010) Role of antioxidants in the skin: Anti-aging effects. *Journal of Dermatological Science* **58**:85-90.

Massaad CA and Klann E (2011) Reactive oxygen species in the regulation of synaptic plasticity and memory. *Antioxidants & redox signaling* **14**:2013-2054.

Matsumura Y and Ananthaswamy HN (2004) Toxic effects of ultraviolet radiation on the skin. *Toxicology and applied pharmacology* **195**:298-308.

Matsuzawa A and Ichijo H (2008) Redox control of cell fate by MAP kinase: physiological roles of ASK1-MAP kinase pathway in stress signaling. *Biochimica et biophysica acta* **1780**:1325-1336.

McKelvey TG, Hollwarth ME, Granger DN, Engerson TD, Landler U and Jones HP (1988) Mechanisms of conversion of xanthine dehydrogenase to xanthine oxidase in ischemic rat liver and kidney. *American Journal of Physiology - Gastrointestinal and Liver Physiology* **254**:G753-G760.

Meier B, Cross AR, Hancock JT, Kaup FJ and Jones OT (1991) Identification of a superoxide-generating NADPH oxidase system in human fibroblasts. *The Biochemical journal* **275 (Pt 1)**:241-245.

Miller DM, Buettner GR and Aust SD (1990) Transition metals as catalysts of "autoxidation" reactions. *Free radical biology & medicine* **8**:95-108.

Miyano K, Ueno N, Takeya R and Sumimoto H (2006) Direct involvement of the small GTPase Rac in activation of the superoxide-producing NADPH oxidase Nox1. *The Journal of biological chemistry* **281**:21857-21868.

Moi P, Chan K, Asunis I, Cao A and Kan YW (1994) Isolation of NF-E2-related factor 2 (Nrf2), a NF-E2-like basic leucine zipper transcriptional activator that binds to the tandem NF-E2/AP1 repeat of the beta-globin locus control region. *Proceedings of the National Academy of Sciences of the United States of America* **91**:9926-9930.

Montgomery MK, Xu S and Fire A (1998) RNA as a target of double-stranded RNA-mediated genetic interference in Caenorhabditis elegans. *Proceedings of the National Academy of Sciences of the United States of America* **95**:15502-15507.

Morand S, Agnandji D, Noel-Hudson MS, Nicolas V, Buisson S, Macon-Lemaitre L, Gnidehou S, Kaniewski J, Ohayon R, Virion A and Dupuy C (2004) Targeting of the dual oxidase 2 N-terminal region to the plasma membrane. *The Journal of biological chemistry* **279**:30244-30251.

Nakano Y, Banfi B, Jesaitis AJ, Dinauer MC, Allen LA and Nauseef WM (2007) Critical roles for $p22^{phox}$ in the structural maturation and subcellular targeting of NOX3. *The Biochemical journal* **403**:97-108.

Nam HJ, Park YY, Yoon G, Cho H and Lee JH (2010) Co-treatment with hepatocyte growth factor and TGF-beta1 enhances migration of HaCaT cells through NADPH oxidase-dependent ROS generation. *Experimental & Molecular medicine* **42**:270-279.

Narendhirakannan RT and Hannah MA (2013a) Oxidative Stress and Skin Cancer: An Overview. *Indian journal of clinical biochemistry : IJCB* **28**:110-115.

Narendhirakannan RT and Hannah MA (2013b) Oxidative Stress and Skin Cancer: An Overview. *Indian Journal of Clinical Biochemistry* **28**:110-115.

Niki E (2009) Lipid peroxidation: Physiological levels and dual biological effects. *Free radical biology & medicine* **47**:469-484.

Niki E (2014) Biomarkers of lipid peroxidation in clinical material. *Biochimica et Biophysica Acta (BBA) - General Subjects* **1840**:809-817.

Nose K (2000) Role of reactive oxygen species in the regulation of physiological functions. *Biological & pharmaceutical bulletin* **23**:897-903.

Nowak JZ (2013) Oxidative stress, polyunsaturated fatty acids-derived oxidation products and bisretinoids as potential inducers of CNS diseases: focus on age-related macular degeneration. *Pharmacological reports : PR* **65**:288-304.

Ochiai S, Mizuno T, Deie M, Igarashi K, Hamada Y and Ochi M (2008) Oxidative stress reaction in the meniscus of Bach 1 deficient mice: potential prevention of meniscal degeneration. *Journal of orthopaedic research* **26**:894-898.

Okada S, Muto A, Ogawa E, Nakanome A, Katoh Y, Ikawa S, Aiba S, Igarashi K and Okuyama R (2010) Bach1-dependent and -independent regulation of heme oxygenase-1 in keratinocytes. *The Journal of biological chemistry* **285**:23581-23589.

Ou-Yang H, Stamatas G, Saliou C and Kollias N (2004) A chemiluminescence study of UVA-induced oxidative stress in human skin in vivo. *The Journal of investigative dermatology* **122**:1020-1029.

Oyake T, Itoh K, Motohashi H, Hayashi N, Hoshino H, Nishizawa M, Yamamoto M and Igarashi K (1996a) Bach proteins belong to a novel

family of BTB-basic leucine zipper transcription factors that interact with MafK and regulate transcription through the NF-E2 site. *Molecular and cellular biology* **16**:6083-6095.

Oyake T, Itoh K, Motohashi H, Hayashi N, Hoshino H, Nishizawa M, Yamamoto M and Igarashi K (1996b) Bach proteins belong to a novel family of BTB-basic leucine zipper transcription factors that interact with MafK and regulate transcription through the NF-E2 site. *Molecular and cellular biology* **16**:6083-6095.

Paletta-Silva R, Rocco-Machado N and Meyer-Fernandes JR (2013) NADPH oxidase biology and the regulation of tyrosine kinase receptor signaling and cancer drug cytotoxicity. *International Journal of Molecular Sciences* **14**:3683-3704.

Pandel R, Poljsak B, Godic A and Dahmane R (2013) Skin photoaging and the role of antioxidants in its Prevention. *International Scholarly Research Notices Dermatology* **2013**:930164.

Pannen BH, Kohler N, Hole B, Bauer M, Clemens MG and Geiger KK (1998) Protective role of endogenous carbon monoxide in hepatic microcirculatory dysfunction after hemorrhagic shock in rats. *The Journal of clinical investigation* **102**:1220-1228.

Park HS, Jin DK, Shin SM, Jang MK, Longo N, Park JW, Bae DS and Bae YS (2005) Impaired generation of reactive oxygen species in leprechaunism through downregulation of Nox4. *Diabetes* **54**:3175-3181.

Parkos CA, Allen RA, Cochrane CG and Jesaitis AJ (1987) Purified cytochrome b from human granulocyte plasma membrane is comprised of two polypeptides with relative molecular weights of 91,000 and 22,000. *The Journal of clinical investigation* **80**:732-742.

Piccoli C, Ria R, Scrima R, Cela O, D'Aprile A, Boffoli D, Falzetti F, Tabilio A and Capitanio N (2005) Characterization of mitochondrial and extra-mitochondrial oxygen consuming reactions in human hematopoietic stem cells. Novel evidence of the occurrence of NAD(P)H oxidase activity. *The Journal of Biological Chemistry* **280**:26467-26476.

Polefka TG, Meyer TA, Agin PP and Bianchini RJ (2012) Effects of solar radiation on the skin. *Journal of cosmetic dermatology* **11**:134-143.

Poljsak B, Dahmane R and Godic A (2013) Skin and antioxidants. *Journal of cosmetic and laser therapy : official publication of the European Society for Laser Dermatology* **15**:107-113.

Pourova J, Kottova M, Voprsalova M and Pour M (2010) Reactive oxygen and nitrogen species in normal physiological processes. *Acta Physiologica* **198**:15-35.

Pozzoli G, Mancuso C, Mirtella A, Preziosi P, Grossman AB and Navarra P (1994) Carbon monoxide as a novel neuroendocrine modulator: inhibition of stimulated corticotropin-releasing hormone release from acute rat hypothalamic explants. *Endocrinology* **135**:2314-2317.

Rada B, Hably C, Meczner A, Timar C, Lakatos G, Enyedi P and Ligeti E (2008) Role of Nox2 in elimination of microorganisms. *Seminars in immunopathology* **30**:237-253.

Rahman M, Kundu JK, Shin JW, Na HK and Surh YJ (2011) Docosahexaenoic acid inhibits UVB-induced activation of NF-kappaB and expression of COX-2 and NOX-4 in HR-1 hairless mouse skin by blocking MSK1 signaling. *PloS one* **6**:e28065.

Raval CM, Zhong JL, Mitchell SA and Tyrrell RM (2012) The role of Bach1 in ultraviolet A-mediated human heme oxygenase 1 regulation in human skin fibroblasts. *Free radical biology & medicine* **52**:227-236.

Raval, C. (2008). Thre role of Bach1 in ultraviolet-A mediated human heme oxygenase-1 gene regulation. Thesis (Doctor of Philosophy (PhD)). *University of Bath*.

Reeve VE and Tyrrell RM (1999) Heme oxygenase induction mediates the photoimmunoprotective activity of UVA radiation in the mouse. *Proceedings of the National Academy of Sciences of the United States of America* **96**:9317-9321.

Rokutan K, Kawahara T, Kuwano Y, Tominaga K, Sekiyama A and Teshima-Kondo S (2006) NADPH oxidases in the gastrointestinal tract: a potential role of Nox1 in innate immune response and carcinogenesis. *Antioxidants & Redox Signaling* **8**:1573-1582.

Rosbrook GO, Stead MA, Carr SB and Wright SC (2012) The structure of the Bach2 POZ-domain dimer reveals an intersubunit disulfide bond. *Acta crystallographica Section D, Biological crystallography* **68**:26-34.

Rosc-Schluter BI, Hauselmann SP, Lorenz V, Mochizuki M, Facciotti F, Pfister O and Kuster GM (2012) NOX2-derived reactive oxygen species are crucial for CD29-induced pro-survival signalling in cardiomyocytes. *Cardiovascular Research* **93**:454-462.

Rossary A, Arab K and Steghens JP (2007) Polyunsaturated fatty acids modulate NOX 4 anion superoxide production in human fibroblasts. *The Biochemical Journal* **406**:77-83.

Royer-Pokora B, Kunkel LM, Monaco AP, Goff SC, Newburger PE, Baehner RL, Cole FS, Curnutte JT and Orkin SH (1986) Cloning the gene for an inherited human disorder--chronic granulomatous disease--on the basis of its chromosomal location. *Nature* **322**:32-38.

Ryter SW, Alam J and Choi AM (2006) Heme oxygenase-1/carbon monoxide: from basic science to therapeutic applications. *Physiological Reviews* **86**:583-650.

Schraufstatter IU, Hinshaw DB, Hyslop PA, Spragg RG and Cochrane CG (1986) Oxidant injury of cells. DNA strand-breaks activate polyadenosine diphosphate-ribose polymerase and lead to depletion of nicotinamide adenine dinucleotide. *The Journal of clinical investigation* **77**:1312-1320.

Schroder K, Zhang M, Benkhoff S, Mieth A, Pliquett R, Kosowski J, Kruse C, Luedike P, Michaelis UR, Weissmann N, Dimmeler S, Shah AM and Brandes RP (2012) Nox4 is a protective reactive oxygen species generating vascular NADPH oxidase. *Circulation Research* **110**:1217-1225.

Singh MM, Irwin ME, Gao Y, Ban K, Shi P, Arlinghaus RB, Amin HM and Chandra J (2012) Inhibition of the NADPH oxidase regulates heme oxygenase 1 expression in chronic myeloid leukemia. *Cancer* **118**:3433-3445.

Sorce S and Krause KH (2009) NOX enzymes in the central nervous system: from signaling to disease. *Antioxidants & Redox Signaling* **11**:2481-2504.

Steinbrenner H, Ramos MC, Stuhlmann D, Mitic D, Sies H and Brenneisen P (2005) Tumor promoter TPA stimulates MMP-9 secretion from human keratinocytes by activation of superoxide-producing NADPH oxidase. *Free radical research* **39**:245-253.

Suh YA, Arnold RS, Lassegue B, Shi J, Xu X, Sorescu D, Chung AB, Griendling KK and Lambeth JD (1999) Cell transformation by the superoxide-generating oxidase Mox1. *Nature* **401**:79-82.

Sun J, Brand M, Zenke Y, Tashiro S, Groudine M and Igarashi K (2004) Heme regulates the dynamic exchange of Bach1 and NF-E2-related factors in the Maf transcription factor network. *Proceedings of the National Academy of Sciences of the United States of America* **101**:1461-1466.

Sun J, Hoshino H, Takaku K, Nakajima O, Muto A, Suzuki H, Tashiro S, Takahashi S, Shibahara S, Alam J, Taketo MM, Yamamoto M and Igarashi K (2002) Hemoprotein Bach1 regulates enhancer availability of heme oxygenase-1 gene. *The European Molecular Biology Organization Journal* **21**:5216-5224.

Taille C, El-Benna J, Lanone S, Dang MC, Ogier-Denis E, Aubier M and Boczkowski J (2004) Induction of heme oxygenase-1 inhibits NAD(P)H oxidase activity by down-regulating cytochrome b558 expression via the reduction of heme availability. *The Journal of Biological Chemistry* **279**:28681-28688.

Takeya R, Ueno N, Kami K, Taura M, Kohjima M, Izaki T, Nunoi H and Sumimoto H (2003) Novel human homologues of p47phox and p67phox participate in activation of superoxide-producing NADPH oxidases. *The Journal of Biological Chemistry* **278**:25234-25246.

Tandara L and Salamunic I (2012) Iron metabolism: current facts and future directions. *The Journal of the Croatian Society of Medical Biochemistry and Laboratory Medicine* **22**:311-328.

Tang G (2005) siRNA and miRNA: an insight into RISCs. *Trends in Biochemical Sciences* **30**:106-114.

Teahan C, Rowe P, Parker P, Totty N and Segal AW (1987) The X-linked chronic granulomatous disease gene codes for the beta-chain of cytochrome b-245. *Nature* **327**:720-721.

Tenhunen R, Marver HS and Schmid R (1968) The enzymatic conversion of heme to bilirubin by microsomal heme oxygenase. *Proceedings of the National Academy of Sciences of the United States of America* **61**:748-755.

Tenhunen R, Marver HS and Schmid R (1969) Microsomal Heme Oxygenase - Characterization of Enzyme. *Journal of biological chemistry* **244**:6388-&.

Thannickal VJ and Fanburg BL (2000) Reactive oxygen species in cell signaling. *American Journal of Physiology - Lung Cellular and Molecular Physiology* **279**:L1005-L1028.

Tobi SE, Paul N and McMillan TJ (2000) Glutathione modulates the level of free radicals produced in UVA-irradiated cells. *Journal of Photochemistry and Photobiology B: Biology* **57**:102-112.

Tobiume K, Matsuzawa A, Takahashi T, Nishitoh H, Morita K, Takeda K, Minowa O, Miyazono K, Noda T and Ichijo H (2001) ASK1 is required for sustained activations of JNK/p38 MAP kinases and apoptosis. *European Molecular Biology Organization Reports* **2**:222-228.

Trakshel GM, Kutty RK and Maines MD (1986) Purification and characterization of the major constitutive form of testicular heme oxygenase. The noninducible isoform. *The Journal of Biological Chemistry* **261**:11131-11137.

Trouba KJ, Hamadeh HK, Amin RP and Germolec DR (2002) Oxidative stress and its role in skin disease. *Antioxidants & Redox Signaling* **4**:665-673.

Turrens JF (2003) Mitochondrial formation of reactive oxygen species. *The Journal of Physiology* **552**:335-344.

Tyrrell RM (1995) Ultraviolet radiation and free radical damage to skin. *Biochemical Society Symposia; Free radicals and oxidative stress: Environment, drugs and food additives*:47-53.

Tyrrell RM (2012) Modulation of gene expression by the oxidative stress generated in human skin cells by UVA radiation and the restoration of redox homeostasis. *Photochemical & photobiological sciences : Official journal of the European Photochemistry Association and the European Society for Photobiology* **11**:135-147.

Tyrrell RM and Pidoux M (1986) Endogenous glutathione protects human skin fibroblasts against the cytotoxic action of UVB, UVA and near-visible radiations. *Photochemistry and Photobiology* **44**:561-564.

Tyrrell RM and Pidoux M (1988) Correlation between endogenous glutathione content and sensitivity of cultured human skin cells to radiation at defined wavelengths in the solar ultraviolet range. *Photochemistry and Photobiology* **47**:405-412.

Tyrrell RM and Pidoux M (1989) Singlet oxygen involvement in the inactivation of cultured human fibroblasts by UVA (334 nm, 365 nm) and near-visible (405 nm) radiations. *Photochemistry and Photobiology* **49**:407-412.

Tyrrell RM and Reeve VE (2006) Potential protection of skin by acute UVA irradiation--From cellular to animal models. *Progress in Biophysics and Molecular Biology* **92**:86-91.

Tyrrell RMaK, S.M. (1990) The interaction of UVA radiation with cultured cells. *Journal of Photochemistry and Photobiology* **4**: 349-361.

Ueyama T, Geiszt M and Leto TL (2006) Involvement of Rac1 in activation of multicomponent Nox1- and Nox3-based NADPH oxidases. *Molecular and cellular biology* **26**:2160-2174.

Unno M, Matsui T and Ikeda-Saito M (2007) Structure and catalytic mechanism of heme oxygenase. *Natural Product Reports* **24**:553-570.

Valencia A and Kochevar IE (2008) Nox1-based NADPH oxidase is the major source of UVA-induced reactive oxygen species in human keratinocytes. *The Journal of Investigative Dermatology* **128**:214-222.

Vallet P, Charnay Y, Steger K, Ogier-Denis E, Kovari E, Herrmann F, Michel JP and Szanto I (2005) Neuronal expression of the NADPH oxidase NOX4, and its regulation in mouse experimental brain ischemia. *Neuroscience* **132**:233-238.

von Sonntag C (1987) *The Chemical Basis of Radiation Biology*. Taylor & Francis, London.

Wagener FA, Dekker D, Berden JH, Scharstuhl A and van der Vlag J (2009) The role of reactive oxygen species in apoptosis of the diabetic kidney. *Apoptosis : an international journal on programmed cell death* **14**:1451-1458.

Wang CC, Chiang YM, Sung SC, Hsu YL, Chang JK and Kuo PL (2008) Plumbagin induces cell cycle arrest and apoptosis through reactive oxygen species/c-Jun N-terminal kinase pathways in human melanoma A375.S2 cells. *Cancer letters* **259**:82-98.

Warnatz HJ, Schmidt D, Manke T, Piccini I, Sultan M, Borodina T, Balzereit D, Wruck W, Soldatov A, Vingron M, Lehrach H and Yaspo ML (2011) The BTB and CNC homology 1 (BACH1) target genes are involved in the oxidative stress response and in control of the cell cycle. *The Journal of Biological Chemistry* **286**:23521-23532.

Weinberger B, Archer FE, Kathiravan S, Hirsch DS, Kleinfeld AM, Vetrano AM and Hegyi T (2013) Effects of bilirubin on neutrophil responses in newborn infants. *Neonatology* **103**:105-111.

Wondrak GT, Jacobson MK and Jacobson EL (2006) Endogenous UVA-photosensitizers: mediators of skin photodamage and novel targets for skin photoprotection. *Photochemical & photobiological sciences : Official journal of the European Photochemistry Association and the European Society for Photobiology* **5**:215-237.

Yang S, Madyastha P, Bingel S, Ries W and Key L (2001) A New Superoxide-generating Oxidase in Murine Osteoclasts. *Journal of Biological Chemistry* **276**:5452-5458.

Yin H, Xu L and Porter NA (2011) Free Radical Lipid Peroxidation: Mechanisms and Analysis. *Chemical Reviews* **111**:5944-5972.

Zhong JL, Raval C, Edwards GP and Tyrrell RM (2010) A role for Bach1 and HO-2 in suppression of basal and UVA-induced HO-1 expression in human keratinocytes. *Free Radical Biology and Medicine* **48**:196-206.

Zhou YD, Fang XF and Cui ZJ (2009) UVA-induced calcium oscillations in rat mast cells. *Cell Calcium* **45**:18-28.

Zollman S, Godt D, Prive GG, Couderc JL and Laski FA (1994) The Btb Domain, Found Primarily in Zinc-Finger Proteins, Defines an Evolutionarily Conserved Family That Includes Several Developmentally-Regulated Genes in Drosophila. *Proceedings of the National Academy of Sciences of the United States of America* **91**:10717-10721.

Appendix

Appendix 1 Flow cytometry data presenting of ROS generation in live cultured human skin cells. Red coloured area represents for the value of the ROS dye (CM-H_2DCFDA) labelled fluoresce intensity which was proportional to the ROS generation. Values were generated by the fluorescence intensity that measured by flow cytometer in the living single cell. The peak (i.e. representing the median value of fluorescence intensity) shifting (black arrow) indicates the UVA induced ROS generation in comparison with control (ctrl).